DCE17

2nd DOCTORAL CONGRESS in ENGINEERING

8 – 9 JUNE 2017 • FEUP • PORTO • PORTUGAL

Book of Abstracts

2nd Symposium on Chemical, Biological and Environmental Engineering

U.PORTO
FEUP FACULDADE DE ENGENHARIA
UNIVERSIDADE DO PORTO

Book of Abstracts

of the

2nd Symposium on Chemical, Biological and Environmental Engineering

Editors:
Alexandra Pinto, Daniel Direito, Helder X. Nunes,
Joana Vilas Boas, Marta Barbosa, Sara Ramos

Porto
June 2017

This volume contains the abstracts presented at the Symposium on Chemical, Biological and Environmental Engineering, within the 2nd Doctoral Congress in Engineering - DCE17, held in Porto, between June 8th and 9th, 2017.

Title: Book of Abstracts of the 2nd Symposium on Chemical, Biological and Environmental Engineering

Edited by **Alexandra Pinto, Daniel Direito, Helder X. Nunes, Joana Vilas Boas, Marta Barbosa, Sara Ramos**

Published by:
FEUP Edições
http://fe.up.pt/dce17/symposia/symposium-on-chemical-biological-and-environmental-engineering/BoAChemBioEnvEng.pdf

First edition June 2017
ISBN. 978-972-752-218-7

Universidade do Porto, Faculdade de Engenharia, Departamento de Engenharia Química, Rua Dr. Roberto Frias s/n 4200-465 Porto, Portugal

Sponsored by

GOLD

BOSCH
Tecnologia para a vida

INESCTEC

INDULATEX
There is no impossible

SYNOPSYS®

SILVER

Addlink
Software Científico

Hovione

BRONZE

inegi driving science & innovation

U.PORTO

Other Contributions

EUROPAC

paralab

Porto.

QrH+

Sociedade Portuguesa de Química

SOGRAPE VINHOS

*

---

* Faculty of Engineering of the University of Porto:
Department of Chemical Engineering | Department of Civil Engineering | Department of Electrical and Computer Engineering | Department of Mechanical Engineering | Department of Metallurgical and Materials Engineering | Department of Mining Engineering | Department of Physics Engineering

Symposium Committee

Scientific Committee

Chair: Alexandra Pinto | FEUP
Arminda Alves | FEUP
Carmen Rangel | LNEG
Cidália Botelho | FEUP
Daniel Direito | FEUP
Fernando Pereira | FEUP
Filomena Barreiro | IPB
Francisco Malcata | FEUP
Helder Xavier Nunes | FEUP
Joana Vilas Boas | FEUP
José Teixeira | U.Minho
Manuel Alves | FEUP
Manuel Simões | FEUP
Marta Barbosa | FEUP
Miguel Madeira | FEUP
Sara Ramos | FEUP

Organizing Committee

Chair: Alexandra Pinto | FEUP
Cidália Botelho | FEUP
Daniel Direito | FEUP
Helder Xavier Nunes | FEUP
Joana Vilas Boas | FEUP
Marta Barbosa | FEUP
Sara Ramos | FEUP

Welcome

Welcome to the Symposium on Chemical, Biological and Environmental Engineering, within the 2nd Doctoral Congress in Engineering - DCE17!

After the first edition (2015) the congress was held again at the Faculty of Engineering of the University of Porto (FEUP). The Symposium on Chemical, Biological and Environmental Engineering was one of the 10 symposia that made up the 2nd Doctoral Congress in Engineering, and was organized by students of the Doctoral Program in Chemical and Biological Engineering and the Doctoral Program in Environmental Engineering from FEUP.

The Organizing Committee of the Symposium on Chemical, Biological and Environmental Engineering received 58 submissions, from 7 countries, being 25 oral and 31 poster presentations selected after revision by the Scientific Committee. Moreover, the Symposium Program also included 2 Keynote Lectures from national recognized scientists, who shared their experience working on engineering field. The Symposium was attended by ca. 90 participants, represented about 27% of the total attendees of DCE17.

Finally, all the submissions were automatically included in contest for Best Oral Presentation and Best Poster awards, sponsored by Sociedade Portuguesa de Química.
We acknowledge the Keynote Speakers and all the authors for their contributions, the Scientific Committee for helping to build the scientific program and the participant Companies and Institutions for their support.

Porto, June 2017

Symposium Organizing Committee

Contents

Keynotes

Oral Presentations

Poster Presentation

Programme

June 8th, Thursday

08:00	**Registration**
09:00	**Welcome Session** (B032)
09:30	**Opening Session** (B032) Professor Alexandra Pinto
09:45	**Keynote** (B032) Doctor Vânia Calisto. *Boosting Circular Economy in Environmental Engineering - Application to water remediation systems*
10:15	**Oral Presentations | Session I** (B032) Moderated by Professor Alexandra Pinto, Professor Cidália Botelho and Doctor Vânia Calisto • João Carlos Sousa, Marta O. Barbosa, Ana R. Ribeiro, M. Fernando, R. Pereira and Adrián M.T. Silva. *Spatial and temporal distribution of contaminants of emerging concern in Ave River* • Nuno Moreira, Carlos Narciso-Da-Rocha, María Polo-López, Luisa Pastrana-Martínez, Joaquim Faria, Célia Manaia, Pilar Fernández-Ibañez, Olga Nunes and Adrián Silva. *Pilot-scale H2O2-assisted heterogeneous photocatalytic treatment of effluents from urban wastewater treatment plants* • Hugo Bacelo, Sílvia Santos and Cidália Botelho. *Tannin-based adsorbents: preparation and use for arsenic removal from water*
11:00	**Coffee Break**
11:30	**Oral Presentations | Session II** (B032) Moderated by Professor Fernando Pereira, Professor Filomena Barreiro and Professor Manuel Simões • A. R. Morgado, M. J. Lima, M. J. Sampaio, C. G. Silva, J. L. Faria and A. M. T. Silva. *Effective visible light phenol degradation using photocatalytically active carbon nitride nanosheets* • Sofia Mota, Filipa Paulo and Lúcia Santos. *Microencapsulation of Eugenol: a promising compound for incorporation in versatile Products* • Marta Pedrosa, Luisa Pastrana-Martinez, Manuel Pereira, Joaquim Faria, José Luis Figueiredo and Adrián Silva. *Catalytic ozonation of oxalic acid using doped graphene derivatives* • Diogo Santos, Manuel Fernando Pereira, Adrián Silva, Salomé Soares and José Figueiredo. *Catalytic Wet Oxidation of Phenol over Carbon Nanotubes in Continuous Operation* • Isabel Neto and Helena Soares. *An environmentally-friendly process to recover Cu and Al from a leaching solution of spent Printed Circuit Boards* • Seghir Dekkouche, Sergio Morales-Torres, Ana Rita Ribeiro, Joaquim Luís Faria, Ounissa Kebiche-Senhadji, Clàudià Fontas and Adrián Manuel Tavares Da Silva. *Microfiltration membranes for photocatalytic degradation of emerging contaminants*
13:00	**Lunch**
14:30	**Oral Presentations | Session III** (B032) Moderated by Professor Francisco Malcata, Professor Miguel Madeira and Doctor Vânia Calisto • Elson Gomes, Inês Mota and Alírio Rodrigues. *Fractionation of acids, ketones and aldehydes from lignin oxidation broth with SP700 resin* • João Pinto, Mohamed Belgacem, Alírio Rodrigues and Filomena Barreiro. *Oxypropylation of lignocellulosic agro-industrial residues – a comparative study* • Diogo Dias, Marta Miguel, Maria Bernardo, Nuno Lapa, Inês Matos, Isabel Fonseca and Filomena Pinto. *Removal of Cr(III) by using activated carbons produced from rice waste chars* • Stephanie Andrade, Joana Loureiro, Maria Pereira and Manuel Coelho. *Effects of Gallic acid on Membrane Biophysical Properties: Relevance for Its Biophysical Effects* • Maria João Ramalho, Joana Angélica Loureiro, Manuel A N Coelho and Maria Do Carmo Pereira. *Liposomes for temozolomide delivery* • R. Vinoth Kumar and G. Pugazhenthi. *Novel low cost ceramic and zeolite-ceramic composite membranes for liquid phase separation applications*
16:30	**Coffee Break**
17:00	**Plenary | Industry 4.0** (B032)
18:30	**Workshops**

June 9th, Friday

08:00	**Registration**
09:00	**Keynote** (B032) Doctor Susana Pereira. *The cycle innovation perspective and the engineering opportunity to support bioeconomy and circular economy development*
09:30	**Oral Presentations | Session IV** (B032) Moderated by Professor Arminda Alves, Professor José Teixeira and Doctor Susana Pereira • Ana Ramos, Rosa Aragão, Carlos Afonso Teixeira and Abel Rouboa. *MSW energetic valorisation: sustainability analysis of a Portuguese incineration plant* • Hélder F.V. Fontes, Luísa M. Pastrana-Martinez, Joaquim L. Faria, Adrian M.T. Silva and José L. Figueiredo. *Evaluation of the parameters affecting the photocatalytic reduction of CO2 over graphene-based composites* • Beatriz Bráz, Catarina Moreira, Vânia Oliveira and Alexandra Rodrigues Pinto. *Performance of a passive Direct Alcohol Fuel Cell* • Adriano Henrique, José A. C. Silva and Alírio E. Rodrigues. *Separation of Hexane Isomers Using ZIF-8*
10:30	**Coffee Break**
11:00	**Oral Presentations | Session V** (B032) Moderated by Professor Alexandra Pinto, Doctor Carmen Rangel and Professor Manuel Alves • Rami S. Arafah, António E. Ribeiro, AlÍrio E. Rodrigues and LuÍs S. Pais. *Optimizing the Separation of Nadolol Stereoisomers by SMB Chromatography using Chiralpak IA Chiral Stationary Phase* • Rubia Risso, Pedro Ferraz, Sara Meireles, Isabel Fonseca and Joaquim Vital. *Soybean oil methanolysis catalyzed by highly active CaO obtained from waste shells* • Isabel Patrícia Fernandes, Maria José Ferreira, Mário Rui Costa and Maria Filomena Barreiro. *New Footwear Materials based on Polyurethane and Polyureas* • João Valentim, Rúbia Risso, Gaelle Cardoso, Sofia Santos, Maria Helena Casimiro, Isabel Fonseca and Joaquim Vital. *Methanolysis of soybean oil in a catalytic membrane reactor. Study of the effect of catalyst loading and polymer crosslinking of CaO/PVA composite membranes* • Margarida Brito, Cláudio Fonte, Madalena Maria Dias, Ricardo Jorge Santos and José Carlos Lopes. *Mixing of Similar Fluids in Mesomixers* • Patrícia Cruz, Fernando Rocha and António Ferreira. *The axial dispersion performance of a novel oscillatory flow reactor – a design of experiments approach*
12:30	**Lunch**
14:00	**Poster Session**
14:30	**Pitch Session | PhDs in Companies** (Auditorium)
15:30	**Keynote** (Auditorium) Doctor Filipa Moraes. *Post-academic careers for PhD holders*
16:00	**Networking Session & Coffee Break**
16:30	**Symposium Awards & Closing Session** (Sala de Atos - DEQ)
17:00	**Round Table Session | PhDs in Companies** (Auditorium)
18:30	**Closing Reception**

Keynote Speakers

Keynote

Vânia Calisto

Post-doctoral researcher
Centre for Environmental and Marine Studies (CESAM), Aveiro University

Topic: Boosting Circular Economy in Environmental Engineering – application to water remediation systems

Vânia Calisto (born in 1985) got her degree in Biochemistry and Food Chemistry at the Chemistry Department of the University of Aveiro (UA). In 2011, she completed her PhD in Chemistry from UA working on the "Occurrence, persistence and fate of psychiatric pharmaceuticals in the environment". In 2012, she joined the Associate Laboratory CESAM as a post-doctoral research fellow. Since then, she has been doing research work in Environmental Engineering, mainly concerning the development of alternative adsorbents for the removal of pharmaceuticals from contaminated water, using industrial wastes as new resources. This work is focused on the application of circular economy approaches to solve environmental problems and is being developed under the scope of the RemPharm project (www.rempharm.com). Vânia Calisto is involved in the scientific supervision of several undergraduate, master and PhD students, published 35 papers in international peer review journals, presented more than 45 communications in national and international conferences and is involved in the participation/organization of science communication actions. The relevance of the developed work in the field of remediation of contaminated water resources by pharmaceuticals has resulted in the attribution of the Honor Medal for Women in Science by L'Oreal, FCT and UNESCO (2014 edition).

Susana Pereira

Researcher
BLC3 - Campus de Tecnologia e Inovação

Topic: The cycle innovation perspective and the engineering opportunity to support bioeconomy and circular economy development

Bachelor degree in Biochemistry and Food Chemistry (2008), MSc. in Materials derived from Renewable Resources (2009) and PhD in Chemical Engineering minor in Bioengineering (2013), all from the University of Aveiro. Having experience in the renewable resources valorisation and biorefineries R&D since 2009 at Aveiro Institute of Materials (CICECO). Currently is a researcher at BLC3 (since 2016) at the Energy and Territory Department, working on the integrated biorefinery project. Author of 7 papers in international peer-reviewed journals, 1 book chapter, 16 posters and oral communications in international and national conferences.

Oral Presentations

Spatial and temporal distribution of contaminants of emerging concern in Ave River

João C. Sousa *, **Marta O. Barbosa, Ana R. Ribeiro, M. Fernando R. Pereira, Adrián M.T. Silva**

Laboratory of Separation and Reaction Engineering - Laboratory of Catalysis and Materials (LSRE-LCM), Faculdade de Engenharia, Universidade do Porto, Rua Dr. Roberto Frias, 4200-465 Porto, Portugal
**jcgsousa@fe.up.pt*

Keywords: Ave River; Contaminants of emerging concern; Commission Decision 2015/495/EU; Solid-phase extraction; Ultra-high performance liquid chromatography-tandem mass spectrometry.

Ave River with an extension of ca. 90 km, is one of the most industrial impacted rivers of Portugal and it was already considered as a highly polluted river. Even after the construction of some WWTPs, the Ave River still shows high levels of pollution. The growing concern about emerging contaminants in the environment and their pseudo-persistence, even when present at trace levels demands the development of novel methodologies for the analysis of these compounds in aquatic matrices (Figure 1).

Figure 1 – Occurrence of contaminants of emerging concern. Localization of Ave river.

A monitoring study was carried out in 15 sampling points of Ave River over four sampling periods (2016 – 2017), in order to evaluate the occurrence and frequency of 11 contaminants of emerging concern (CECs) included in the first Watch List of European Commission Decision 2015/495 (Barbosa et al. 2016). Water samples were treated by solid phase extraction followed by multi-residue analysis on a triple quadrupole mass spectrometer instrument coupled to liquid chromatography (LC-MS/MS) to determine the CECs during the sampling campaigns The optimized mobile phase in a Kinetex™ 1.7 µm XB-C_{18} 100 Å column (100 x 2.1 mm) was methanol/water at gradient mode with a flow rate of 0.25 mL min^{-1}. The highest recoveries for most target analytes were achieved with Oasis® HLB cartridges, using ethanol as conditioning and eluting solvent and 500 mL of water acidified samples. The method was validated as recommended by the international guidelines. The range of method detection limits (MDL) was 0.01 – 2.67 ng L^{-1} and the method quantification limits (MQL) were between 0.03 and 8.08 ng L^{-1}. The identification of the compounds was performed according to European Commission Decision 2002/657, namely by analysing the retention time, two MS/MS transitions for each substance and their ion ratio.

From the 11 studied compounds, diclofenac, 2-ethylhexyl 4-methoxycinnamate, erythromycin, clarithromycin, azithromycin, imidacloprid, thiamethoxam and clothianidin were detected and quantified in Ave River samples. Much higher concentrations were detected in the dry season than those found in the wet season probably due to the low river flow.(Li et al. 2015)

Acknowledgments

This work was financially supported by Project POCI-01-0145-FEDER-006984 – Associate Laboratory LSRE-LCM funded by FEDER through COMPETE2020 - Programa Operacional Competitividade e Internacionalização (POCI) – and by national funds through FCT - Fundação para a Ciência e a Tecnologia. ARR and MOB acknowledge the research grants from FCT (Ref. SFRH/BPD/101703/2014 and Ref. SFRH/BD/115568/2016, respectively), and AMTS acknowledges the FCT Investigator 2013 Programme (IF/01501/2013), with financing from the European Social Fund and the Human Potential Operational Programme. JCGS acknowledge the research grant FEUP-LSRE-LCM-AFR2016 Laboratório Associado LSRE-LCM supported by Project POCI-01-0145-FEDER-006984.

References

Barbosa, M.O., N.F.F. Moreira, A.R. Ribeiro, F.M. Pereira, and A. M.T. Silva. 2016. "Occurrence and removal of organic micropollutants: an overview of the watch list of EU Decision 2015/495." *Water Research*. doi: 10.1016/j.watres.2016.02.047.

Li, W., L. Gao, Y. Shi, J. Liu, and Y. Cai. 2015. "Occurrence, distribution and risks of antibiotics in urban surface water in Beijing, China." *Environ Sci Process Impacts* no. 17 (9):1611-9. doi: 10.1039/c5em00216h.

Pilot-scale H_2O_2-assisted heterogeneous photocatalytic treatment of effluents from urban wastewater treatment plants

N. F. F. Moreira[1,4*], C. Narciso-da-Rocha[2], M. I. Polo-López[3], L. M. Pastrana-Martínez[1], J. L. Faria[1], C. M. Manaia[2], P. Fernández-Ibañez[5], O. C. Nunes[4] and A. M. T. Silva[1]

[1]Laboratory of Separation and Reaction Engineering – Laboratory of Catalysis and Materials (LSRE-LCM), Faculdade de Engenharia, Universidade do Porto, Rua Dr. Roberto Frias, Porto, 4200-465 Porto, Portugal
[2]Universidade Católica Portuguesa, CBQF - Centro de Biotecnologia e Química Fina – Laboratório Associado, Escola Superior de Biotecnologia, Rua Arquiteto Lobão Vital, Apartado 2511, 4202-401 Porto, Portugal
[3]Plataforma Solar de Almeria – CIEMAT, P.O. Box 22, 04200 Tabernas, Almeria, Spain
[4]Laboratory for Process Engineering, Environment, Biotechnology and Energy (LEPABE), Faculdade de Engenharia, Universidade do Porto, Rua Dr. Roberto Frias, Porto, 4200-465 Porto, Portugal
[5]Nanotechnology and Integrated BioEngineering Centre, School of Engineering, University of Ulster, Newtownabbey, Northern Ireland, BT37 0QB, United Kingdom
*nmoreira@fe.up.pt

Keywords: Solar oxidative treatments, urban wastewater, organic micropollutants, antibiotic resistant bacteria and genes, *Proteobacteria.*

The continuous disposal of organic pollutants, including antibiotics, and bacteria of human/animal origin into the environment significantly contributes to the proliferation of antibiotic resistant bacteria and related genes (ARB&ARG). Urban wastewater treatment plants (WWTPs) are considered one of the main hotspots of this type of contamination. To face this problem, new technologies able to remove simultaneously human pathogens and organic micropollutants are being developed, among them, tertiary treatments such as advanced oxidation processes (AOPs), including H_2O_2 assisted photocatalysis, UV/Vis-H_2O_2, heterogeneous photocatalysis, ozonation and photo-Fenton like processes (Barbosa et al. 2016).

In the present work, a set of solar-driven oxidation processes, namely, solar-H_2O_2 and heterogenous photocatalysis with and/or without the addition of H_2O_2, were investigated at pilot-scale for the treatment of urban wastewater samples collected after activated sludge biological treatment in an urban WWTP located in Southern Spain (Almeria). Degussa (Aeroxide) TiO_2 P25 and a graphene oxide-TiO_2 composite (GO-TiO_2) prepared as described elsewhere (Pastrana-Martínez et al. 2012) were chosen as photocatalysts. Pilot-scale compound parabolic collector (CPC) photo-reactors (with a total illuminated volume of 14 L) were used for all the solar-driven processes (Rodríguez-Chueca et al. 2014). Three model contaminants widely and frequently found in water streams, were selected - carbamazepine (CBZ), sulfamethoxazole (SMX) and diclofenac (DFC). In each experiment, wastewater samples were spiked with 100 µg L^{-1} of each model micropollutant and their concentrations were measured by high performance liquid chromatography (HPLC-DAD). The membrane filtration method was used to quantify cultivable bacteria, specifically, fecal coliforms and enterococci and the respective subpopulations resistant to the antibiotics tetracycline and ciprofloxacin. Furthermore, the abundance of the genes 16S rRNA, *intI1*, *bla*$_{TEM}$, *qnrS*, *sul1*, *bla*$_{CTX\text{-}M}$ and *vanA* was assessed based on quantitative polymerase chain reaction assays (qPCR). The bacterial community was assessed using Illumina sequencing before and after 3-days storage at room temperature.

Regarding the degradation of organic micropollutants, heterogeneous photocatalysis was an efficient process regardless of the catalyst used (P25 or GO-TiO_2), leading to a complete degradation of SMX and DFC. A complete removal of CBZ was only possible when H_2O_2 was added to P25 photocatalysis. Simultaneously, ARB were removed to values under the detection limit (1 CFU 100 mL^{-1}). However, after 3-days storage, ARB regrowth occurred for P25 photocatalysis, suggesting that at least some bacterial populations were only transiently inactivated. Regarding the removal of genes, higher removal rates for 16S rRNA, *intI1*, *qnrS*, *bla*$_{TEM}$, *bla*$_{CTX\text{-}M}$ and *sul1* were found in the experiments where H_2O_2 was used. Moreover, reactivation occurred for all the genes after 3-days storage when P25 was used without H_2O_2. The gene *vanA* was under the limit of quantification before treatment. Finally, irrespective of the solar treatment applied, higher relative abundance of *Proteobacteria* was found after 3-days storage, in agreement with previous studies (Becerra-Castro et al. 2016).

Acknowledgements

This work was supported by Project nº P1404290052 under the EU SFERA Program (FP7-SFERA grant no 228296), and by NORTE 2020 (AIProcMat@N2020 NORTE-01-0145-FEDER-000006 and LEPABE-2-ECO-INNOVATION NORTE-01-0145-FEDER-000005), under the Portugal 2020 Partnership Agreement, through ERDF, Projects POCI-01-0145-FEDER-006984 (UID/EQU/50020/2013) and POCI-01-0145-FEDER-006939 (UID/EQU/00511/2013), and COMPETE2020 – and by national funds through FCT, UID/Multi/50016/2013-CBQF and Water JPI/0001/2013 STARE. NFFM, LMPM and AMTS acknowledge PD/BD/114318/2016, IF/01248/2014 and IF/01501/2013, respectively.

References

Barbosa, Marta O., Nuno F. F. Moreira, Ana R. Ribeiro, Manuel F. R. Pereira, and Adrián M. T. Silva. 2016. "Occurrence and removal of organic micropollutants: An overview of the watch list of EU Decision 2015/495." *Water Research* 94:257-279. doi: http://dx.doi.org/10.1016/j.watres.2016.02.047.

Becerra-Castro, Cristina, Gonçalo Macedo, Adrian M. T. Silva, Célia M. Manaia, and Olga C. Nunes. 2016. "Proteobacteria become predominant during regrowth after water disinfection." *Science of The Total Environment* 573:313-323. doi: http://dx.doi.org/10.1016/j.scitotenv.2016.08.054.

Pastrana-Martínez, Luisa M., Sergio Morales-Torres, Vlassis Likodimos, José L. Figueiredo, Joaquim L. Faria, Polycarpos Falaras, and Adrián M. T. Silva. 2012. "Advanced nanostructured photocatalysts based on reduced graphene oxide–TiO_2 composites for degradation of diphenhydramine pharmaceutical and methyl orange dye." *Applied Catalysis B: Environmental* 123–124:241-256. doi: http://dx.doi.org/10.1016/j.apcatb.2012.04.045.

Rodríguez-Chueca, J., M. I. Polo-López, R. Mosteo, M. P. Ormad, and P. Fernández-Ibáñez. 2014. "Disinfection of real and simulated urban wastewater effluents using a mild solar photo-Fenton." *Applied Catalysis B: Environmental* 150–151:619-629. doi: http://dx.doi.org/10.1016/j.apcatb.2013.12.027.

Tannin-based adsorbents: preparation and use for arsenic removal from water

H.A.M. Bacelo, C.M.S. Botelho, S.C.R. Santos*
Laboratory of Separation and Reaction Engineering - Laboratory of Catalysis and Materials (LSRE-LCM), Chemical Engineering Department, Faculdade de Engenharia da Universidade do Porto
*scrs@fe.up.pt

Keywords: tannins, arsenic, biopolymer, adsorption, water and wastewater treatment.

Tannins are ubiquitous natural polymers, polyphenolic secondary metabolites of higher plants, mainly present in soft tissues. Maritime pine (*Pinus pinaster*) is one of the most common trees in Portugal. The extraction of tannins from these vegetable residues and the subsequent production of tannin-based adsorbents (TBA) may constitute an important contribute for their reuse and valorisation. The presence of phenolic groups (anionic nature) makes them potential adsorbents for cationic species. However, by chemical modifications, adsorption of anionic species, which arsenic is an example of, can also be possible. Iron-based adsorbents have been identified as promising adsorbents for arsenic. Based on that, this work aimed to assess the arsenic removal from aqueous solutions using a lab-produced TBA, loaded with iron.

Tannin extraction from *Pinus pinaster* bark was carried out in hot alkaline solution (100 g bark, 600 mL H_2O, 5 g NaOH, 85 °C, 90 min) (adapted from Sanchez-Martin (2011)). The precipitant recovered by evaporation was considered the tannin extract (TE). The average extractable content was 59 mg per g of bark. Considering that tannins are water-soluble compounds, an immobilization treatment is required before their use as adsorbents. The tannin gelification procedure was executed at 80 °C, in alkaline medium and using formaldehyde as cross-linking agent (procedure adapted from Xie et al. (2013)). The resultant product was considered the tannin gel (TG). In order to prepare iron-loaded TG, an oxidation step was considered before iron-loading. The procedure of oxidation was optimized for the pine tannins. One gram of TG was stirred with 100 mL of 1 mol L^{-1} nitric acid solution at 60 °C for 30, 50 or 120 min, or 2 mol L^{-1}, at 40 or 60 °C for 90 min. One gram of oxidized TG was then added to 50 mL of a saturated solution of $FeCl_3$ at pH 2 and the mixture was kept under stirring at room temperature for 48 h (procedure adapted from Ogata et al. (2011)). The resultant product was considered the iron-loaded TG. Non-oxidized TG was also subjected to same iron treatment. To optimize the oxidation conditions, a correlation between oxidation parameters and the iron content of the adsorbents was evaluated (Table 1). It was concluded that the oxidation step prior to the treatment with iron is of great importance. The optimal oxidation conditions for posterior iron treatment was found to be 50 min in 1 mol L^{-1} HNO_3 at 60 °C, where a content of 24.4 ± 0.7 mg of iron per g of adsorbent was achieved.

Adsorption assays were executed by stirring TG-Ox1-50-Fe (dosage: 5 g L^{-1}) with As(III) or As(V) solutions (10 mg L^{-1}) at different pH (2.5-4.5), at 20 °C for 24 h. The maximum adsorbed amounts were achieved at pH 3.5 for As(V) (1.8 mg g^{-1}) and at pH 4.5 for As(III) (1.7 mg g^{-1}). Considering that As(III) and As(V) are present in solution as neutral or anionic species, and considering the

pH_{PZC} of the adsorbent (2.93±0.02), adsorption must be happening mostly through chemical interaction with iron and not through electrostatic attraction.

Table 1. *Iron content of several TBAs (value ± deviation between average and duplicate measurements).*

Adsorbent	Oxidation conditions	Iron-treatment	Iron content (mg g^{-1})
TG	-	-	0.20 ± 0.01
TG-Fe	-	+	2.1 ± 0.4
TG-Ox2-40-Fe	2 M, 90 min, 40 °C	+	5.9 ± 0.1
TG-Ox2-60-Fe	2 M, 90 min, 60 °C	+	13 ± 1
TG-Ox1-30-Fe	1 M, 30 min, 60 °C	+	10 ± 1
TG-Ox1-50-Fe	1 M, 50 min, 60 °C	+	24.4 ± 0.7
TG-Ox1-120-Fe	1 M, 120 min, 60 °C	+	7.8 ± 0.2

Adsorption kinetics was studied using arsenic (III or V) solutions (500 mL, 10 mg L^{-1}) and 5.0 g of TG-Ox1-50-Fe, at pH 3.5 and 20 °C. Samples were retrieved at different contact times. Arsenic adsorption was found to be rapid with equilibrium achieved after 2 h. Equilibrium isotherms for As(III) and As(V) adsorption by TG-Ox1-50-Fe were obtained at pH 3.5 and 20 °C (adsorbent dosage: 10 g L^{-1} g; initial As concentrations: 1-40 mg L^{-1}). In the experimental conditions, removal percentages ranged from 40 to 83 % and from 49 to 90 % for As(III) and As(V), respectively. According to the Langmuir model fitting (not illustrated), the maximum adsorption capacities of the adsorbent were 1.92 ± 0.09 and 2.3 ± 0.2 mg g^{-1}, respectively for As(III) and As(V). These values fit somewhat reasonably when compared with other values reported in literature for unconventional adsorbents. The adsorbent also seems to have affinity towards both oxidation states of arsenic, making it advantageous for real scenario applications, since some arsenic-contaminated waters, like those leached from mines, contain both trivalent and pentavalent species. Future work needs to be done to assess adsorption mechanism and to try to minimize iron leaching to the aqueous solution.

References

Ogata, T., S. Morisada, Y. Oinuma, Y. Seida, and Y. Nakano. 2011. "Preparation of adsorbent for phosphate recovery from aqueous solutions based on condensed tannin gel." *Journal of Hazardous Materials* 192 (2):698-703.

Sanchez-Martin, J., Beltran-Heredia, J., Gibello-Perez, P. 2011. "Adsorbent biopolymers from tannin extracts for water treatment." *Chemical Engineering Journal* 168 (3):1241-1247.

Xie, F., Z. J. Fan, Q. L. Zhang, and Z. R. Luo. 2013. "Selective Adsorption of Au3+ from Aqueous Solutions Using Persimmon Powder-Formaldehyde Resin." *Journal of Applied Polymer Science* 130 (6):3937-3946.

Acknowledgments

This work is a result of project "AIProcMat@N2020 - Advanced Industrial Processes and Materials for a Sustainable Northern Region of Portugal 2020", with the reference NORTE-01-0145-FEDER-000006, supported by Norte Portugal Regional Operational Programme (NORTE 2020), under the Portugal 2020 Partnership Agreement, through the European Regional Development Fund (ERDF) and of Project POCI-01-0145-FEDER-006984 – Associate Laboratory LSRE-LCM funded by ERDF through COMPETE2020 - Programa Operacional Competitividade e Internacionalização (POCI) – and by national funds through FCT - Fundação para a Ciência e a Tecnologia.

Effective visible light phenol degradation using photocatalytically active carbon nitride nanosheets

A.R. Morgado*, M.J. Lima, M.J. Sampaio, C.G. Silva, J.L. Faria
and A.M.T. Silva

Laboratory of Separation and Reaction Engineering – Laboratory of Catalysis and Materials (LSRE-LCM),
Departamento de Engenharia Química, Faculdade de Engenharia, Universidade do Porto, Rua Dr. Roberto Frias s/n,
4200-465 Porto, Portugal
* eq12019@fe.up.pt

Keywords: carbon nitride, nanosheets, photocatalysis, phenol

Photocatalysis is known to be an efficient technique used for the degradation of organic pollutants in water and wastewater. Phenol and its derivatives can be found in a wide range of industrial effluents and are known as toxic and refractory organic compounds, therefore hard to be reduced using conventional biological treatment processes. Being a relatively simple organic molecule with a very-well established photochemical behaviour, phenol is often used as model compound to assess catalysts' efficiency for photocatalytic wastewater treatment (Sampaio et al. 2017).

Graphitic carbon nitride, g-C_3N_4, is a polymeric layered material composed by C, N and some minor content of H, all earth abundant elements (Masih et al. 2017). Its unique electronic and optical properties make this a suitable material to be used as photocatalyst, in particular the possibility of being photo-excited with visible light (Wen et al. 2017). Moreover, the polymeric nature of g-C_3N_4 allows its easy modification seeking for enhanced photoefficiency. In the present work, bulk g-C_3N_4 was synthesized by thermal decomposition of dicyandiamide. The base photocatalytic g-C_3N_4 nanosheets were obtained by thermal exfoliation of the bulk material at 500 °C (T500). Figure 1 shows TEM images of bulk (a) and thermal exfoliated g-C_3N_4 (b).

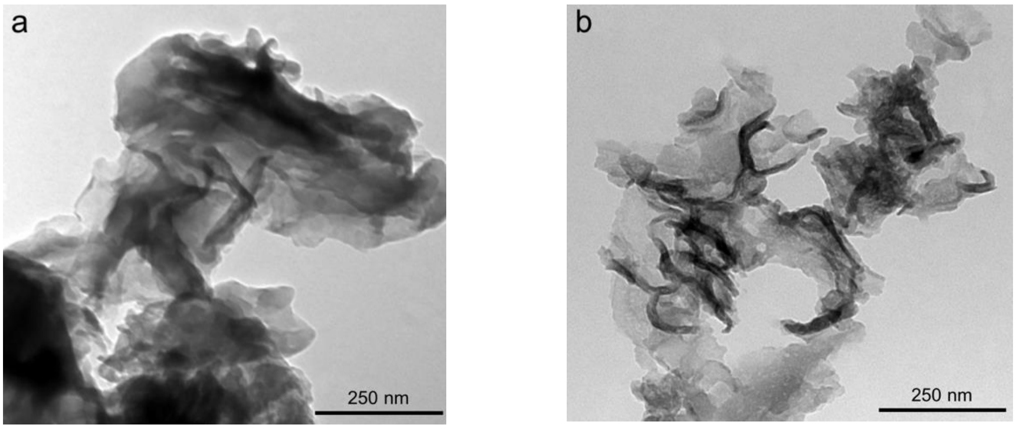

Figure 1. *TEM images of bulk g-C_3N_4 (a) and T500 (b).*

In this preliminary study, the initial substrate concentration (Fig. 2a) and photocatalyst load (Fig. 2b) were varied in order to optimize the reaction conditions for the photocatalytic degradation of phenol in aqueous media under Vis-LED irradiation (417 nm). Experiments using bulk g-C_3N_4 and commercial TiO_2-P25 (the benchmark material in photocatalytic advanced oxidation processes for water treatment) were performed for comparison purposes (Fig. 2b).

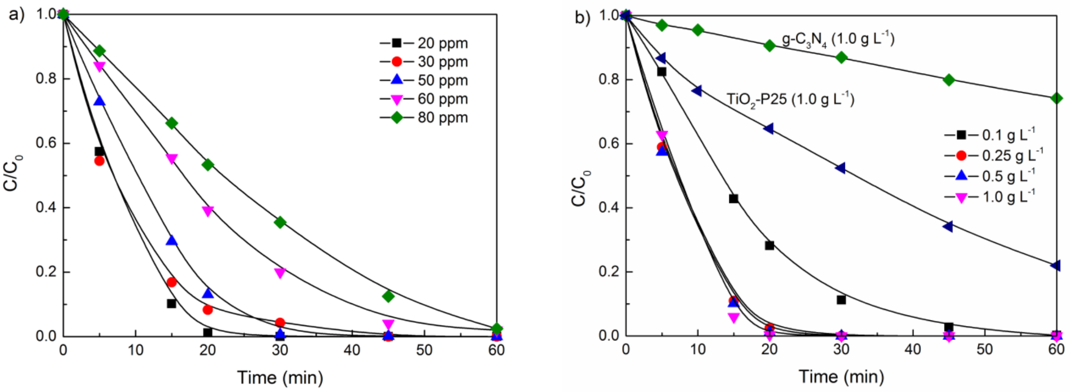

Figure 2. *Effect of (a) initial phenol concentration using 0.5 g L^{-1} of T500 and (b) catalyst load for 20 ppm of phenol.*

As the initial concentration increased, phenol removal was progressively slower, which may be attributed to a lower availability of active sites in the catalyst for adsorption and reaction (Fig. 2a). It has to be noticed that even for highly concentrated solutions, phenol was totally removed at the end of merely 60 min of irradiation. Moreover, T500 revealed to be much more active than bulk g-C_3N_4 and TiO_2-P25 (Fig. 2b), which demonstrates the enormous potential of this material for treating phenolic effluents using highly-efficient and low cost irradiation sources (Vis-LEDs). Further studies are being carried out to disclose the mechanism of phenol degradation under the tested conditions.

Acknowledgments

This work was financially supported by Project POCI-01-0145-FEDER-006984 – Associate Laboratory LSRE-LCM funded by FEDER through COMPETE2020 - Programa Operacional Competitividade e Internacionalização (POCI) – and by national funds through FCT - Fundação para a Ciência e a Tecnologia. M.J.L. acknowledges FCT for the research grant PD/BD/52623/2014, while A.M.T.S. and C.G.S. acknowledge the FCT Investigator Programme (IF/01501/2013 and IF/00514/2014, respectively) with financing from the European Social Fund and the Human Potential Operational Programme.

References

Masih, Dilshad, Yuanyu Ma, and Sohrab Rohani. 2017. "Graphitic C_3N_4 based noble-metal-free photocatalyst systems: A review." *Applied Catalysis B: Environmental*. doi: 10.1016/j.apcatb.2017.01.061.

Sampaio, Maria J., Maria J. Lima, Daniel L. Baptista, Adrián M. T. Silva, Cláudia G. Silva, and Joaquim L. Faria. 2017. "Ag-loaded ZnO materials for photocatalytic water treatment." *Chemical Engineering Journal* 318:95-102. doi: 10.1016/j.cej.2016.05.105.

Wen, Jiuqing, Jun Xie, Xiaobo Chen, and Xin Li. 2017. "A review on g-C_3N_4-based photocatalysts." *Applied Surface Science* 391:72-123. doi: 10.1016/j.apsusc.2016.07.030.

Microencapsulation of Eugenol: a promising compound for incorporation in versatile products

Sofia Mota[1], Filipa Paulo[2], Lúcia Santos[2]*

[1]Department of Chemical Engineering, Faculty of Engineering, University of Porto
[2]LEPABE – Laboratory for Process Engineering, Environment, Biotechnology and Energy, Faculty of Engineering, University of Porto
***Corresponding author:** Tel.: +351 22 5081682, Fax: +351 22 508 1440, e-mail address: lsantos@fe.up.pt

Keywords: Microencapsulation, controlled release, eugenol, double emulsion, solvent evaporation.

The increasing consumer's interest in natural and biological products (Aguiar et al., 2016; Carvalho et al., 2016) created the demand for new valuable products as well as the reformulation of others with new or improved functionalities (Carvalho et al., 2016). Added-value products for cosmetic, personal care and food sectors need to be differentiate, which can be accomplished using innovative technologies such as microencapsulation (Casanova and Santos, 2016). Therefore, food and cosmetic industries apply microencapsulation processes mainly for the protection of the core material from environment degradation (e.g. heat, moisture, air and light) and the study of the controlled release of compounds over time (Desai and Park, 2005). Several active ingredients for cosmetic applications have been studied. Some examples are antioxidants, essential oils, fragrances, sun filters, anti-aging molecules, moisturisers, and tanning, whitening or lightening agents. Depending the application intended, the active ingredient may be controlled released on the surface of the skin or in specific layers in the skin (Casanova and Santos, 2016). Moreover, active ingredients intended for food applications can be vitamins, enzymes, flavours, minerals, seasonings, or preservatives (Desai and Jin Park, 2005), being mostly sustained released in human body. Essential oils are volatile and usually present low stability, since they are easily oxidized or decomposed in the presence of oxygen, light, enzymatic degradation, or heat, during processing, storage and/or utilization. Therefore, these compounds can be microencapsulated in order to keep their physicochemical properties. Eugenol, an essential oil, is a clear to pale yellow oil mainly extracted from clove, basil, nutmeg, cinnamon and bay leafs. This compound is soluble in water as well as in organic solvents and presents a characteristic pleasant, floral and spicy odour. It has been widely studied and used in cosmetic and food industries. In fact, eugenol is used as flavouring, antimicrobial and fragrance agent. Chemically, it is defined as a phenolic compound which present antibacterial, antifungal and antioxidant properties (Goñi et al., 2016) which also makes this compound attractive to food and cosmetics sectors due to its preservative properties. There are numerous possibilities to microencapsulate compounds in order to obtain products with added-value. Regard microencapsulation approaches, several encapsulation methods are described (Dubey et al., 2009; Ghosh, 2006; Gouin, 2004), being the double emulsion solvent evaporation one of the most applied techniques. The water-oil-water, double emulsion solvent evaporation technique was never reported for eugenol microencapsulation, which brings originality into this work. The main advantage of using the double emulsion solvent evaporation is due to the not requirement of high temperatures during the process, considering that this compound is thermosensitive.

Ethyl cellulose (EC) is a biocompatible polymer and one of the most studied encapsulating material for controlled release purposes. Two common organic solvents used in the preparation of microparticles are dichloromethane (DCM) and methanol (MeOH). The use of DCM is more prevalent due to the fact it is able to dissolve the most common used polymers. Nevertheless, DCM is toxic (suspected carcinogen and mutagen) and therefore a removal step of this solvent is required during microencapsulation process. Usually, co-solvents may be added to the organic phase. Methanol is widely reported as co-solvent for microencapsulation purposes. Additionally, is reported that this mixture (DCM/MeOH) favors the polymer precipitation and improve the diffusion of the active ingredient from the internal aqueous phase to the external aqueous phase, allowing a better encapsulation efficiency.

The purpose of this study is to prepare and characterize eugenol-loaded microparticles by double emulsion solvent evaporation technique, using EC as encapsulating material and PVA as surfactant, as well as to study the controlled release of eugenol from microparticles, intended for industrial applications. Moreover, specific aims include the validation of the analytical method for eugenol quantification (UV-Vis spectrophotometry), including the analysis of linearity, sensitivity, detection and quantification limits, as well as repeatability and intermediate precision. Particle size distribution, encapsulation efficiency, product yield and water content were determined for microparticles characterization. Additionally, controlled release studies were performed. The analytical methods (quantification of eugenol in ultrapure water, acid and basic environments) were validated. The preliminary obtained results of this study were 79%, 80% and 67% related to encapsulation efficiency of eugenol, product yield and water content in microparticles, respectively. Regard the particle size distribution, the mean diameter of the microparticles obtained was 153 ± 4 **μ**m (R.S.D. of 2.7%) and the SPAN obtained was 4.4 ± 0.2 (R.S.D. of 5.5%). The controlled release studies were performed in neutral and basic mediums (respectively, pH 5.7 and pH 9.0) obtaining a eugenol release of 10.1% and 7.4% after 24h, respectively.

References

Aguiar, J., Estevinho, B. N., & Santos, L. (2016). Microencapsulation of natural antioxidants for food application: The specific case of coffee antioxidants - A review. *Trends in Food Science and Technology*, *58*, 21–39.

Carvalho, I. T., Estevinho, B. N., & Santos, L. (2016). Application of microencapsulated essential oils in cosmetic and personal healthcare products - A review. *International Journal of Cosmetic Science*, *38*(2), 109–119.

Casanova, F., & Santos, L. (2015). Encapsulation of cosmetic active ingredients for topical application – a review. *Journal of Microencapsulation*, 1–17.

Desai, K. G. H., & Jin Park, H. (2005). *Recent Developments in Microencapsulation of Food Ingredients*. *Drying Technology*, 23 (7).

Dubey, R., Shami, T. C., & Bhasker Rao, K. U. (2009). Microencapsulation technology and applications. *Defence Science Journal*, *59*(1).

Ghosh, S. K. (2006). Functional coatings and microencapsulation: a general Perspective. In Functional coatings (pp.1-28). Weinheim: WILEY-VCH Verlag GmbH and CO KGaA

Goñi, M. L., Gañán, N. A., Strumia, M. C., & Martini, R. E. (2016). Eugenol-loaded LLDPE films with antioxidant activity by supercritical carbon dioxide impregnation. *Journal of Supercritical Fluids*, *111*, 28–35.

Gouin, S. (2004). Microencapsulation: Industrial appraisal of existing technologies and trends. *Trends in Food Science and Technology*, *15*(7–8), 330–347.

Acknowledgements

This work was the result of the project: POCI-01-0145-FEDER-006939 (Laboratory for Process Engineering, Environment, Biotechnology and Energy – UID/EQU/00511/2013) funded by the European Regional Development Fund (ERDF), through COMPETE2020 - Programa Operacional Competitividade e Internacionalização (POCI) and by national funds, through FCT - Fundação para a Ciência e a Tecnologia; NORTE-01-0145-FEDER-000005 – LEPABE-2-ECO-INNOVATION, supported by North Portugal Regional Operational Programme (NORTE 2020), under the Portugal 2020 Partnership Agreement, through the European Regional Development Fund (ERDF);

Catalytic ozonation of oxalic acid using doped graphene derivatives

M. Pedrosa*, L.M. Pastrana-Martinez, M.F.R. Pereira, J.L. Faria,
J.L. Figueiredo, A.M.T. Silva
Laboratory of Separation and Reaction Engineering - Laboratory of Catalysis and Materials (LSRE-LCM), Faculdade de Engenharia, Universidade do Porto, Rua Dr. Roberto Frias, 4200-465 Porto, Portugal
*pedrosa.marta@fe.up.pt

Keywords: doped graphene-based materials, graphene oxide-TiO_2 composites, ozonation, water treatment.

Catalytic ozonation appears as a possible technology for future water/wastewater treatment and reuse. Carbon materials have been employed as catalysts on their own and/or catalyst supports in this and several other processes. The introduction of nitrogen (N-) and sulphur (S-) heteroatoms affects the catalytic activity of these carbon materials (Figueiredo and Pereira 2010, Rocha *et al*. 2015). In this work, the catalytic activity of N- and S- doped graphene-based materials was investigated for the degradation of oxalic acid by catalytic ozonation. Moreover, a protective layer of titanium dioxide (TiO_2) nanoparticles was added on these graphene derivatives (doped and undoped) as an attempt to shield the carbon materials from the erosive attack of ozone (Yang *et al*. 2014). A schematic illustration of the catalytic ozonation of oxalic acid with GO derivatives and the GO derivatives-TiO_2 (GOT) composites is represented in Figure 1.

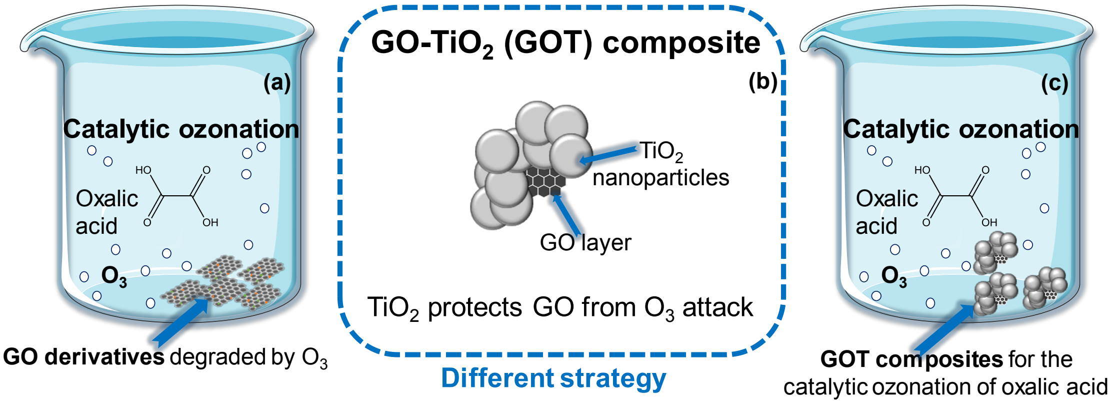

Figure 1. Illustration of the catalytic ozonation of oxalic acid with (a) GO derivatives and (c) GOT composites, and schematic representation (b) of the GOT composites.

Graphene oxide (GO) was prepared by the oxidation of synthetic graphite, employing the Brodie and modified Hummers methodologies followed by mechanical exfoliation (ultrasonication). N- and S- doped reduced GO (rGO) materials were produced by thermal annealing using as precursors ammonia gas and benzyl disulphide, respectively. GOT composites were prepared by liquid phase deposition (LPD) (Pastrana-Martinez et al. 2012) with ammonium hexaflurorotitanate (IV), boric acid and GO aqueous dispersion. The synthesized materials were characterized by XPS, SEM, nitrogen adsorption at 77 K, elemental analysis and TGA. The metal-free carbon materials exhibited a good catalytic activity in the ozonation of oxalic acid. However, it was observed a significant degradation of the carbon materials by ozone (Yang *et al*. 2014). To prevent the GO degradation, GOT composites were synthetized and tested in the catalytic ozonation of oxalic acid. The results showed that the GOT materials presented a higher stability under the strongly erosive ozonation conditions, since the TiO_2 nanoparticles protected the GO nanoplatelets. The composite rGOT-H-N presented the highest oxalic acid removal (87%) and TOC mineralization (85%). Thus, nitrogen functionalities applied in rGOT composites prepared by the Hummers method improved the removal of oxalic acid using catalytic ozonation, comparatively to the composites obtained from the Brodie method and the undoped ones.

Acknowledgments: This work is a result of project “AIProcMat@N2020 - Advanced Industrial Processes and Materials for a Sustainable Northern Region of Portugal 2020”, with the reference NORTE-01-0145-FEDER-000006, supported by Norte Portugal Regional Operational Programme (NORTE 2020), under the Portugal 2020 Partnership Agreement, through the European Regional Development Fund (ERDF) and of Project POCI-01-0145-FEDER-006984 – Associate Laboratory LSRE-LCM funded by ERDF through COMPETE2020 - Programa Operacional Competitividade e Internacionalização (POCI) – and by national funds through FCT - Fundação para a Ciência e a Tecnologia. MP acknowledges the research grant from FCT (Ref. SFRH/BD/102086/2014). AMTS and LMPM acknowledge the FCT Investigator Programme (IF/01501/2013 and IF/01248/2014, respectively), with financing from the European Social Fund and the Human Potential Operational Programme.

References

Figueiredo, J. L., and M. F. R. Pereira. 2010. "The role of surface chemistry in catalysis with carbons." Catalysis Today 150 (1-2): 2-7.

Pastrana-Martínez, L. M., S. Morales-Torres, V. Likodimos, J. L. Figueiredo, J. L. Faria, P. Falaras, and A. M. T. Silva. 2012. "Advanced nanostructured photocatalysts based on reduced graphene oxide–TiO_2 composites for degradation of diphenhydramine pharmaceutical and methyl orange dye." Applied Catalysis B: Environmental 123–124: 241-256.

Rocha, R. P., A. G. Goncalves, L. M. Pastrana-Martínez, B. C. Bordoni, O. S. G. P. Soares, J. J. M. Órfão, J. L. Faria, J. L. Figueiredo, A. M. T. Silva, and M. F. R. Pereira. 2015. "Nitrogen-doped graphene-based materials for advanced oxidation processes." Catalysis Today 249: 192-198.

Yang, F., M. Zhao, Z. Wang, H. Ji, B. Zheng, D. Xiao, L. Wu, and Y. Guo. 2014. "The role of ozone in the ozonation process of graphene oxide: oxidation or decomposition?" RSC Advances 4 (102): 58325-58328.

Catalytic Wet Oxidation of Phenol over Carbon Nanotubes in Continuous Operation

D.F.M. Santos*, O.S.G.P. Soares, A.M.T. Silva, J.L. Figueiredo, M.F.R. Pereira

Laboratory of Separation and Reaction Engineering – Laboratory of Catalysis and Materials (LSRE-LCM), Chemical Engineering Department., Faculty of Engineering University of Porto, Porto, Portugal;
*diogosantos@fe.up.pt

Keywords: Catalytic Wet Oxidation, Phenol, Carbon nanotubes, Continuous operation.

The industrial growth has brought an increase in the production of wastewaters, which need to be treated before being released into the aquatic environment. Some of these wastewaters contain highly recalcitrant and bio-toxic organic compounds, which renders infeasible the traditional treatment options. Wet oxidation (WO) is a process that can be used to remove these organic compounds from wastewaters. This process implements very high temperature and pressure in order to oxidize (with dissolved oxygen) the organic compounds into H_2O and CO_2, but some other by-products can also be formed (Wang, 2014).

In this process, noble metal based catalysts and metal oxide catalysts are the most commonly used to reduce the operating temperature and pressure (process called catalytic wet oxidation – CWO). However, the cost of the noble metals and the typical deactivation observed due to the formation of carbonaceous deposits and leaching of the active phase are limitations to the implementation of this technology. Carbon materials are interesting catalysts for this application since they are very stable at the standard reaction conditions, cheap, generally present high surface areas and their chemical and textural properties can be easily optimized, improving their catalytic activity. In particular, carbon nanotubes (CNTs) have attracted attention due to their non-microporous nature, which minimizes mass transfer limitations (Ovejero, 2006).

In this work, multi-walled carbon nanotubes (MWCNTs) were treated by ball milling, with and without a nitrogen precursor (melamine), to introduce nitrogen functionalities. CWO experiments for the degradation of phenol were performed in both batch and continuous mode. The influence of the reaction temperature, the dissolved oxygen concentration and the initial phenol concentration was evaluated in both operation modes for the most active catalyst. Deactivation and regeneration of the N-doped catalyst were also investigated. An experiment in continuous operation under intensified conditions, i.e. using a higher initial phenol concentration, was also performed to assess the efficiency of the catalyst under more realistic conditions.

Catalyst screening experiments were performed in batch mode at 160 °C, 6 bar of oxygen partial pressure and an initial phenol concentration of 75 mg L^{-1}. After 2 h of reaction, the original nanotubes (CNT-O) achieved 40% of phenol removal, while the N-doped nanotubes (CNT-BM-M) achieved a phenol removal of 98 %. The different reaction parameters were then studied over the CNT-BM-M catalyst. Temperature was found to be the most influential parameter, an optimal temperature of 160 °C being determined. Higher oxygen partial pressures slightly increased the phenol removal, while higher initial phenol concentrations improved the efficiency of the process, especially in terms of the total organic carbon (TOC) removal. Deactivation of the N-doped catalyst was clearly observable in the experiments performed in continuous mode. The deactivation was ascribed to two phenomena (Santos, 2016): (i) the decrease of pyridine groups during the reaction; (ii) the formation of carbonaceous deposits on the surface of the catalyst. Several regeneration procedure were attempted. A significant regeneration was achieved by thermal treatment at 600 °C under nitrogen atmosphere. An experiment under intensified conditions was also performed. In this experiment, an initial phenol concentration of 500 mg L^{-1} was used. The mass of catalyst was also increased in order to maintain the ratio "mass of catalyst/mass flow rate of phenol" constant. A phenol conversion of 80% and a TOC removal of 50% were achieved at near steady state over the N-doped catalyst, while the original catalyst only achieved 64% and 38% removals, respectively (Figure 1).

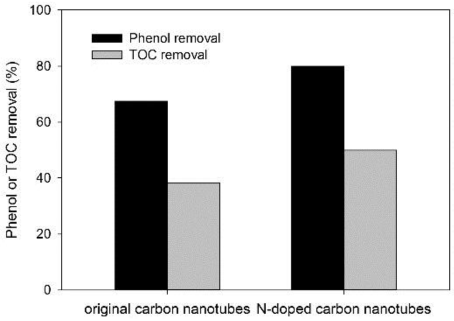

Figure 1. Phenol and TOC removal at near steady state the intensified reaction.

Acknowledgments

This work is a result of project "AIProcMat@N2020 - Advanced Industrial Processes and Materials for a Sustainable Northern Region of Portugal 2020", with the reference NORTE-01-0145-FEDER-000006, supported by Norte Portugal Regional Operational Programme (NORTE 2020), under the Portugal 2020 Partnership Agreement, through the European Regional Development Fund (ERDF) and of Project POCI-01-0145-FEDER-006984 – Associate Laboratory LSRE-LCM funded by ERDF through COMPETE2020 - Programa Operacional Competitividade e Internacionalização (POCI) – and by national funds through FCT - Fundação para a Ciência e a Tecnologia. DS and AMTS acknowledge FCT (PD/BD/105983/2014 and IF/01501/2013, respectively). The authors also acknowledge Dr. Carlos M. Sá (CEMUP) for assistance with XPS analyses.

References

Wang, Jianbing, Wantao Fu, Xuwen He, Shaoxia Yang, and Wanpeng Zhu. 2014. "Catalytic Wet Air Oxidation of Phenol with Functionalized Carbon Materials as Catalysts: Reaction Mechanism and Pathway." Journal of Environmental Sciences 26, no. 8: 1741-49.

Ovejero, G., J. L. Sotelo, M. D. Romero, A. Rodríguez, M. A. Ocaña, G. Rodríguez, and J. García. 2006. "Multiwalled Carbon Nanotubes for Liquid-Phase Oxidation. Functionalization, Characterization, and Catalytic Activity." Industrial & Engineering Chemistry Research 45, no. 7: 2206-12.

Diogo F.M. Santos, Olívia S.G.P. Soares, Adrián M.T. Silva, José L. Figueiredo, Manuel F.R. Pereira. 2016." Catalytic wet oxidation of organic compounds over N-doped carbon nanotubes in batch and continuous operation", Applied Catallysis B: Environmental 199 361-371.

An environmentally-friendly process to recover Cu and Al from a leaching solution of spent Printed Circuit Boards

I.F.F Neto and H.M.V.M. Soares*
REQUIMTE/LAQV, Chemical Engineering Dpt., Faculty of Engineering University of Porto, Porto, Portugal
*hsoares@fe.up.pt

Keywords: Printed circuit boards, bispicolylamine resin, Al recovery, Cu purification

Recycling of metals from Printed Circuit Boards (PCBs) has many environmental benefits: energy savings; reduction of metals obtained from traditional extractive metallurgical processes and reduced CO_2 emissions. The large percentage of Cu present in PCBs residues, usually about ten times more than the Cu amount present in rich-content minerals, makes these residues an attractive secondary source of Cu. Recovery of metals from PCBs is usually performed by pyrometallurgical and/or hydrometallurgical methods, combined with mechanical pretreatments. Hydrometallurgical processes have high metal recoveries with a flexible mode of operation and suitability for small scale applications (Yazici and Deveci, 2013).

There is an urgent need for achieving environmentally sustainable methods to separate metals from solutions leached from PCBs. Therefore, the main aim of this work was to develop a zero waste process to recover Cu and Al with high purity from PCBs residues.

From the leaching of pre-processed (crushed and roasted) PCBs, with HNO_3 2 mol/L for 210´at 50ºC, a multi-metal solution containing 78 and 85% of the total amount of Cu and Al present in the original residue, respectively, together with other metals, was achieved. The leached solution was constituted by: 66% of Cu and 28% of Al and smaller amounts of Fe, Sn, Zn, Ni and Ag.

In a second step, a bispicolylamine resin (Dowex M4195^{TM}) was used to recover Cu with high selectivity. A flow rate of 0.17 mL/(min.g of resin) was applied to allow maximizing Cu recovery (99.5% of Cu retained). Almost no Al, Fe, Sn and Zn were retained. H_2SO_4 4 mol/L was used as eluent and 96% of Cu was eluted.

The use of the bispicolylamine resin allowed concentrating the Cu in the final solution (from 18 to 31 mM of Cu) and enabled purifying Cu into a final Cu solution with high grade of purity (99.0%).

Aluminum, which was the major constituent of the raffinate solution, was recovered by precipitation increasing the pH to 8.5 with NaOH 10 mol/L, and recovered as $Al(OH)_3$ solid with a purity grade of 76%, being Fe and Na the major contaminants (11 and 8%, respectively). The filtrate solution and the water used for washing the solid of Al were the only effluents of the process. These effluents were composed mainly by Na ions (99.9% of the metals), which can be recovered in a two stages process with diffusion dialysis followed by electrodialysis for the removal and recovery of sodium hydroxide (Imran et al., 2016).

References

Imran, B., S.J. Khan, I.A. Qazi and M. Arshad. 2016. “Removal and recovery of sodium hydroxide (NaOH) from industrial wastewater by two-stage diffusion dialysis (DD) and electrodialysis (ED) processes”. Desalination and Water Treatment 57:7926–7932.

Yazici, E.Y. and H. Deveci. 2013. “Extraction of metals from waste printed circuit boards (WPCBs) in H2SO4–CuSO4–NaCl solutions”. Hydrometallurgy 139: 30–38.

Microfiltration membranes for photocatalytic degradation of emerging contaminants

S. Dekkouche[1, 2*], S. Morales-Torres[1], A.R. Ribeiro[1], J.L. Faria[1], O. Kebiche-Senhadji[2], C. Fontàs[3] and A.M.T. Silva[1]

[1]Laboratory of Separation and Reaction Engineering - Laboratory of Catalysis and Materials (LSRE-LCM), Faculdade de Engenharia, Universidade do Porto, Porto, Portugal;
[2]Laboratoire des procédés membranaires et téchniques de séparation et récupération, Université de Béjaia, Algeria;
[3]Department of Analytical Chemistry, University of Girona, Girona, Spain
[*] dekkouche-gp@hotmail.fr

Keywords: titanium dioxide, membranes, photocatalysis, diclofenac, 17-α-ethinylestradiol.

Over the last decades, pharmaceuticals like diclofenac (DCF) and 17-α-ethinylestradiol (EE2) have been detected in surface water and groundwater at ng L^{-1} to µg L^{-1} levels. These contaminants of emerging concern are not completely biodegradable and might resist to conventional wastewater treatments (Ribeiro et al. 2015). Heterogenous photocatalysis has been successfully applied to the removal of both DCF and EE2. However, most of studies employed suspended particle photocatalysts, requiring at some stage the separation of the material from the treated water. Previously, it was demonstrated how immobilization of photocatalysts in membranes circumvents this limitation and allows to operate in continuous mode (Pastrana-Martínez et al. 2015). Aiming to develop new separation strategies, in the present work, we prepared microfiltration (MF) membranes containing TiO_2 particles, by a two-step method using polysulfone (PS) and polyvinylidene fluoride (PVDF). The performance of these TiO_2-MF membranes was assessed in the photodegradation of DCF and EE2 using UV-LED radiation under continuous mode operation.

Photocatalytic membranes were prepared following a two-step method adapted from the literature (Fischer et al 2015). Briefly, commercial hydrophilic PS and PVDF membranes were soaked in water and then, immersed in an ethanolic solution of titanium isopropoxide (2 µmol L^{-1}) for 2 h under stirring. The resulting TiO_2-MF membranes were washed, dried in air at 25 °C and finally, treated hydrothermally with water vapour at 110 °C for 2 h. The so obtained T-PS and T-PVDF membranes were characterized by thermogravimetric analysis (TGA), physical adsorption of N_2, scanning electron microscopy (SEM) and contact angle measurements. Their performances were studied in dark adsorption and UV-LED (393 nm) photocatalytic experiments with an aqueous solution containing ca. 300 µg L^{-1} of DCF and/or EE2 under recirculation mode (Q_{feed} = 5 mL min^{-1}). Product analysis was carried out by HPLC with fluorescence detection. Neat PS and PVDF membranes were also tested for comparison purposes.

Following our preparation method, a homogeneous layer of TiO_2 particles was assembled on the surface of both PS and PVDF membranes. The top surface of the PS membrane before (PS) and after (T-PS) TiO_2 assembling is shown in Figures 1a and 1b. The amount of TiO_2 on T-PS was larger than on T-PVDF, as confirmed by TGA. Higher BET surface areas and lower contact angles (higher surface hydrophilicity) were obtained for the TiO_2-MF membranes in comparison with neat membranes, regardless of the type of support used. The removals of both DCF and EE2 contaminants were below 25% by simple adsorption. Photocatalysis by UV-LED irradiation significantly increased the conversion, reaching almost complete degradation in the case of the T-PS membrane (Figure 1c).

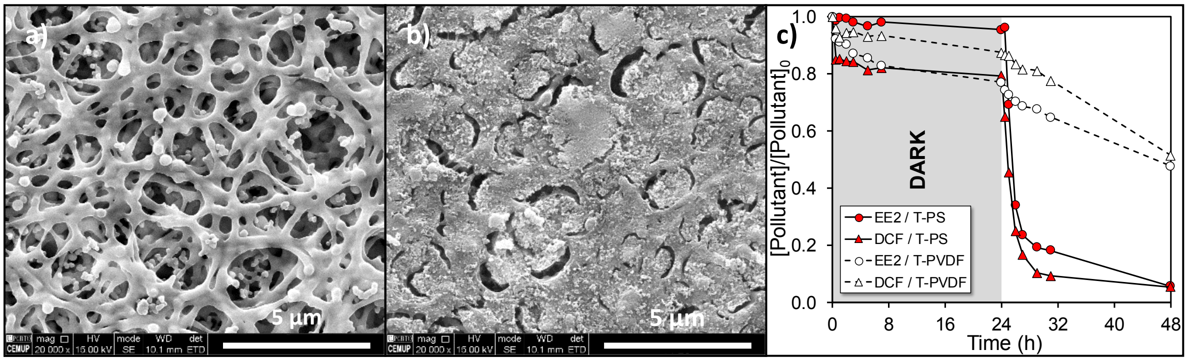

Figure. 1. SEM micrographs for a) neat PS and b) T-PS membranes; c) normalized DCF and EE2 concentrations for dark adsorption experiments and UV-LED (393 nm) photocatalytic experiments.

PVDF is a very unreactive fluorocarbon known by its inertness towards oxidation, thermal degradation, as well as its resistance to most acids and alkalis. These superior resistance properties may also be responsible by the low performance, which is most probably due to the adsorptive properties.

Acknowledgments: Financial support was provided by "AIProcMat@N2020 - Advanced Industrial Processes and Materials for a Sustainable Northern Region of Portugal 2020", with the reference NORTE-01-0145-FEDER-000006, supported by Norte Portugal Regional Operational Programme (NORTE 2020), under the Portugal 2020 Partnership Agreement, through the European Regional Development Fund (ERDF) and of Project POCI-01-0145-FEDER-006984 – Associate Laboratory LSRE-LCM funded by ERDF through COMPETE2020 - Programa Operacional Competitividade e Internacionalização (POCI) – and by national funds through FCT-Fundação para a Ciência e a Tecnologia. SK acknowledge to the Erasmus Mundus Programme. SMT and AMTS acknowledge the FCT Investigator Programme (IF/00573/2015 and IF/01501/2013, respectively) and ARR acknowledges the research grant from FCT (Ref. SFRH/BPD/101703/2014), with financing from the European Social Fund and the Human Potential Operational Programme.

References

Fischer, K., M. Grimm, J. Meyers, C. Dietrich, R. Gläser, and A. Schulze. 2015. "Photoactive microfiltration membranes via directed synthesis of TiO_2 nanoparticles on the polymer surface for removal of drugs from water." Journal of Membrane Science 478:49-57. doi: 10.1016/j.memsci.2015.01.009.

Pastrana-Martínez, L. M., S. Morales-Torres, J. L. Figueiredo, J. L. Faria, and A. M. T. Silva. 2015. "Graphene oxide based ultrafiltration membranes for photocatalytic degradation of organic pollutants in salty water." Water Research 77:179-190. doi: 10.1016/j.watres.2015.03.014.

Ribeiro, A. R., O. C. Nunes, M. F.R. Pereira, and A. M. T. Silva. 2015. "An overview on the advanced oxidation processes applied for the treatment of water pollutants defined in the recently launched Directive 2013/39/EU." Environment International 75:33-51. doi: 10.1016/j.envint.2014.10.027.

Fractionation of acids, ketones and aldehydes from lignin oxidation broth with SP700 resin

E. Gomes[1], I. Mota[1] and A. E. Rodrigues[1*]

[1]1 Laboratory of Separation and Reaction Engineering, Associate Laboratory LSRE/LCM, Department of Chemical Engineering, Faculty of Engineering, University of Porto, Rua Dr. Roberto Frias s/n, 4200-465 Porto, Portugal; * elson@fe.up.pt; Phone: +351 22 508 1400; Fax: +351 22 508 1440
[*]arodrig@fe.up.pt

Keywords: vanillin, syringaldehyde, acetovanillone, acetosyringone, lignin, sp700, biorefinery, adsorption.

Lignin is a biopolymer that binds cellulose and hemicellulose in the plant cell walls granting its rigidity and support. Plants can have a lignin composition up to 30 % (w/w), thus making it the second most abundant biopolymer next to cellulose (McKendry,2002). Side streams from the pulp and paper industry are very rich in lignin and the common route employed for the valorization of these streams are the production of steam and electricity, making the pulp and paper industry a net seller of energy. A more noble route for the valorization of lignin involve its oxidative depolymerization into highly functionalized monomers like vanillin and syringaldehyde, among other compounds (Changzhi,2015).

One of the aspects hindering the adoption of lignin and other biomass sources as platform chemical feedstock is the difficulty of separation of the compounds produced during the oxidative depolymerization without resorting to complex sequence of processes employing harmful solvents. Different approaches have been tried ranging from membranes, precipitations and solvent extractions or any combination of these (Mota,2016).

In this work, an oxidation mixture containing several phenolic monomers, among other compounds, is treated by an adsorption process onto SP700 resin after ultrafiltration with a membrane with an average molecular weight cut-off of 5000 Da. This preprocessing is performed to remove the higher molecular weight lignin structures that were not depolymerized. The phenolic monomers quantified by HPLC-UV were *p*-hydroxybenzaldehyde, vanillic acid, vanillin, syringic acid syringaldehyde, acetovanillone and acetosyringone. The initial feed concentrations are given in **Table 1**. The oxidation mixture was fed for a certain period of time (3h) and then, the adsorbed monomers were initially desorbed with water and afterwards, with ethanol. The recovery, concentration and fractionation of these monomers was made with success.

Table 1. Feed concentrations for the adsorption experiments performed at pH values of 9 and 11. Values are averages of 3 injections.

Compound	Concentration of feed at pH = 9 (g/L)	Concentration of feed at pH = 11 (g/L)
***p*-hydroxybenzaldehyde (H)**	0.015 ± 0.001	0.011 ± 0.003
vanillic acid (VA)	0.151 ± 0.006	0.153 ± 0.009
vanillin (V)	0.114 ± 0.005	0.095 ± 0.007
syringic acid (SA)	0.155 ± 0.008	0.155 ± 0.004
syringaldehyde (S)	0.057 ± 0.003	0.017 ± 0.002
acetovanillone (VO)	0.036 ± 0.002	0.037 ± 0.003
acetosyringone (SO)	0.033 ± 0.002	0.033 ± 0.002

Experiments at two different pH values (9 and 11) were performed in order to understand the influence of the pH on the adsorption of the phenolic monomers of interest and take advantage of the presence of compounds in the mixture with different pKa values (Ragnar).

Concentration histories of the experiments performed at pH 9 and 11 are presented in **Figure 1.** These experiments revealed that operating at alkaline conditions the phenolic acids will not be adsorbed and that operating at pH 11 has the additional advantage of separating the aldehydes V and S, that are mainly collected in the water desorption step, from the respective ketones, VO and SO, that are mainly obtained in the ethanolic fraction. Therefore, tuning the adsorption pH can be important to fractionate the aldehydes from the ketones during adsorption/desorption with a non-polar resin.

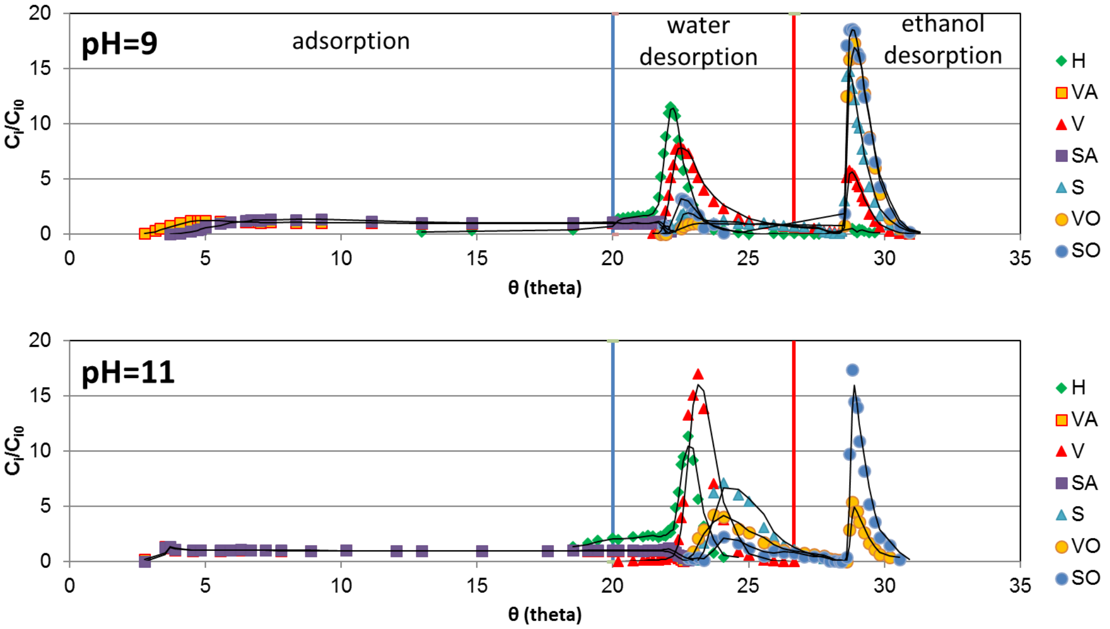

Figure 1 – Adsorption and desorption normalized concentration histories of the experiments conducted at pH = 9 (top) and pH = 11 (bottom). Blue line – start of desorption with deionized water, red line – start of desorption with pure ethanol. $\theta = t/\bar{t}_r$, $\bar{t}_r = 540\ s$. $T = 25$°C, $Q_L = 10\ ml/min$, column of 446 x 26 mm and porosity of 0.37. Feed concentrations presented in **Table 1**.

References

Changzhi Li, Xiaochen Zhao, Aiqin Wang, George W. Huber, and Tao Zhang (2015) Catalytic Transformation of Lignin for the Production of Chemicals and Fuels Chemical Reviews 2015 115 (21), 11559-11624 DOI: 10.1021/acs.chemrev.5b00155

McKendry P (2002) Energy production from biomass (part 1): overview of biomass. Bioresource Technology 83(1):37–46.

Mota, M. I. F., Rodrigues Pinto, P. C., Loureiro, J. M. and Rodrigues, A. E. (2016) Recovery of Vanillin and Syringaldehyde from Lignin Oxidation: A Review of Separation and Purification Processes. Sep. Purif. Rev., 45: 227-259.

Ragnar, M.; Lindgren, C.T.; Nilvebrant, N-O. (2000) pKa-Values of guaiacyl and syringyl phenols related to lignin. J. Wood. Chem. Technol., 20:277–305.

Oxypropylation of lignocellulosic agro-industrial residues – a comparative study

J.A. Pinto[1*], M.N. Belgacem[3], A.E. Rodrigues[2], and M.F. Barreiro[1]

[1]Laboratory of Separation and Reaction Engineering – Laboratory of Catalysis and Materials (LSRE-LCM), Bragança Polytechnic Institute, Bragança, Portugal;

[2]Laboratoire de Génie des Procédés Papetiers (UMR 5518 - CNRS), Grenoble INP, Domaine Universitaire, St. Martin d'Hères, France

[3]Laboratory of Separation and Reaction Engineering – Laboratory of Catalysis and Materials (LSRE-LCM), Faculty of Engineering, University of Porto, Portugal;

*jpinto@ipb.pt

Keywords: Oxypropylation, agro-industrial residues, biopolyols.

Introduction

Nowadays a great interest is devoted to the production and use of biobased products. The main scope of the oxypropylation process is to obtain polyols, in the form of viscous liquids, which can be used as co-monomers to produce polyurethanes and polyesters. Oxypropylation is a polymerization process that forms grafts of poly (propylene oxide), from available hydroxyls leading to the conversion of biomass residues into liquid polyols. Theoretically, any biomass residue containing hydroxyl groups (e.g. lignin, sugar beet pulp, cork, olive stone, date seed, rapeseed cake, etc.) can be transformed by oxypropylation into liquid polyols.

Oxypropylation reactions are normally performed using a basic catalyst such as potassium hydroxide (KOH), which is also the most frequently used (Figure 1). The oxypropylation reaction is always accompanied by the occurrence of propylene oxide homopolymerization. The homopolymerization of propylene oxide takes places when some residual moisture is present in the reaction medium.

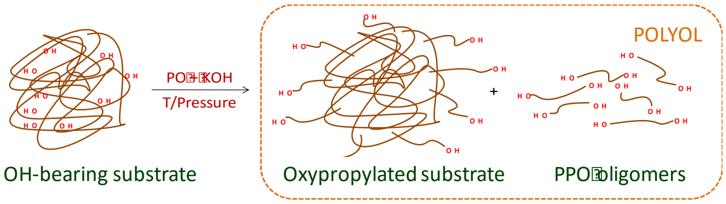

Figure 1. Schematic representation of oxypropylation reaction

Biomass can be directly oxypropylated, nevertheless sometimes a pre-treatment (pre-activation) can be used. This pre-treatment increases the reactivity of the biomass by activating its hydroxyl groups. Pre-activation called upon KOH dissolved in ethanol that is let in contact with the biomass. This strategy is particularly useful when rough granulometries are used. In fact, the efficiency of an oxypropylation process depends on several variables, which can be related with the substrate nature and used oxypropylation conditions. In lignocellulosic biomasses, the content of each fraction (lignin, cellulose and hemicellulose) can differ, as well as, the crystalline organization, which may limit reagent's access to biomass. Also, the hydroxyl content can vary among biomasses. In general, high values demand higher amounts of reactants, namely catalyst content, and more severe reaction conditions.

In this work, and as a preliminary study to the topic of the present PhD thesis, the oxypropylation process of two biomasses (almond shell and Brazilian pine fruit shell) is compared.

Experimental

The biomasses (almond shell and Brazilian pine fruit shell) have been characterized in what concerns the lignocellulosic composition and extractables using the procedures described elsewhere (Matos et al., 2010). In what concerns the oxypropylation process a pressure reactor of 450 mL equipped with a heating mantle, mechanical stirrer, thermocouple and manometer, was used. Three Biomass/PO ratios were tested (30/70, 20/80 and 10/90, w/v, g/ml) by using 3 catalyst contents (5, 10 and 15%, w/w, biomass-based). The polyols were characterized in what concerns homopolymer content (HOMO, %(w/w)), viscosity (Pa.s, 20°C), hydroxyl number (IOH, mg KOH/g) and unreacted biomass(UB, w/w, biomass-based).

Discussion and conclusions

Comparing the two biomasses, almond shell is characterized by higher content of ashes (2.5% comparatively with 1.9%) and a lower content of extractables (9.2% comparatively with 14.4%). In fact, pine fruit shell comprises 6.3% of OH-bearing compounds (methanol extractables) and 7.5% of more polar substances (water extractables). Concerning the lignocellulosic composition (cellulose, hemicellulose and lignin), the almond shell comprises 54.8% of holocellulose (39.0% of cellulose and 15.8% of hemicellulose), and 45.2% of lignin. For the pine fruit shell, the total amount of holocellulose was 52.7% (34.9% of cellulose and 17.8 % of hemicellulose). For this material lignin accounts with 47.3%.

Figure 2 presents the results obtained for the produced polyols in terms of HOMO, IOH and UB. The viscosity results reveled, in general, very high values for the pine fruit shell-based polyols, when compared with their homologues obtained with almond shell. In particular, for the pine-fruit shell-based polyols, the series 30/70 gives values over 500 Pa.s, as well as, the polyol 20/80/5. For this last polyol, also an apparently abnormal high UB was obtained, as well as for the pine-fruit shell-based polyols of the series 30/70. These differences are hard to be explained solely in terms of lignocellulosic composition. To get further insights, SEM and TEM analysis are being carried out to inspect morphology and crystallinity of the two studied biomasses.

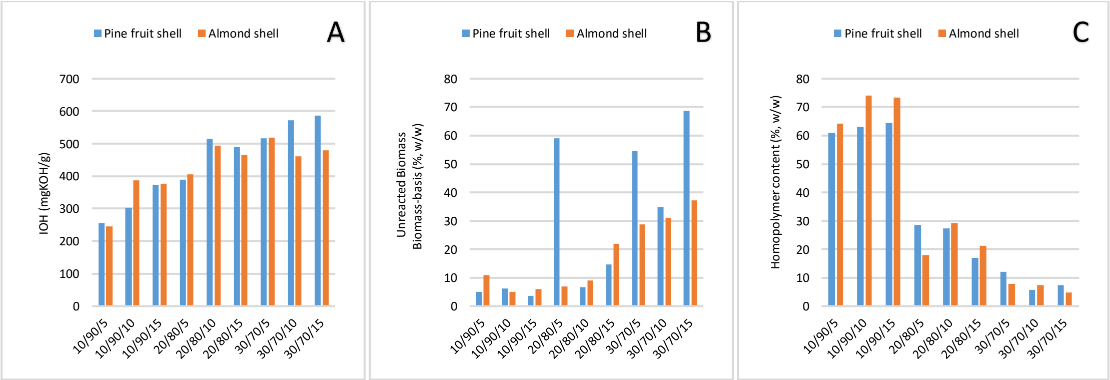

Figure 2. Polyols characterisation: **A**-Hydroxyl number; **B**-Unreacted Biomass; **C**-Homopolymer content.

References

Matos, M., Barreiro, M.F., Gandini, A., (2010). "Olive stone as a renewable source of biopolyols". *Industrial Crops and Products* 32: 7–12.

Acknowledgments: POCI-01-0145-FEDER-006984 (LA LSRE-LCM), funded by FEDER, through POCI-COMPETE2020 and FCT; Project NORTE-01-0145-FEDER-000006, funded by NORTE2020 under PT2020, through ERDF.

Removal of Cr(III) by using activated carbons produced from rice waste chars

D. Dias[1*], M. Miguel[1], M. Bernardo[2], N. Lapa[1], I. Matos[2], I. Fonseca[2], F. Pinto[3]
[1]LAQV, REQUIMTE, Department of Sciences and Technology of Biomass, Faculdade de Ciências e Tecnologia, Universidade Nova de Lisboa, Lisboa, Portugal;
[2]LAQV, REQUIMTE, Department of Chemistry, Faculdade de Ciências e Tecnologia, Universidade Nova de Lisboa, Lisboa, Portugal;
[3]Bionergy Unit, Laboratório Nacional de Energia e Geologia, Lisboa, Portugal.
[*]da.dias@campus.fct.unl.pt

Keywords: Pyrolysis, Rice wastes, adsorption, chars, chromium

Introduction

Rice is the second most produced cereal worldwide, generating high amounts of wastes, especially rice husk (RH), rice straw (RS) and polyethylene (PE) from plastic bags. Due to their interesting calorific value, these wastes can be submitted to thermal processes, such as pyrolysis, in order to generate energy carriers (mainly, gas and bio-oils). The chars (solid fraction) generated by pyrolysis are seen as by-products, and their use to produce high-performance adsorbents is being tested to substitute the commercial activated carbons (CAC), which are more costly and less environmental sustainable (Cha et al., 2016). On the other hand, chromium is one of the most economically valuable raw materials for Europe; its recovery from liquid effluents is a priority for EU (European Comission, 2014). The main aim of this work is to recover Cr(III) from aqueous media by using activated carbons (AC) produced from chars obtained from the pyrolysis of rice wastes.

Material and Methods

A blend of 50% RH + 50% PE (w/w) was pyrolysed at 390 °C, 6 bar, for 35 min. The pyrolysis char (PC) was separated from the liquid fraction through settling and was further extracted with hexane (hexane/char ratio: 17 mL g^{-1}), for 3 h, in a Soxhlet apparatus.

PC was up-graded to improve its adsorptive capacity through the following two processes: (1) Physical activation (p-PC) – it was performed in a quartz reactor, heated-up in an electric vertical tube furnace at 800 °C, for 4 h, under 150 cm^3 min^{-1} CO_2 flow; (2) Physical activation and chemical treatment (pc-PC) – the physical activation was followed by a treatment with HNO_3 (13 M) under a solid to liquid (S/L) ratio of 50 g L^{-1}, in a silicone bath at 90 °C, for 6 h. The acid activated carbon obtained was then washed with distilled water until stable pH and dried at 100 °C overnight. For comparison purposes, a commercial activated carbon (CAC) was also chemically treated under the same conditions(c-CAC).

Cr(III) adsorption assays were performed in a roller-table agitator, at 150 rpm, for 24 h. The Cr(III) starting solution was of 70 mg Cr(III) L^{-1} and an initial pH of 4.5. Solid/liquid ratios (S/L) of 5 and 10 g L^{-1} were used. The samples were then filtered with cellulose nitrate membranes (0.45 µm); the final pH values were measured and Cr concentrations were quantified by ICP-AES.

Results and Discussion

Above a pH of 5, Cr(III) removal is ruled by precipitation. Bellow a pH of 5 Cr(III) removal is ruled by adsorption. So the final pH of each assay is crucial to understand which process occurred.

Figure 1 shows the results of (a) Cr(III) removal percentage and (b) uptake capacity (q_e) in the adsorption assays (bars), as well as the final pH values in each assay (dots).

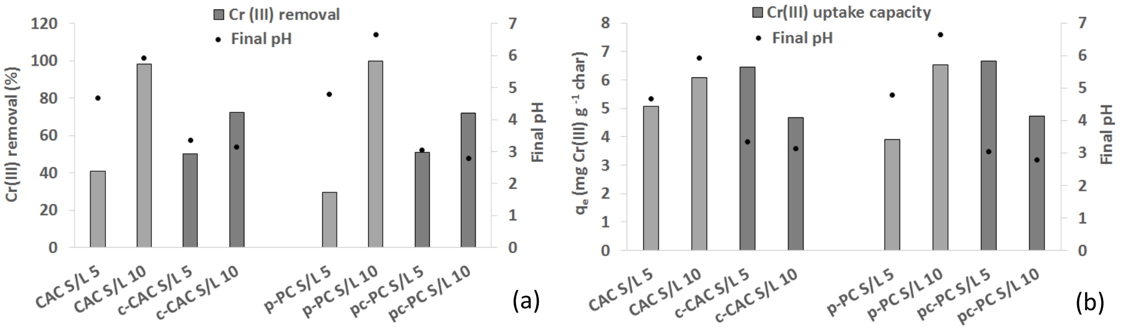

Figure 1. Cr(III) removal (a) and uptake capacity (b) for each activated carbon, and final pH values in each adsorption assay (S/L ratio expressed in g L^{-1}).

For the AC p-PC, only submitted to physical activation, Cr(III) removal was lower than for CAC at S/L 5 g L^{-1} (29.7% and 40.9%, respectively). In both cases adsorption ruled (pH<5). At S/L 10 g L^{-1}, both AC removed almost 100% Cr(III), because precipitation occurred (pH>5). Cr(III) uptake capacity reflected these same tendencies. For S/L 10 g L^{-1}, both AC removed more than the double of Cr(III) when compared to S/L 5 g L^{-1}. This was more significant for p-PC, for which q_e increased from 3.89 mg Cr(III) g^{-1} at S/L 5 g L^{-1} to 6.53 mg Cr(III) g^{-1} at S/L 10 g L^{-1}.

For the activated carbons submitted to physical activation followed by chemical treatment (pc-PC and c-CAC), no precipitation occurred (pH<5). For these AC, adsorption was the main process ruling Cr(III) removal. The results for both AC were very similar; at S/L 5 g L^{-1}, both AC removed *ca.* 50% Cr(III), while at S/L 10 g L^{-1} the removal percentage increased to *ca.* 70%. The uptake capacity, q_e, was higher at S/L 5 g L^{-1} than for S/L 10 g L^{-1} for both AC, meaning that doubling the mass of these AC cannot be an advantage for Cr(III) uptake. q_e achieved the highest value for pc-PC, being comparable to the adsorption assays in which Cr(III) was almost completely removed due to chemical precipitation.

Conclusions

The uptake capacity of p-PC, at S/L 5 g L^{-1}, was lower than for CAC. However, when the mass was doubled (S/L 10 g L^{-1}), its behaviour was similar to CAC, due to Cr(III) chemical precipitation.

The physical activation followed by chemical treatment improved the adsorption capacity of both AC, and reduced the removal through precipitation. pc-PC showed a similar behaviour to chemically treated CAC, being a promising alternative for further studies on Cr(III) removal, namely under continuous-flow conditions and using real liquid effluents.

References

Cha, J.S., Park, S.H., Jung, S.-C., Ryu, C., Jeon, J.-K., Shin, M.-C., Park, Y.-K., 2016. Production and utilization of biochar: A review. J. Ind. Eng. Chem. 40, 1–15. doi:10.1016/j.jiec.2016.06.002

European Comission, 2014. On the review of the list of critical raw materials for the EU and the implementation of the Raw Materials Initiative. Brussels.

Effects of Gallic acid on Membrane Biophysical Properties: Relevance for Its Biophysical Effects

Stephanie Andrade[1*], Joana A. Loureiro[1], Manuel A. N. Coelho[1] and Maria do Carmo Pereira[1]

[1]LEPABE, Department of Chemical Engineering, Faculty of Engineering University of Porto, Porto, Portugal

*stephanie@fe.up.pt

Keywords: Liposomes, Membrane models, Partition coefficient, Alzheimer's disease.

The incidence of Alzheimer's disease (AD), a neurodegenerative disease, is promoted by the increase of the age. This disease affects the memory and other cognitive functions with sufficient intensity to produce functional losses, and it is the most common cause of dementia in the elderly (Brookmeyer et al. 2007). The neuropathological characteristics of AD include extracellular senile plaques, which consist of deposits of amyloid beta-peptide (Aβ) and neurofibrillar tangles that are formed by hyperphosphorilation and abnormal deposition of tau protein (Clippingdale, Wade, and Barrow 2001; Klafki et al. 2006; Selkoe 2001). Protein misfolding or partially folded structure is responsible for the fibrillation of various amyloidogenic proteins/peptides (Ahn et al. 2007). Thus, it is essential to find molecules that prevent or interrupt the aggregation of proteins.

Various natural compounds have been suggested as therapeutics for AD. Among these compounds, gallic acid (GA) arouses great interest. GA is a type of phenolic acid that can improve spatial learning and memory impairment due to their antioxidant (Mansouri et al. 2013) and anti-inflammatory properties (Kim et al. 2011). Moreover, GA inhibits the fibril formation and Aβ oligomerization (Liu et al. 2013; Valizadeh et al. 2012).

This work aims the systematic study of the biophysical interactions of GA with membrane models of different lipid composition. Liposomes of 1,2-dimyristoyl-sn-glycero-3-phosphocholine (DMPC) with and without cholesterol (CHOL) were used as mimetic models of human cell membranes to evaluate the GA membrane partition.

The GA lipophilicity was evaluated by spectroscopic methods, which enabled the determination of the partition coefficient (Kp). The results of derivative spectrophotometry indicate that GA has a Kp of 2377 ± 91 in absence of cholesterol and 1321 ± 162 in your presence, at 37℃. The high partition values reveal a strong interaction between GA and the membrane models whereby and that GA is able to be incorporated into DMPC liposome model systems. Moreover, these results suggests that GA has greater affinity for the DMPC bilayers than for DMPC:CHOL [5.67:1] membrane models. CHOL plays the essential function of regulating the physical properties of the cell membrane as it controls the lipid organization and phase behavior, and regulates the membrane fluidity and its mechanical strength (Pan et al. 2008; Rog et al. 2009). From the molecular perspective, CHOL is considered to produce a condensing effect and induce ordering to fluid phase lipids, which results in decreasing the Kp (Rog et al. 2009; Hung et al. 2007).

Acknowledgements

This work was financially supported by POCI-01-0145-FEDER-006939 (Laboratory for Process Engineering, Environment, Biotechnology and Energy – UID/EQU/00511/2013) funded by the European Regional Development Fund (ERDF), through COMPETE2020 - Programa Operacional Competitividade e Internacionalização (POCI) and by national funds, through FCT - Fundação para a Ciência e a Tecnologia; and NORTE-01-0145-FEDER-000005 – LEPABE-2-ECO-INNOVATION, supported by North Portugal Regional Operational Programme (NORTE 2020), under the Portugal 2020 Partnership Agreement, through the European Regional Development Fund (ERDF). Stephanie Andrade acknowledges INCENTIVO/EQB/UI0511-Engª Biomédica grant and Joana A. Loureiro also acknowledges postdoctoral grant FEUP-TRANSCAN/0001/2012.

References

Ahn, Jung Sun, Jung-Ho Lee, Je-Hoon Kim, and Seung R. Paik. 2007. 'Novel method for quantitative determination of amyloid fibrils of α-synuclein and amyloid β/A4 protein by using resveratrol', *Analytical Biochemistry*, 367: 259-65.

Brookmeyer, Ron, Elizabeth Johnson, Kathryn Ziegler-Graham, and H. Michael Arrighi. 2007. 'Forecasting the global burden of Alzheimer's disease', *Alzheimer's & Dementia*, 3: 186-91.

Clippingdale, A. B., J. D. Wade, and C. J. Barrow. 2001. 'The amyloid-beta peptide and its role in Alzheimer's disease', *J Pept Sci*, 7: 227-49.

Hung, W. C., M. T. Lee, F. Y. Chen, and H. W. Huang. 2007. 'The condensing effect of cholesterol in lipid bilayers', *Biophys J*, 92: 3960-7.

Kim, M. J., A. R. Seong, J. Y. Yoo, C. H. Jin, Y. H. Lee, Y. J. Kim, J. Lee, W. J. Jun, and H. G. Yoon. 2011. 'Gallic acid, a histone acetyltransferase inhibitor, suppresses beta-amyloid neurotoxicity by inhibiting microglial-mediated neuroinflammation', *Mol Nutr Food Res*, 55: 1798-808.

Klafki, Hans-Wolfgang, Matthias Staufenbiel, Johannes Kornhuber, and Jens Wiltfang. 2006. 'Therapeutic approaches to Alzheimer's disease', *Brain*, 129: 2840-55.

Liu, Y., T. L. Pukala, I. F. Musgrave, D. M. Williams, F. C. Dehle, and J. A. Carver. 2013. 'Gallic acid is the major component of grape seed extract that inhibits amyloid fibril formation', *Bioorg Med Chem Lett*, 23: 6336-40.

Mansouri, M. T., Y. Farbood, M. J. Sameri, A. Sarkaki, B. Naghizadeh, and M. Rafeirad. 2013. 'Neuroprotective effects of oral gallic acid against oxidative stress induced by 6-hydroxydopamine in rats', *Food Chem*, 138: 1028-33.

Pan, J., T. T. Mills, S. Tristram-Nagle, and J. F. Nagle. 2008. 'Cholesterol perturbs lipid bilayers nonuniversally', *Phys Rev Lett*, 100: 198103.

Rog, T., M. Pasenkiewicz-Gierula, I. Vattulainen, and M. Karttunen. 2009. 'Ordering effects of cholesterol and its analogues', *Biochim Biophys Acta*, 1788: 97-121.

Selkoe, Dennis J. 2001. 'Alzheimer's Disease: Genes, Proteins, and Therapy', *Physiological Reviews*, 81: 741-66.

Valizadeh, Z., A. Eidi, A. Sarkaki, Y. Farbood, and P. Mortazavi. 2012. 'Dementia type of Alzheimer's disease due to beta-amyloid was improved by Gallic acid in rats', *Healthmed*, 6: 3648-56.

Liposomes for temozolomide delivery

M. J. Ramalho[1], Joana A. Loureiro[1], M. A. N Coelho[1] and M. C. Pereira[1*]
[1]LEPABE, Chemical Engineering Dpt., Faculty of Engineering University of Porto, Porto, Portugal;

*mcsp@efe.up.pt

Keywords: Temozolomide, Glioblastoma multiform, Blood-brain barrier, Nanosystem, Nanotechnology, Drug delivery, Liposomes, Cancer therapy

Glioblastoma multiform is the most common primary brain cancer and presents high morbidity and mortality. Its classical treatment consists of combination of surgery, radiation and chemotherapy with temozolomide, an alkylating agent (Morais et al. 2015). However, in these aggressive tumours, this treatment is rarely successfully curative, due to this tumour high resistance to therapy and low drug bioavailability in tumour tissue, due to the inability of most molecules to cross the blood-brain barrier (BBB) (van Tellingen et al. 2015). Therefore, new therapeutic strategies, as specific drug delivery systems, must be developed to overcome those limitations. In this work, temozolomide was encapsulated in liposomes. Liposomes with controlled sizes and properties were prepared by the lipid film hydration method. After synthesis, the liposomes were physicochemically characterized in terms of size, shape and zeta potential. The attained systems for temozolomide delivery showed mean diameters of approximately 80 nm and remained stable at storage conditions for several weeks. Two different phospholipids, 1-palmitoyl-2-oleoyl-sn-glycero-3-phosphocholine (POPC), 1,2-distearoyl-sn-glycero-3-phosphocholine (DSPC) and 1,2-distearoyl-sn-glycero-3-phosphoethanolamine-N-[amino(polyethylene glycol)-2000] (DSPE-PEG), were used, as different lipid/lipid and lipid/drug ratios, to optimize the encapsulation efficiency values. Liposomes failed to encapsulate temozolomide when DSPC was used in the formulation, due to the amphipathic nature and small size of temozolomide, being able to escape the bilayer. The efficiency encapsulation values reached a maximum of 36% when using POPC due to the differences in the packing geometry of the hydrophobic carbon chains among DSPC and POPC. Since POPC exhibits an unsaturated double bond, the lipids packaging is hindered leading to an increased membrane fluidity, allowing a higher drug encapsulation in the bilayer. Also, variations on the cholesterol content showed an influence on the fluid state of the phospholipid bilayer, resulting in variations of the encapsulation efficiency values as shown in table 1.

Table 1. Encapsulation efficiency (EE) values of the prepared POPC liposomes.

Lipids	Lipids molar ratio	Lipids:drug ratio	Drug phase	EE%
POPC:Chol:DSPE-PEG	52:45:3	10:1	Aqueous	25
POPC:Chol:DSPE-PEG	87:10:3	10:1	Aqueous	30
POPC:Chol:DSPE-PEG	87:10:3	2:1	Aqueous	33
POPC:Chol:DSPE-PEG	87:10:3	2:1	Aqueous with 10% DMSO	36

The attained results showed the developed POPC liposomes are suitable for temozolomide encapsulation. Though, further studies are required to conclude whether the nanoformulation is able to improve its therapeutic efficacy.

Acknowledgements

This work was financially supported by: Project POCI-01-0145-FEDER-006939 (Laboratory for Process Engineering, Environment, Biotechnology and Energy – LEPABE funded by FEDER funds through COMPETE2020 - Programa Operacional Competitividade e Internacionalização (POCI) – and by national funds through FCT - Fundação para a Ciência e a Tecnologia; FCT doctoral grant PD/BD/105984/2014.

References

Morais, L. C., V. C. J. Queiroz, J. E. S. Cavalcante, H. H. S. Matozinho, F. H. R. Silva, M. G. P. Costa, F. Y. Pereira I, L. C. P. Tavares, and G. M. Guimarães. 2015. "Treatment and prognosis of glioblastoma multiforme: a literature review." *Journal of the Neurological Sciences* no. 357:e183. doi: 10.1016/j.jns.2015.08.630.

van Tellingen, O., B. Yetkin-Arik, M. C. de Gooijer, P. Wesseling, T. Wurdinger, and H. E. de Vries. 2015. "Overcoming the blood–brain tumor barrier for effective glioblastoma treatment." *Drug Resistance Updates* no. 19:1-12. doi: http://dx.doi.org/10.1016/j.drup.2015.02.002.

Novel low cost ceramic and zeolite-ceramic composite membranes for liquid phase separation applications

R. Vinoth Kumar* and G. Pugazhenthi
Department of Chemical Engineering, Indian Institute of Technology Guwahati, Guwahati - 781039 (Assam) India.
*vinoth@iitg.ernet.in

Keywords: Low cost ceramic membrane, zeolite membrane, wastewater treatment, BSA separation.

Preparation of ceramic membrane and its potential in wastewaters treatment

A novel tubular configured ceramic membrane fabricated using an inexpensive raw materials (ball clay, kaolin, feldspar, quartz, pyrophyllite and calcium carbonate) by extrusion technique. The properties of the prepared membrane were porosity 53%, water permeability 5.93×10^{-7} m^3/m^2s kPa, average pore size 0.309 µm and mechanical strength 12 MPa. Furthermore, the manufacturing cost of the acquired membrane is estimated to be \$0.5 (or 69 $\$/m^2$). In order to explore the potential application of this novel tubular membrane, treatment of two different type of wastewater, viz. synthetic oily and local dairy wastewater was studied. The effect of various process conditions, namely applied pressure, feed concentration and cross flow rate was examined on the wastewater treatment efficiency. An increase in both applied pressure and cross flow rate on the treatment process reduced the percentage rejection of oil in the oily wastewater and chemical oxygen demand (COD) removal from the dairy wastewater. An applied pressure of 69 kPa was found to be the best for achieving the highest rejection (99.98%) of oily wastewater with a permeate flux of 3.16×10^{-5} m^3/m^2s. A maximum COD reduction of up to 91% in the membrane permeate stream with a flux of 2.59×10^{-6} m^3/m^2s was achieved for treating the dairy wastewater.

Fabrication of zeolite-ceramic composite membranes

The novel low cost tubular ceramic membrane was further used as a support for preparing Faujasite (FAU) and Mordenite framework inverted (MFI) type zeolite membranes following the hydrothermal treatment method. Solution containing a mixture of silicate and aluminate with molar composition of $70Na_2O:Al_2O_3:20SiO_2:2000H_2O$ was used to create a FAU zeolite separation layer on the support under hydrothermal condition in Teflon made autoclave reactor operated at 75°C for 12 h. For MFI zeolite layer formation on the porous support, hydrothermal solution prepared using silicate solution with a gel composition of $100SiO_2:5(TPA)2O:5.3Na_2O:1420H_2O$, was subjected to hydrothermal treatment at 185°C for 4 h. To eliminate the template (TPAOH) from the zeolite channels, the membrane was calcined at 400°C for 5 h in an air atmosphere. XRD analysis of the FAU zeolite membrane revealed a peak at 2θ value of 12.40 confirming the highly pure and crystal nature of the material (Huang 2012). Similarly, the distinctive peaks obtained at the 2θ value of 7.5 and 23.5 for MFI zeolite powder revealed its high purity (Wegner 1999). The reduction in the porosity, pore size and water permeability, and an increase in weight of the membranes as compared to those in the support confirmed the incorporation of the zeolite layers on the ceramic support by hydrothermal treatment.

Separation of chromium and BSA protein

The separation efficiency of FAU and MFI type zeolite membranes supported on the low cost tubular ceramic support was evaluated for chromium removal from aqueous solution. The effect of various process parameters, such as applied pressure, initial feed concentration and cross flow rate on permeate flux and chromium removal efficiency by the composite membrane was studied. Results showed that chromium removal efficiency increased with an increase in the applied pressure and feed concentration. On the other hand, chromium removal reduced slightly with an increase in the cross flow rate for both the zeolite membranes. A maximum chromium removal of 82% and 78% is obtained with FAU and MFI membrane, respectively, at 345 kPa applied pressure, 1000 ppm initial feed concentration and unadjusted solution pH 2.35. These novel membranes showed excellent performance in the removal of chromium with 1 to 6 order higher fluxes than other membranes reported in the literature for chromium removal. The FAU and MFI type zeolite membranes were further tested for the separation of bovine serum albumin (BSA) protein from aqueous solution followed by optimization of critical parameters of the microfiltration system using response surface methodology (RSM) and bi-objective genetic algorithm (GA) approaches. The optimum levels of these variables are: 100 ppm BSA concentration, solution pH 2 and applied pressure 276 kPa. At these optimum conditions of the process parameters, a higher permeate flux and BSA rejection of 2.66×10^{-5} m^3/m^2s and 88% respectively, were obtained for the FAU membrane. In case using the MFI membrane, these values were 4.63×10^{-5} m^3/m^2s and 82%, respectively.

Major findings and conclusions

To minimize membrane fabrication cost and make process more commercially attractive, a prototype novel low cost tubular ceramic membrane with excellent characteristics was effectively fabricated. The elaborated membrane was highly fulfilled in oily wastewater as well as dairy wastewater. The obtained rejection values for both these wastewaters were well within the permissible limits for wastewater discharge into the environment. FAU and MFI type zeolite membranes were effectively fabricated on low cost porous tubular ceramic substrate with good properties by hydrothermal synthesis technique. Potential of the prepared FAU & MFI membrane investigated by chromium and BSA separation. Separation efficiency of the FAU & MFI zeolite membrane exhibited better separation efficiency than others reported in the literatures. Owing to its high removal efficiency and low synthesis temperature, and no requirement of calcinations step for its preparation. In addition to the excellent properties and performance of the novel low cost tubular membrane, the use of simple fabrication method, reduced sintering temperature and inexpensive raw materials used for its fabrication clearly establish its potential large scale liquid phase separation applications as compared with high cost commercial α- alumina, zirconia and titania based microfiltration membranes.

References

Huang, A., N. Wang, and J. Caro. 2012. "Seeding-free synthesis of dense zeolite FAU membranes on 3-aminopropyltriethoxysilane-functionalized alumina supports". Journal of Membrane Science, 389: 272-279. doi: 10.1016/j.memsci.2011.10.036.

Wegner, K., J. Dong, and Y.S. Lin. 1999. "Polycrystalline MFI zeolite membranes: xylene pervaporation and its implication on membrane microstructure", Journal of Membrane Science, 158 (1-2): 17-27. doi: 10.1016/S0376-7388(98)00339-1.

MSW energetic valorisation: sustainability analysis of a Portuguese incineration plant

Ana Ramos[1*], Rosa Aragão[2], Carlos Afonso Teixeira[2], Abel Rouboa[1,2]
[1]CIENER-INEGI, Institute of Science and Innovation in Mechanical and Industrial Engineering, Faculty of Engineering of the University of Porto, Porto, Portugal
[2]CITAB, Centre for the Research and Technology of Agro-Environmental and Biological Sciences, University of Trás-os-Montes and Alto Douro, Vila Real, Portugal
*aramos@inegi.up.pt

Keywords: MSW, waste management, incineration, sustainability, LCA.

The exponential population growth, the substantial improvement of their living conditions and daily needs have inevitably entailed problems regarding emergent waste production. This has become a global concern, waste management being in the spotlight as strongly evidenced by the rising number of field-related published literature (Chen, Jiang et al. 2015). This study assesses the environmental impact of the energetic valorisation process in a Portuguese incineration facility with electricity production. The environmental evaluation was performed modelling data for 2015 into environmental impact categories by means of a dedicated life cycle assessment (LCA) software. A well-defined frontier was set for the system, with a functional unit of 1ton of MSW. The LCA methodology followed was CML 2001, and the selected impact categories were: global warming potential (GWP), acidification potential (AP), eutrophication potential (EP), abiotic depletion potential (ADP), human toxicity potential (HTP), freshwater aquatic ecotoxicity potential (FAETP), marine aquatic ecotoxicity potential (MAETP) and terrestric ecotoxicity potential (TETP). The main processes in MSW energetic valorisation are incineration, flue gas treatment and ash inertization (Figure 1).

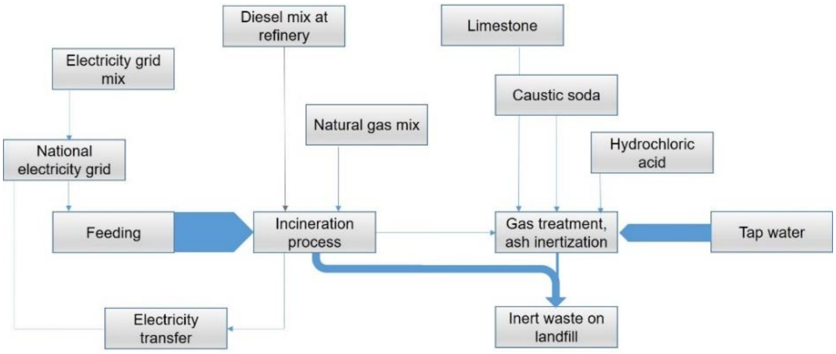

Figure 1. Schematics of the energetic recovery plant with electricity production.

To verify the environmental contribution given by the electricity production, a hypothetical scenario with no energy production was settled, bypassing the electricity transfer process. As expected the scenario with electricity production performed better, presenting negative values for all the impact categories. This supports the alleviation of the environmental injury caused by some of the processes involved in this waste treatment technology, as well as savings on material resources and avoidance of emissions to environmental compartments (Morselli, Bartoli et al. 2005, Hong, Li et al. 2010, Parkes, Lettieri et al. 2015).

Comparing the results for the environmental impact categories of this assessment to the international panorama, similar values for the total contribution of AP (Jeswani and Azapagic 2016), EP (Gunamantha and Sarto 2012, Jeswani and Azapagic 2016) and ADP (fossil) (Fernández-Nava, del Río et al. 2014, Menikpura, Sang-Arun et al. 2016) were reported. Nevertheless, enhanced results for GWP (Toniolo, Mazzi et al. 2014, Jeswani and Azapagic 2016), ecotoxicity (Hong, Li et al. 2010, Toniolo, Mazzi et al. 2014) and HTP (Bueno, Latasa et al. 2015, Jeswani and Azapagic 2016) were herein registered. This absolute sustainable situation grants this Portuguese plant a solid position amongst the concurrent results and validates the LCA approach methodology as a favourable and reproducible procedure to take into account when evaluating environmental profiles for waste management scenarios.

References

Bueno, G., I. Latasa and P. J. Lozano. 2015. "Comparative LCA of two approaches with different emphasis on energy or material recovery for a municipal solid waste management system in Gipuzkoa." Renewable and Sustainable Energy Reviews 51:449-459.

Chen, H., W. Jiang, Y. Yang, Y. Yang and X. Man. 2015. "Global trends of municipal solid waste research from 1997 to 2014 using bibliometric analysis." Journal of the Air & Waste Management Association 65(10):1161-1170.

Fernández-Nava, Y., J. del Río, J. Rodríguez-Iglesias, L. Castrillón and E. Marañón. 2014. "Life cycle assessment of different municipal solid waste management options: a case study of Asturias (Spain)." Journal of Cleaner Production 81:178-189.

Gunamantha, M. and Sarto. 2012. "Life cycle assessment of municipal solid waste treatment to energy options: Case study of KARTAMANTUL region, Yogyakarta." Renewable Energy 41:277-284.

Hong, J., X. Li and C. Zhaojie. 2010. "Life cycle assessment of four municipal solid waste management scenarios in China." Waste Management 30(11):2362-2369.

Jeswani, H. K. and A. Azapagic. 2016. "Assessing the environmental sustainability of energy recovery from municipal solid waste in the UK." Waste Management 50:346-363.

Menikpura, S. N. M., J. Sang-Arun and M. Bengtsson. 2016. "Assessment of environmental and economic performance of Waste-to-Energy facilities in Thai cities." Renewable Energy 86:576-584.

Morselli, L., M. Bartoli, M. Bertacchini, A. Brighetti, J. Luzi, F. Passarini and P. Masoni. 2005. "Tools for evaluation of impact associated with MSW incineration: LCA and integrated environmental monitoring system." Waste Management 25(2):191-196.

Parkes, O., P. Lettieri and I. D. L. Bogle. 2015. "Life cycle assessment of integrated waste management systems for alternative legacy scenarios of the London Olympic Park." Waste Management 40:157-166.

Toniolo, S., A. Mazzi, V. G. Garato, F. Aguiari and A. Scipioni. 2014. "Assessing the "design paradox" with life cycle assessment: A case study of a municipal solid waste incineration plant." Resources Conservation and Recycling 91:109-116.

Evaluation of the parameters affecting the photocatalytic reduction of CO_2 over graphene-based composites

H.F.V. Fontes, A.M.T. Silva, J.L. Figueiredo,
J.L. Faria, L.M. Pastrana-Martínez*
Laboratory of Separation and Reaction Engineering - Laboratory of Catalysis and Materials (LSRE-LCM), Faculdade de Engenharia, Universidade do Porto, Rua Dr. Roberto Frias, 4200-465 Porto, Portugal
*lpastrana@fe.up.pt

Keywords: reduced graphene oxide, TiO_2, CdS, photocatalysis, solar fuels, CO_2 conversion.

Introduction

Fossil fuels, one of the most common sources of energy, have a significant impact in the environment, resulting in considerable climate changes (Ozin 2015). Nowadays, new photocatalytic technologies are being developed to transform renewable energy (i.e solar light) to chemical fuels and products, such as carbon dioxide reduction (Dhakshinamoorthy et al. 2012). Selecting an efficient semiconductor is a hard task mainly due to the limited selectivity, recombination of photo-generated charge carriers and and the poor light-harvesting ability (Ola and Maroto-Valer 2015, Sun and Wang 2014). To outcome this limitation, the coupling of a main semiconductor with graphene or its derivatives (e.g., graphene oxide, GO and reduced graphene oxide, rGO) may create a synergistic effect that can improve the overall process efficiency (Sun and Wang 2014, Pastrana-Martínez et al. 2016).

In the present work a series of composites (rGO-TiO_2 or rGO-CdS) with graphene-based materials and titanium dioxide or cadmium sulphide were prepared with different rGO loadings (1.5, 3.0 and 6.0 wt.%) and applied to the photoreduction of CO_2 with water using near UV-Vis ($\lambda \geq 366$ nm) radiation. The photocatalytic runs were carried out in a cylindrical glass immersion photo-reactor (200 mL) with a Heraeus TQ 150 medium-pressure mercury vapor lamp located axially in the reactor and held in a quartz immersion tube. The analysis of CO_2 and reaction products was carried out by gas chromatography (Agilent 7890A GC). The effect of different parameters (such as, pH, reaction temperature and solvent properties), as well as important scientific aspects of the photocatalytic mechanism for graphene based composites, were investigated in detail.

Results and discussion

Results showed that the presence of graphene derivatives in the graphene-based semiconductor composites increased their absorption in the visible spectral range and enhanced the CO_2 photoreduction in aqueous phase. Liquid solar fuels such as methanol (MeOH) and ethanol (EtOH) were the main products under UV-Vis light irradiation. SEM images revealed that when 3.0 wt.% rGO is introduced, the semiconductor nanoparticles are assembled uniformly on the surface of rGO (not shown). The pH of the aqueous medium was identified as the key variable in the product distribution. The synthesized rGO-TiO_2 composites containing 3.0 wt.% rGO revealed high photocatalytic activity for both MeOH and EtOH production at the initial solution pH of 4.0 and 11.0, respectively, exceeding that of the benchmark P25 photocatalyst. The addition of rGO to the CdS-rGO composites up to 3.0 wt.% leads to higher CO_2 conversion than that observed for the bare CdS material (Figure 1) at natural pH. This superior performance was attributed to the synergistic interaction encompassing both interfacial electron-transfer between the two constituent phases, as well as to the lower band-gap energy and maybe to the quenching of photoluminescence.

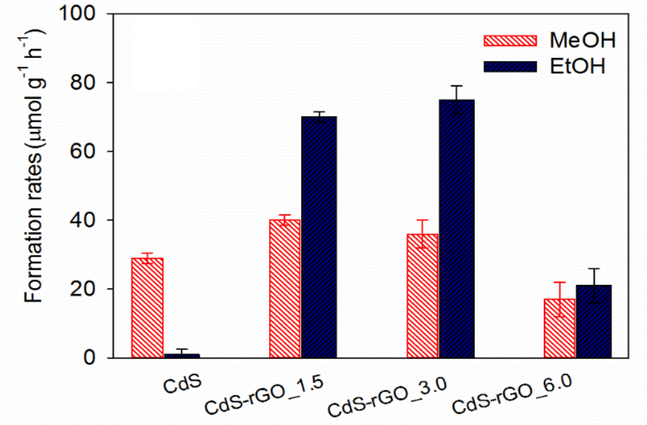

Figure 1. Methanol and ethanol formation rates using CdS and CdS-rGO composites at natural pH and at 180 min.

Acknowledgements

Financial support for this work was provided by “AIProcMat@N2020 - Advanced Industrial Processes and Materials for a Sustainable Northern Region of Portugal 2020”, with the reference NORTE-01-0145-FEDER-000006, supported by Norte Portugal Regional Operational Programme (NORTE 2020), under the Portugal 2020 Partnership Agreement, through the European Regional Development Fund (ERDF) and of Project POCI-01-0145-FEDER-006984 – Associate Laboratory LSRE-LCM funded by ERDF through COMPETE2020 - Programa Operacional Competitividade e Internacionalização (POCI) – and by national funds through FCT - Fundação para a Ciência e a Tecnologia. LMPM and AMTS acknowledge the FCT Investigator Programme (IF/01248/2014 and IF/01501/2013, respectively) with financing from the European Social Fund and the Human Potential Operational Programme.

References

Ozin, G. A. 2015. "Throwing New Light on the Reduction of CO_2." *Advanced Materials* no. 27 (11):1957-1963. doi: 10.1002/adma.201500116.

Dhakshinamoorthy, A., S. Navalon, A. Corma, and H. Garcia. 2012. "Photocatalytic CO_2 reduction by TiO_2 and related titanium containing solids." *Energy & Environmental Science* no. 5 (11):9217-9233. doi: 10.1039/c2ee21948d.

Ola, Oluwafunmilola, and M. Mercedes Maroto-Valer. 2015. "Review of material design and reactor engineering on TiO_2 photocatalysis for CO_2 reduction." *Journal of Photochemistry and Photobiology C: Photochemistry Reviews* no. 24:16-42.

Sun, H., and S. Wang. 2014. "Research advances in the synthesis of nanocarbon-based photocatalysts and their applications for photocatalytic conversion of carbon dioxide to hydrocarbon fuels." *Energy and Fuels* no. 28 (1):22-36. doi: 10.1021/ef401426x.

Pastrana-Martínez, L. M., A. M. T. Silva, N. N. C. Fonseca, J. R. Vaz, J. L. Figueiredo, and J. L. Faria. 2016. "Photocatalytic Reduction of CO_2 with Water into Methanol and Ethanol Using Graphene Derivative–TiO_2 Composites: Effect of pH and Copper(I) Oxide." *Topics in Catalysis* no. 59 (15-16):1279-1291. doi: 10.1007/s11244-016-0655-2.

Performance of a passive Direct Alcohol Fuel Cell

Catarina Moreira[1], Beatriz Braz[1], Vânia Oliveira[1], Alexandra Rodrigues Pinto[1*]

[1]CEFT, Department of Chemical Engineering, Faculty of Engineering University of
Porto, Porto, Portugal;
*apinto@fe.up.pt

Keywords: Direct alcohol fuel cell, methanol, ethanol, electrochemical impedance spectroscopy, polarization curves, performance

Abstract

The direct methanol fuel cells (DMFCs) have been the target of several studies due to its high potential of implementation in portable applications. However, the use of methanol as fuel has some disadvantages and thus ethanol appears as an alternative and more attractive fuel. Ethanol is less toxic and has higher energy density than methanol and can be obtained from renewable sources. Nevertheless, the performance of direct ethanol fuel cells (DEFCs) is lower than the DMFCs due to the sluggish ethanol electrochemical oxidation. To combine the advantages of both fuels, a mixture of methanol and ethanol for two different concentrations and different ethanol and methanol volume ratios were tested in a direct alcohol fuel cell (DAFC) towards its optimization. In this work, electrochemical impedance spectroscopy (EIS) measurements were carried out to identify and quantify the different losses affecting the DAFC performance (activation, ohmic and mass transfer losses).

Introduction

In recent years, the demand for efficient, renewable and sustainable energy sources has been increasing in order to obtain a more diverse use of portable power devices. Direct alcohol fuel cells (DAFCs) appear as a power solution with potential since they offer high energy densities and use liquids as fuel. Direct methanol fuel cells (DMFCs) have been developed and optimized in the last years. However, the use of methanol presents some disadvantages, based on its toxicity, volatility and inflammability. Therefore, ethanol emerges as an alternative and promising fuel due to its non-toxicity, natural availability, renewability and higher power densities (Badwal et al. 2015).

In direct alcohol fuel cells (DAFCs), part of the fuel (methanol or ethanol) fed to the anode permeates through the membrane to the cathode side without being oxidized, due to the concentration gradient between the anode and the cathode, leading to a decrease of the cell performance. Ethanol appears as an attractive fuel to minimize that, since ethanol has low permeation rates mainly due to its larger molecular size (Badwal et al. 2015). Despite that, the performance of the direct ethanol fuel cells is lower that the DMFCs since the electrochemical ethanol oxidation reaction is slower than the methanol one, due to the difficulty of breaking the carbon-carbon bond, resulting in higher anodic overpotentials. In order to take the advantages of both fuels, the use of aqueous solutions with different methanol and ethanol ratios on the anode side of DAFCs have been proposed and tested (Wongyao et al. 2011).

Electrochemical impedance spectroscopy (EIS), a diagnostic tool that has been widely used in studying the electrochemical systems, has been, also, applied by the researchers in the PEM fuel cell field (Yuan et al. 2007). EIS is a method used to perform the diagnose of the fuel cell performance since it allows to identify and quantify separately the individual contributions of each component and process, particularly, it allows the identification and quantification of the activation, charge and mass transfer losses (Mallick et al. 2016).

Materials and Methods

In the experiments, a passive DAFC with an open area of 10.2 cm2 was operated at atmospheric pressure and the temperature was monitored and set near ambient conditions, 25°C. Aqueous ethanol and methanol solutions were fed to the anode at two different concentrations (2 M and 3 M) and different volume ratios of ethanol in the solution were tested (25 %, 50 %, 75 % and 100 %) in order to analyze the effect of the ethanol concentration on the fuel cell power density. Towards a cost reduction, a Nafion 117 membrane with a lower catalyst loading on the anode and cathode electrodes was used. The catalyst used at the anode side was Pt/Ru black with a loading of 3 mg/cm2 and Pt black with a loading of 1.1-1.4 mg/cm2 was used at the cathode. The experimental tests were performed with a commercial fuel cell test station (Zahner Elektrik GmbH &Co. kG) and the effect of the ethanol concentration on the DAFC power output was evaluated through the polarization curves performed galvanostatically and from the EIS measurements. These measurements were carried out on potentiostac mode with an amplitude of 10 mV and a frequency range from 0.01 Hz to 100 kHz. These results were further fitted to an equivalent electric circuit to estimate the different losses that affect the cell performance (activation, ohmic and mass transfer losses).

References

Badwal, S.P.S., S. Giddey, A. Kulkarni, J. Goel, and S. Basu. 2015. “Direct Ethanol Fuel Cells for Transport and Stationary Applications – A Comprehensive Review.” Applied Energy 145: 80–103. Accessed 20 February, 2017. doi:10.1016/j.apenergy.2015.02.002.

Mallick, Ranjan K., Shashikant B. Thombre, Ramani V. Motghare, and Rakesh R. Chillawar. 2016. “Analysis of the Clamping Effects on the Passive Direct Methanol Fuel Cell Performance Using Electrochemical Impedance Spectroscopy.” Electrochimica Acta 215: 150-161. Accessed 15 February, 2017. doi:10.1016/j.electacta.2016.08.080.

Wongyao, N., A. Therdthianwong, and S. Therdthianwong. 2011. “Performance of Direct Alcohol Fuel Cells Fed with Mixed Methanol/ethanol Solutions.” Energy Conversion and Management 52 (7): 2676–2681. Accessed 20 February, 2017. doi:10.1016/j.enconman.2011.01.005.

Yuan, Xiaozi, Haijiang Wang, Jian Colin Sun, and Jiujun Zhang. 2007. “AC Impedance Technique in PEM Fuel Cell Diagnosis - A Review.” International Journal of Hydrogen Energy 32 (17): 4365–4380. Accessed 15 February, 2017. doi:10.1016/j.ijhydene.2007.05.036.

Separation of Hexane Isomers Using ZIF-8

Adriano Henrique[1,2*], José A. C. Silva[1,2] and Alírio E. Rodrigues[2]
[1] School of Technology and Management, Polytechnic Institute of Bragança, Bragança, Portugal;
[2] Laboratory of Separation and Reaction Engineering, Chemical Engineering Dpt., Faculty of Engineering University of Porto, Porto, Portugal.
*adriano_henrique@ipb.pt

Keywords: Hexane isomers, MOF ZIF-8, Multicomponent sorption, Breakthrough curves.

An important process in petrochemical industry is the octane upgrading of gasoline by the separation of paraffin isomers in the range C5/C6. The gasoline obtained from crude oil has a high fraction of linear and monobranched alkanes, which must be converted into isomers with high degree of ramification to improve the research octane number (RON) (Ferreira et al. 2013).

The RON is one of the parameters of gasoline quality and as higher its value, better is the combustion, reducing the tendency of a rapid and inefficient detonation of the hydrocarbons. In other words, the combustion occurs like a smooth explosion, improving the performance of the motor (Mendes et al. 2014).

The separation of n/iso-paraffins is actually realized by the Total Isomerization Process (TIP), which consist in performing the isomerization of normal paraffins, with low levels of RON to mono or di-branched isomers, and then, the paraffins with a high octane degree are separated from the others (Peralta et al. 2012). The research octane number increase as the branching degree of the paraffin increases.

In this way, the objective of this work is to study the separation of hexane isomers using a Metal Organic Framework (MOF) *i.e.* ZIF-8 (Zeolitic Imidazolate Framework) to improve the octane rating of gasoline in TIP processes. The MOF ZIF-8 shows chemical and thermal robustness and its structure consist of a cubic arrangement with 8 sodalite cages in the corner (Park et al. 2006).

In this work, several studies of the adsorption of hexane isomers on ZIF-8 were performed, with an equimolar mixture of: n-hexane (n-HEX), 2,2-dymethilbutane (22DMB), 2,3-dymethilbutane (23DMB), 3-methylpentane (3MP) and 2-methypentane. During those experiments the temperatures and hydrocarbon pressure covers temperatures 373, 423 and 473 K and pressure range 2-10 kPa. Figure 1 shows a typical breakthrough curves for the C6 isomers at hydrocarbon pressure 5 kPa and temperature at 373 K.

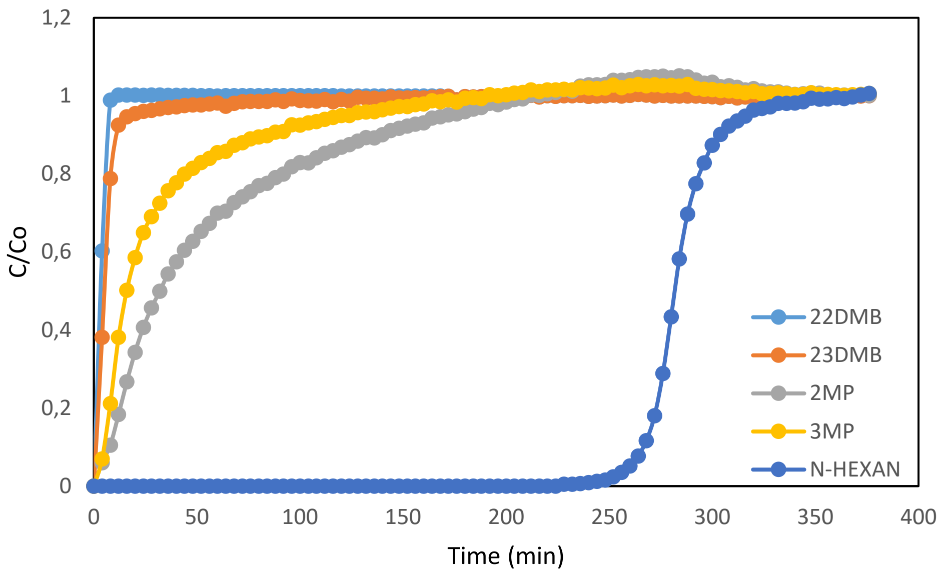

Figure 1. Experimental breakthrough curve of an equimolar mixture of hexane isomers n-HEX/22DMB/23DMB/3MP/2MP at 373 K and hydrocarbon pressure at 5 kPa.

Figure 1 show that ZIF-8 is capable to perform the kinetic separation of hexane isomers in different classes, where the sorption hierarchy is: nHEX>>>2MP>3MP>>23DMB>22DMB. It is also being developed a numerical package using the Method of Lines (MOL) (Schiesser and Griffiths 2009) in MATLAB code to simulate the breakthrough-curves experiments.

From this work, it can be concluded that ZIF-8 can be an efficient separator of hexane isomers in classes: linear>monobrached>dibranched paraffins, with a high impact in the upgrading of actual TIP processes in petrochemical industry.

References

Ferreira, A. F. P., M. C. Mittelmeijer-Hazeleger, M. A. Granato, V. F. D. Martins, A. E. Rodrigues, G. Rothenberg. 2013. “Sieving Di-Branched from Mono-Branched and Linear Alkanes Using ZIF 8: Experimental Proof and Theoretical Explanation.” Phys. Chem. Chem. Phys. 15 (22): 8795–804. Accessed 27 Feb, 2017. DOI: 10.1039/C3CP44381G.

Mendes, P.A.P., A.E. Rodrigues, P. Horcajada, C. Serre, J.A.C. Silva. 2014. “Single and multicomponent adsorption of hexane isomers in the microporous ZIF-8.” Micropor. Mesopor. Mater. 194: 146–156. Accessed 27 Feb, 2017. DOI: 10.1016/j.micromeso.2014.04.009.

Park, K.S., Z. Ni, A.P. Côte, J.Y. Choi, R. Huang, F.J. Uribe-Romo, H.K. Chae, M. O’Keeffe, O.M. Yaghi. 2006. “Exceptional chemical and thermal stability of zeolitic imidazolate frameworks.” PNAS 103 (27):10186–10191. Accessed 27 Feb, 2017. DOI: 10.1073/pnas.0602439103.

Peralta, D., G. Chaplais, A. Simon-Masseron, K. Barthelet, G. D. Pirngruber. 2012. “Separation of C6 Paraffins Using Zeolitic Imidazolate Frameworks: Comparison with Zeolite 5A.” Ind. Eng. Chem. Res. 51: 4692-4702. Accessed 27 Feb, 2017. DOI: 10.1021/ie202995g.

Schiesser, W. E. and G. W Griffiths. 2009. A Compendium of Partial Differential Equation Models. Method of Lines Analysis with Matlab. Cambridge: Cambridge University Press.

Optimizing the Separation of Nadolol Stereoisomers by SMB Chromatography using Chiralpak IA Chiral Stationary Phase

RAMI S. ARAFAH[1], ANTÓNIO E. RIBEIRO[1], ALÍRIO E. RODRIGUES[2] AND LUÍS S. PAIS[1] *
Laboratory of Separation and Reaction Engineering, Associate Laboratory LSRE/LCM
[1]School of Technology and Management, Polytechnic Institute of Bragança
Campus de Santa Apolónia, 5300-253 Bragança, Portugal
[2]Department of Chemical Engineering, Faculty of Engineering, University of Porto
Rua Dr. Roberto Frias s/n, 4200-465 Porto, Portugal
*pais@ipb.pt

Keywords: Simulated moving bed, Chiralpak IA, Nadolol stereoisomers, Optimization of solvent composition.

Abstract

One of the main goals of the pharmaceutical industry nowadays is to have more safe and efficient drugs, mainly by obtaining single enantiomers and stereoisomers. Nadolol is a nonselective beta-adrenergic receptor antagonist (b-blocker) pharmaceutical drug, still commercially used as a racemic pharmaceutical drug.

The main objective of this work is to study the chiral separation of nadolol stereoisomers by simulated moving bed (SMB) chromatography and to optimize its preparative scale separation using an immobilized chiral stationary phase (Chiralpak® IA), particularly to obtain the more retained stereoisomer, referred as the most active, separated from the other three nadolol stereoisomers.

The screening of the solvent composition is carried out to find the best solvent or solvent mixtures to perform the pseudo-binary separation (1+2+3/4) of the more retained stereoisomer using SMB technology: the three least retained components (1, 2 and 3) to be co-eluted in the raffinate, while the more retained component (4) to be eluted pure in the extract outlet stream.

Different mobile phases were identified as promising solvents for the (1+2+3)/4 pseudo-binary preparative separation, using ethanol, methanol, heptane, acetonitrile and tetrahydrofuran mixtures and compositions.

This work presents a comparison of two preparative pseudo-binary separations of nadolol stereoisomers using two different mobile phase compositions: the 100:0.1 methanol-diethylamine and the 25:75:0.1 methanol-acetonitrile-diethylamine.

The use of pure methanol presents good selectivity between the trio 1+2+3 and the more retained component 4. Nevertheless, its use seems to introduce significant retention and a non-linear adsorption behaviour for the more retained component; this can be a drawback at preparative scale. The use of methanol with acetonitrile significantly decreases the non-linear

behaviour, together with a decrease on the retention of the more retained component and, consequently, also a decrease on the selectivity for the (1+2+3)/4 pseudo-binary separation is observed. So, if the loss in selectivity is not significant, the methanol-acetonitrile mixture can be a promising solvent to perform the SMB separation of nadolol stereoisomers.

The comparative study was carried out at different levels, including elution chromatography, adsorption isotherms measurements, breakthrough experiments, and simulated moving bed operation. The SMB separations were carried out on a laboratory scale unit, the FlexSMB-LSRE® [1], equipped with six Chiralpak® IA chromatographic columns.

Using pure methanol as solvent and a 2 g/L total feed concentration, a 100% pure extract was obtained, with a productivity of 0.58 $g_{target\ product}/(L_{bed}.hr)$ and a solvent consumption of 15.8 $L_{solvent}/g_{target}$ product [2]. Using the same feed concentration, a second SMB run was performed using the methanol-acetonitrile mixture. For this mixture, an improvement in the performance parameters was observed: the more retained stereoisomer was 100% pure recovered at the extract outlet stream, with a system productivity of 0.77 $g_{target\ product}/(L_{bed}.hr)$ and a solvent consumption of 9.43 $L_{solvent}/g_{target\ product}$.

This study shows that the 25:75 methanol-acetonitrile mixture is a good alternative to pure methanol for the SMB separation of the more retained nadolol stereoisomer, using a Chiralpak® IA chiral stationary phase.

Acknowledgements

This work is a result of project "AIProcMat@N2020 - Advanced Industrial Processes and Materials for a Sustainable Northern Region of Portugal 2020", with the reference NORTE-01-0145-FEDER-000006, supported by Norte Portugal Regional Operational Programme (NORTE 2020), under the Portugal 2020 Partnership Agreement, through the European Regional Development Fund (ERDF) and of Project POCI-01-0145-FEDER-006984 – Associate Laboratory LSRE-LCM funded by ERDF through COMPETE2020 - Programa Operacional Competitividade e Internacionalização (POCI) – and by national funds through FCT - Fundação para a Ciência e a Tecnologia.

References

[1] Sá Gomes P., Zabkova M., Zabka M., Minceva M., and Rodrigues A. 2010. "Separation of chiral mixtures in real SMB units: the FlexSMB-LSRE®". AIChE J., 56:125–142.

[2] Arafah R., Ribeiro A., Rodrigues A., and Pais L. 2016. "Separation of Nadolol Stereoisomers Using Chiralpak IA Chiral Stationary Phase". Chirality., 28:399-408.

Soybean oil methanolysis catalyzed by highly active CaO obtained from waste shells

R. Risso*, P. Ferraz, S. Meireles, I. Fonseca and J. Vital
Department of Chemistry, Faculty of Sciences and Technology, NOVA University of Lisbon, Lisbon, Portugal
*r.risso@campus.fct.unl.pt

Keywords: Biodiesel, Catalysis, Calcium oxide, Kinetic model.

Calcium oxide (CaO) derived from waste shells of egg, oyster and clam was synthesized and explored as biodiesel production catalyst. Eggshell was subjected to ultrasound irradiation technique and the mollusk shells were subjected to hydration–dehydration cycles to increase the surface area of CaO and improve its catalytic activity. The catalysts were characterized by XRD, TPD-CO_2, TG-DSC, DLS and N_2 adsorption, while the catalytic activity for the methanolysis of soybean oil was evaluated as the maximum reaction rate value (r_{max}). Two cycles of hydration-dehydration with oyster shell derived CaO provided the maximum values of BET surface area (26.4 m^2 g^{-1}) and transesterification rate of this work, the latter was almost 3 times that of the untreated CaO. New considerations for the kinetic of heterogeneous catalysis were proposed and validated in this work.

Scope

Heterogeneous basic catalysts have been widely studied as alternative to reduce the cost and the environmental pollution of biodiesel production process. Test results have indicated the good catalytic performance of CaO, an alkaline oxide generally produced by thermal decomposition of calcium carbonate ($CaCO_3$). Its main drawback is the long reaction time required, which is due to the low basicity and low surface area (Chouhan and Sarma 2011; Viriya-Empikul et al. 2010). In this study, ultrasound irradiation technique was tested with eggshell to reduce the particle size, and hydration-dehydration cycles were tested with oyster and clam shells to develop porosity. A kinetic model based on the Eley-Rideal mechanism was proposed to describe the transesterification catalyzed by resulted CaO.

Powdered CaO was obtained by ball milling and calcination (900 °C, 4 h, N_2 flow) of egg, oyster and clam shells. The eggshell samples (EULT*n*) were subjected to ultrasound irradiation for *n* hours (*n* = 0,1,3,5,7). The oyster and clam shells samples were subjected to 5 hydration-dehydration cycles. In the hydration step, the CaO remains in suspension in water for 4 h. In the dehydration step, the product is dried at 120 °C and calcined, closing the cycle. The catalyst activity was evaluated as the r_{max} value. The experiments carried out in a batch reactor.

Results and Discussion

According to DLS analysis, the average particle diameter of eggshell derived catalyst just milled (EULT0) was 101 nm and decreased with increasing the ultrasound irradiation time up 5 h of proceeding. However, the average size of the EULT7 sample was increased to 115 nm. The particle size distribution of EULT7 indicates the agglomerates formation. The smaller the catalyst particle size, the higher the catalytic activity. The transesterification results obtained (r_{max}) are in accordance with this. Five hours of ultrasound irradiation reduced the CaO particle size by 34%, which resulted in an increase of 56% in the catalytic activity.

As shown in Figure 1, the trend observed in the BET surface areas (S_{BET}), obtained through N_2 adsorption analysis, coincided with changes in the activity of oyster (OHYD*m*) and clam (CHYD*m*) shells derived catalysts subjected to *m* hydration-dehydration cycles (*m* = 0,1,2,3,4,5). For oyster shell, the best result was obtained in the OHYD2 sample: the S_{BET} (26.4 $m^2 g^{-1}$) was about 8 times that OHID0, while its r_{max} value was almost 3 times higher. For clam shell, the best result occurred in the CHYD3 sample: the S_{BET} (11.5 $m^2 g^{-1}$) was 11 times that of CHYD0, and the r_{max} value was almost twice. Oyster shell derived CaO presented better response to the treatment than CaO from clam shell. This difference is probably justified by the difference in the crystalline structures and in the $CaCO_3$ content of both natural shells.

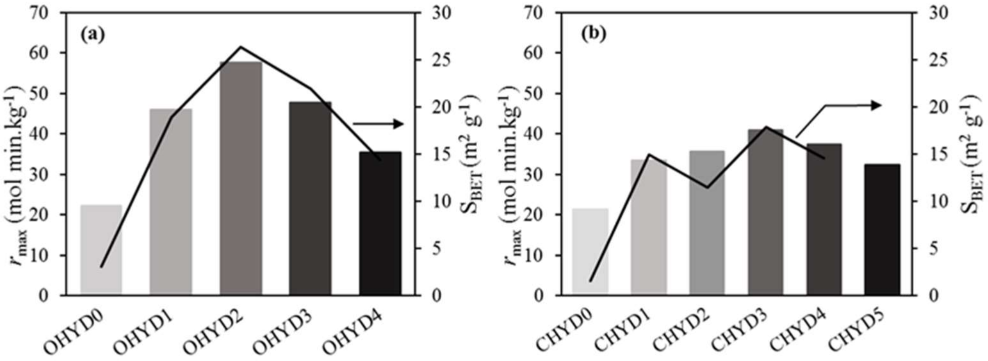

Figure 1. The maximum transesterification rate and the BET surface area of catalysts subjected to *m* hydration-dehydration cycles. (a) Oyster shell derived catalysts (OHYD*m*). (b) Clam shell derived catalysts (CHYD*m*).

In the kinetic study, the conversion of triglyceride into fatty acid methyl esters was assumed to be single step and rate-determining. In order to ensure kinetic control and to avoid interphase mass transfer, a very large excess methanol was used. Consequently, methanol concentration was assumed to be constant. The initial induction period observed in most of the kinetic curves is attributed to the removal of a small layer of $Ca(OH)_2$ formed due to air exposure. The model assumes first order kinetics for that removal and consequent increase of the catalyst active weight. Thus, an activation constant was added to the model that can be related to the reaction induction period.

Conclusions

In the present study, egg, oyster and clam shells were used as renewable sources of CaO catalyst and tested in the transesterification of soybean oil. Ultrasound irradiation and hydration-dehydration cycles were efficient to improve the properties, thus obtaining highly active CaO, which indicates its great potential for use in biodiesel production. The kinetic model calculation had a great agreement with the experimental data.

References

Chouhan, A. P. S., and A. K. Sarma. 2011. “Modern Heterogeneous Catalysts for Biodiesel Production: A Comprehensive Review.” Renewable and Sustainable Energy Reviews 15 (9): 4378–99. doi:10.1016/j.rser.2011.07.112

Viriya-Empikul, N., P. Krasae, B. Puttasawat, B. Yoosuk, N. Chollacoop, and K. Faungnawakij. 2010. “Waste Shells of Mollusk and Egg as Biodiesel Production Catalysts.” Bioresource Technology 101 (10): 3765–67. doi:10.1016/j.biortech.2009.12.079

New Footwear Materials Based on Polyurethane and Polyureas

I.P. Fernandes[1*], M.J. Ferreira[2], M.R. Costa[3] and M.F. Barreiro[1]
[1]Laboratory of Separation and Reaction Engineering – Laboratory of Catalysis and Materials (LSRE-LCM), Bragança Polytechnic Institute, Bragança, Portugal;
[2]Portuguese Footwear Technological Center (CTCP), São João da Madeira, Portugal,
[2]Laboratory of Separation and Reaction Engineering – Laboratory of Catalysis and Materials (LSRE-LCM), Faculty of Engineering, University of Porto, Portugal.
[*]ipmf@ipb.pt

Keywords: Polyurethane-urea, biodegradable, flame retardant, water-based adhesives, footwear.

Introduction

The footwear industry in Portugal is the nucleus of an important cluster of the national economy. According to the strategic lines defined for the sector in its FOOTure 2020 program, the focus is on the development of new materials, with emphasis on bio- and nano-materials, advanced components and devices, new products and designs, equipment and processes. The new materials target specific markets, such as health, wellness, safety and environmentally sustainable footwear, among others. Following this trend, the present work presents the developments carried out in the scope of cooperation between the Laboratory of Separation and Reaction Engineering (LSRE) and the Portuguese Footwear Technological Centre (CTCP), in the field of the development of novel polyurethane-polyureas solutions for application in the footwear sector. More specifically, it addresses the development of solutions for shoe soles modification, aiming to increase the biodegradability and flame resistance and the development of a new process for the synthesis of aqueous polyurethane-urea based adhesives in accordance with recent legal requirements.

Development of solutions for increasing TPU biodegradability

Among the several tested strategies, the increase of the biodegradability of TPU shoe soles was achieved by additivation with 4% (w/w) of natural products (starch, cellulose and lignin). This resulted, for lignin, in materials that presented disintegration at the fourth month, in the test in soil at 58ºC. This formulation was validated in the production of the prototypes presented in figure 1, that have demonstrated to fully comply with the standard specifications imposed for application as shoe soles.

Figure 1. Shoes soles prototypes produced at pilot scale.

Microcellular Polyurethane with flame retardant properties

With respect to the introduction of flame resistance properties, low density microcellular polyurethanes were modified. The tested solutions, which comprised the use of different additives (reactive and inert) and protective coatings, showed that the coating C3 (polyurethane based coating modified with phosphorus compounds, solids content: 45.0%, viscosity: 500 mPa.s) and the inert additive F (ammonium polyphosphate, phosphorus content: 72.0%), introduced at a content of 5% phosphorus (w/w), were the best solutions. The two solutions were tested in the prototypes shown in figure 2, and the boot produced using microcellular PU added with the F additive shown to be in compliance with the standard EN 15090: 2012 specifications (Footwear for Firefighters).

Figure 2. Prototypes produced following the two developed strategies, after flame resistant testing.

NMP-free water-based polyurethane-urea adhesives

In the field of aqueous polyurethane dispersions (PUD) development, the pre-polymer process was studied, and its modification carried out to obtain n-Methyl-2-pyrrolidone free (NMP-free) process in accordance with the legislation, also reviewed in the present work. The products obtained by the two processes (traditional pre-polymer process (PUD-TP) and modified pre-polymer process (PUD-MP)) were compared with commercial counterparts used in a wide range of applications (Table 1). The developed product showed to have a good stability to the presence of electrolytes (the highest one among the tested PUDs) and a stability to temperature comparable to the majority of the tested products.

Table 1. Properties of the laboratorial (PUD-TP and PUD-MP) and commercial dispersions.

PUD	pH	Solids (%)	Viscosity (mPa.s)	Mean particle size (nm)*	Stability to temperature (Nº cycles)	Stability to electrolytes (V_{NaCl} (ml))
Biocol BS 28	7.9	34.7	183.0	Volume: 1301.0(m) Number: 64.0(u)	1 Total coagulation	10.6
Dispercoll U54	8.0	48.0	150.0	Volume: 140.0(u) Number: 133.0(u)	1 Total coagulation	10.6
Cydrothane HP1035	8.8	34.9	80.3	Volume: 229.6(b) Number: 55.3(u)	2 Total coagulation	10.6
PUD-TP	8.4	40.8	152.1	Volume: 107.3(u) Number: 103.0(u)	15 Total coagulation	13.0
PUD-MP	7.2	43.0	18.0	Volume: 121.0(u) Number: 116.0(u)	1 Total coagulation	45.0

***** u – unimodal; m- multimodal.

Acknowledgements

POCI-01-0145-FEDER-006984 (LA LSRE-LCM), funded by FEDER, through POCI-COMPETE2020 and FCT.

Methanolysis of soybean oil in a catalytic membrane reactor. Study of the effect of catalyst loading and polymer crosslinking of CaO/PVA composite membranes

J. Valentim[1*], R. Risso[1], G. Cardoso[1], S. Santos[1], M. H. Casimiro[2], I. Fonseca[1] and J. Vital[1]

[1]Deparment of Chemistry, Faculty of Sciences & Technology, NOVA University of Lisbon; [2]Centre for Nuclear Sciences and Technologies - Instituto Superior Técnico

* j.valentim@campus.fct.unl.pt

Keywords: Biofuel, Chemical Process, Biodiesel, Membrane Reactor, CaO, PVA.

Nowadays the world aims to alternatives for fossil fuels due to crude oil prices and environmental issues. Biodiesel is an alternative but the actual technology make it more expensive than fossil fuels. Using a membrane reactor, with a basic catalyst, would be possible to produce biodiesel with a very good grade and the simultaneous separation of the by-product glycerol. The catalytic assays achieved high conversions and an efficient separation behaviour.

Introduction

Biodiesel is biodegradable and made from biological resources like vegetable oils, animal fats or used cooking oils (Marinković 2016). The transesterification reaction converts triglycerides into fatty acid alkyl esters in the presence of an alcohol and a catalyst (Maia Filho 2016). Basic catalysts provide a low reaction time and more friendly conditions. Homogeneous basic catalysts cannot be reused or regenerated, which requires more separation steps and large amounts of water in the purification step (Marinković 2016). The development of a contactor membrane reactor would increase the reaction selectivity, and the catalytic membrane can also be used to promote the contact between two immiscible reactants in different phases. For this study propose, a PVA catalytic membrane loaded with eggshell CaO and cross-linked with HDI, was developed.

Materials and Methods

Preparation of catalytic membranes

PVA (≥ 99% hydrolyzed) was dissolved in a 20 wt% DMSO and 80 wt% DMF solution. CaO was then suspended in the solution, which was sonicated for 30 min at 80 °C. The mixture was heated at 105 °C and agitated for 15 min. After that, the suspension was poured into a teflon dish and cooled until a viscous membrane was formed. The cooled membrane was then immersed in a 20% DMSO/80% DMF HDI (cross-linker) solution. After 24 h, the cross-linked membrane was washed with methanol in order to change the swelling solvent. Membranes were identified according to the cross-linker and the catalyst amount and codified as PVAESCxxHDIyy, where ESC refers to ”EggShell Calcined” and HDI to the cross-linker, ”xx” and ”yy” refers to the percentage of each one relative to PVA.

Membrane’s characterization

The catalytic membranes were characterized by FTIR and SEM.

Catalytic experiments

The reactor is composed by two chambers separated by the membrane. Methanol (MeOH) is continuously distilled during the process and feed to the reactor's methanol chamber. The MeOH permeated to the oil side is also distilled and added to the methanol distillation flask. To start the each experiment, the oil flask was loaded with 75 mL of soybean oil and 15 mL of undecane as GC standard. The MeOH flask was loaded with 75 mL of dried methanol and 1 mL of benzyl alcohol as GC standard. To evaluate the conversion and the permeability towards the membrane, samples were taken from the oil flask and the distillate flask and analysed by GC.

Discussion

Membrane's characterization

Spectra analysis, allowed the calculation of the real cross-linking. Membranes PVAESC25HDI10 and PVAESC25HDI14 were used as standard to compare results. Most of membranes had an error less than 2%. SEM analysis allowed understanding how the catalyst deposits on the membrane surface and helped to develop a diffusion-kinetic model.

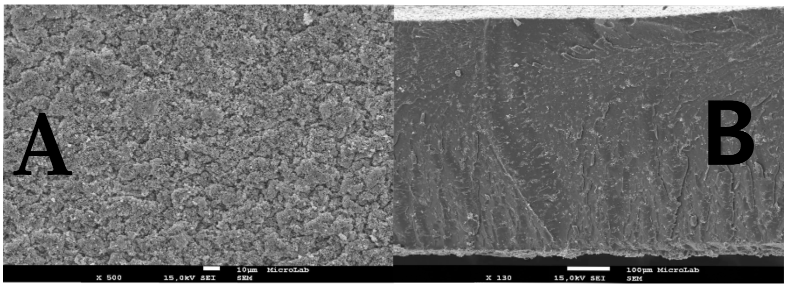

Figure 1. SEM images of membrane PVAESC25HDI14 surface (A) and lateral cut (B).

Catalytic Assays

With catalytic assays and application of a diffusion-kinetic model, it was possible to calculate the initial diffusivity, maximum reaction rate and the permeability of glycerol, FAME and triglycerides through the membrane.

Conclusions

The highest catalytic activity was achieved with the membrane PVAESC15HDI12. With the membrane PVAESC20HDI14 it was possible to achieve a conversion near 95%, which is similar to the conversion obtained with conventional processes, with the simultaneous complete separation of the formed glycerol.

References

Maia Filho, D.C., Salim, V.M.M. & Borges, C.P., 2016. Membrane contactor reactor for transesterification of triglycerides heterogeneously catalysed. Chemical Engineering and Processing: Process Intensification, 108, pp.220–225.

Marinković, D.M. et al., 2016. Calcium oxide as a promising heterogeneous catalyst for biodiesel production: Current state and perspectives. Renewable and Sustainable Energy Reviews, 56, pp.1387–1408.

Mixing of Similar Fluids in Mesomixers

M. A. Brito[1*], C. P. Fonte[2], M. M. Dias[1], R. J. Santos[1], J. C. Lopes[1]
[1] Laboratory of Separation and Reaction Engineering – Laboratory of Catalysis and Materials (LSRE-LCM), Faculty of Engineering, University of Porto, Portugal;
[2]School Chemical Engineering and Analytical Science, Manchester, UK
[*]mbrito@fe.up.pt

Keywords: Mixing, Plate/plate rotational geometry, Computational Fluid Dynamic, Similar fluids

Opposed-jets mixers, such as Confining Impinging Jets (CIJs) and T-jets reactors, are generally small-scale devices where two liquid streams are contacted in a mixing chamber. These devices have many applications in industrial processes, such as in Reaction Injection Moulding (RIM). Nowadays, these mixers are increasingly used in different industrial processes because of their short mixing times, on the order of 10^1 to 10^2 milliseconds (Santos and Sultan 2013). Due to the short mixing times, molecular diffusion is not expected to play a major role and thereby mixing occurs mainly due to stretching and folding of the liquids, forming a lamellar structure (Fonte 2012).

In 1978, Ottino, Ranz, and Macosko (1978) introduced the lamellar model which describes the mechanisms for the decrease of the thickness of lamella of two fluids under a given velocity gradient. When two liquids are disposed in layers, or lamella, shear stretches out these fluids striating the lamella. Thereby, Ottino, Ranz, and Macosko (1978) defined the concept of striation thickness, $s = \frac{\delta_A + \delta_B}{2}$, where δ_A and δ_B are the thickness of each lamella of each component. The thickness of the lamella should be brought down to values that allow chemical reaction to fully occur without mass transfer limitations: in the case of RIM this thickness is around 1 $\mu\mathrm{m}$. RIM machines have production rates of 10 to 100 kg/min, even for industrial reactors with a volume of approximately 50 cm^3. It means that it is possible to work at three different flow regimes: at $\mathrm{Re} < 105$, the flow is laminar with poor mixing dynamics; at $105 \leq \mathrm{Re} \leq 110$, there is a disturbance of the two jets' interface and the formation of vortices in the chamber; at $110 \leq \mathrm{Re} \leq 600$, the regime is laminar chaotic with good mixing dynamics (Fonte 2012). So, since the production rates are high, formulation development for this process is quite challenging in a laboratory, being generally made in pilot scale machines (Ranz 1986).

Mixing in CIJs and T-jets can be studied from flows where there is a well-defined direction for shearing, as those used in rheometry, using a small volume of liquid, approximately 1 cm^3. This type of flow leads to quite homogenous mixing scales between two fluids throughout the flow domain, which is particularly useful for generating data for this kind of mixers.

In this work mixing in a plate/plate rotational rheometer is studied using 3D Computational Fluid Dynamics (CFD) simulations. The goal of this work is the determination of striation thickness values achieved during the mixing in a plate/plate rotational rheometer.

Materials and Methods

Plate/plate rheometers have two circular plates, one plate is fixed and the other rotating. Mixing in these devices is studied using 3D Computational Fluid Dynamics (CFD) simulations. The simulated fluid domain consists of two plates with a diameter of 10 mm spaced by 1 mm and was discretized with $6.6\text{x}10^6$ elements with an edge of 0.05 mm.

The boundary conditions imposed to simulation are the velocities of the plates, where the bottom of the cylinder is a stopped plate and the top is rotating. The angular speed of the top plate is 0.01 rad/s. On the other hand, the side walls have zero shear stress condition. The working fluids were two similar fluids with the physical properties of glycerol.

Results and discussion

Figure 1 shows a cylinder with two fluids: black and white. Initially, the two phases are side by side (Figure 1a). When the top plate starts to rotate, the fluids are stretched out and a lamellar structure is formed. Figure 1b and 1c show the cylinder at different states of rotation of top plate. After one turn, one stria is formed (Figure 1b) while two strias are formed in the end of two turns. Note that each stria is composed by a white and a black strip.

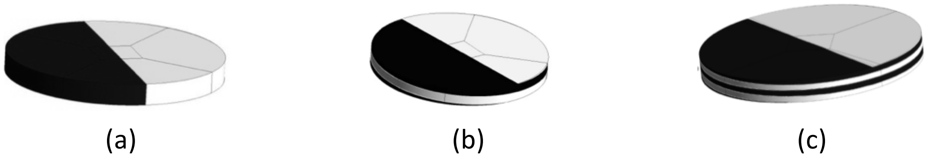

Figure 1. Plate/plate geometry in different states of rotation (a) initial time (b) one turn (c) two turns.

For this system, the striation thickness can be determined as $s = \frac{h}{2n}$, where h is the space between plates and n is the number of turns. Therefore, in mixing that occurs in a plate/plate geometry, the rate of reduction of mixing scales and the generation of the interfacial area are entirely set by the top plate rotational speed. This method enables to set the exact evolution of mixing scales on the product development stage, which makes the production scale-up to industrial machines a direct process without changes on the material properties.

Conclusions

This work shows that plate/plate rheometers can set an exact evolution of mixing scales between two fluids following the law: $s = \frac{h}{2n}$. This well-defined flow can be used for product development in challenging conditions that occur in industrial devices, such as the abovementioned RIM process. The main advantage is the use of a small volume of reactants that minimizes the costs of formulation development.

References

Fonte, C P. 2012. "Mixing Studies with Impinging Jets: PIV/PLIF Experiments and CFD Simulation." PhD, Chemical engineering department, Faculty of Engineering of The University of Porto.

Ottino, J M, W E Ranz, and C W Macosko. 1978. "A lamellar model for analysis of liquid-liquid mixing." *Chemical Engineering Science* 34:877-890.

Ranz, W. 1986. "Analysis of Reaction Processes in which microscopic Heterogeneities Appear: Scale-Up and Scale-Down of Polymerization Reactions." *Industrial & Engineering Chemistry Fundamentals* 25:561-565.

Santos, R J, and M A Sultan. 2013. "State of the Art of Mini/Micro Jet Reactors." *Chemical Engineering and Technology* 36 (6):937-949.

The axial dispersion performance of a novel oscillatory flow reactor – a design of experiments approach

P. Cruz*, F. Rocha and A. Ferreira
[1] LEPABE – Laboratory for Process Engineering, Environment, Biotechnology and Energy, Faculty of Engineering of the University of Porto, Porto, Portugal
*pcruz@fe.up.pt

Keywords: Oscillatory flow reactor, Mixing, Residence time distribution, Axial dispersion

The oscillatory flow reactor (OFR) consists of a tubular device containing evenly spaced baffles which are transversely assembled to a periodically oscillating flow. The mixing is provided by the interaction of the fluid with the constrictions, which may be designed with different configurations according to the application (McDonough, Phan, and Harvey 2015). The novel OFR presented in this work was designed with smooth periodic constrictions and differs from the typical integral baffle configuration in the cross-section format, which is rectangular rather than circular. This new feature was developed to improve the suspension and flow of solids in continuous processing operations, such as crystallization. To properly characterize the mixing efficiency of the present device, residence time distribution (RTD) experiments were conducted by monitoring the response of a pulse dye tracer. A full factorial experiment was designed through a design of experiments (DoE) approach to assess the effects of different hydrodynamic conditions on the axial dispersion coefficient, D.

The present OFR consists of a 3.3 m long Perspex® plate-like reactor, with an internal diameter of 8 mm in the straight section and 3.3 mm in the constriction, and a total volume of 145 mL. A continuous net flow of deionized water was injected into the reactor by a peristaltic pump (BT300-2J, YZ1515X head, Longer Pump) and oscillated by a linear motor (Festo). At time zero, 1 mL of a 0.2 g/L aqueous tracer solution (Indigo carmine, Merck) was injected by a syringe pump (NE-4000, New Era Pump Systems, Inc.) with an inlet flowrate of 25 mL/min at 25 cm downstream of the water inlet. The tracer concentration was measured in the reactor outlet by a spectrometer (Spec Res+ UV/Vis, Sarspec) using an absorbance integral in the wavelength range of 585-635 nm. The axial dispersion coefficient was obtained by fitting the experimental data to a plug flow with axial dispersion model (Zheng and Mackley 2008). Two different levels of net flow Reynolds number, Re_n, frequency of oscillation, f, and amplitude of oscillation, x_0, were used. Each experimental condition was performed in triplicate. The Minitab® 17.3.1 software was used to design the full factorial experiment and to analyse the results.

Several DoE analysis tools were obtained from the Minitab® software, including the plots of main effects, interactions, Pareto, normal probability and normal probability of residuals. The main effects plot shows that all the three input variables have significant effects on D: i) Re_n has a positive effect; and ii) f and x_0 have negative effects. This means that D is lower for low levels of Re_n and high levels of f and x_0, and therefore a high level of mixing intensity may be afforded without compromising the axial dispersion within the reactor. In addition, the interactions plot shows that Re_n and x_0 have a strong interaction, f and x_0 have a weak interaction and Re_n and f do not interact at all. The Pareto plot (Figure 1) and the normal probability plot provide us further detail on this analysis. All the effects, except the interaction of Re_n with f, were found significant with a confidence interval of 95 %, being $\mathrm{Re_n}$ the most important input variable affecting D. These results were confirmed by the normal probability plot and are in accordance with previous findings.

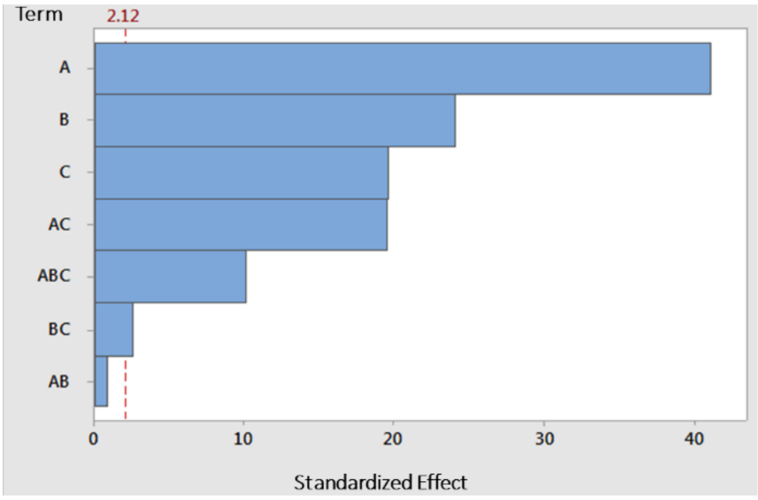

Figure 1. Pareto plot of effects with a confidence interval of 95 %. (A – $\mathrm{Re_n}$, B – f, C – x_0).

A regression model was formulated considering the significant effects and the key assumption of normal distributed data was verified on the normal probability plot of residuals. The main effects and interactions were also studied with respect to the axial dispersion coefficient variability, as Ln(σ), where σ is the standard deviation for the three replicates of each experimental condition. It was found that the interaction of $\mathrm{Re_n}$ and f, which has no effect on the axial dispersion coefficient itself, is the only significant effect on variability. The DoE approach was thus proved effective in providing substantial conclusions with a minimum number of experimental runs.

Acknowledgments

This work was financially supported by: I) Project UID/EQU/00511/2013-LEPABE (Laboratory for Process Engineering, Environment, Biotechnology and Energy – EQU/00511) funded by FEDER funds through COMPETE2020 – Programa Operacional Competitividade e Internacionalização (POCI) – and by national funds through Fundação para a Ciência e a Tecnologia (FCT); II) Project POCI-01-0145-FEDER-016816 (PTDC/QEQ-PRS/3787/2014) funded by the Project 9471 – Reforçar a Investigação, o Desenvolvimento Tecnológico e a Inovação, by the European Regional Development Fund (ERDF) and by national funds through FCT; III) IF exploratory project [IF/01087/2014] funded by FCT. P. Cruz gratefully acknowledges doctoral scholarship [SFRH/BD/119391/2016] from FCT. A. Ferreira is an Investigador FCT.

References

McDonough, J. R., A. N. Phan, and A. P. Harvey. 2015. "Rapid Process Development Using Oscillatory Baffled Mesoreactors – A State-of-the-Art Review." Chemical Engineering Journal 265. Elsevier B.V.: 110–21. doi:10.1016/j.cej.2014.10.113.

Zheng, Mingzhi, and Malcolm Mackley. 2008. "The Axial Dispersion Performance of an Oscillatory Flow Meso-Reactor with Relevance to Continuous Flow Operation." Chemical Engineering Science 63: 1788–99. doi:10.1016/j.ces.2007.12.020.

Poster Session

Continuum mechanical model for cross-linked actin networks with contractile bundles

Ferreira, J. P. S.* †, Parente, M. P. L. *† and Natal Jorge R. M. *†

*Instituto de Engenharia Mecânica e Gestão Industrial (INEGI)
University of Porto
† Mechanical Engineering Department, Faculty of Engineering (FEUP)
University of Porto, Porto

e-mail: e-mail: j.ferreira@fe.up.pt, mparente@fe.up.pt, rnatal@fe.up.pt

Keywords: Continuum Mechanics, Actin Networks, Myosin, Contraction, Micro-sphere

Abstract

The actin cytoskeleton is involved in a large range of cellular processes including morphogenesis and motility. In the context of a mechanical approach to cell biology, there is a close relationship between cellular function and mechanical properties, there is a tight coupling between biochemical and mechanical signals. In recent years, an increasing amount of attention has been given to the integration of this knowledge into the development of constitutive models. Therefore, in this work we use a microstructurally motivated continuum model to describe the passive mechanical properties of in vitro crosslinked actin networks. Virtual experiments qualitatively predict how the contraction influence the network response, which is to a large extent governed by the time-scale of applied deformations/forces.

References

[1] Unterberger, M.J., Schmoller, K.M., Wurm, C., Bausch, A.R., Holzapfel, G.A.: Viscoelasticity of cross-linked actin networks: Experimental tests, mechanical modeling and finite-element analysis. Acta Biomaterialia 9(7), 7343–7353 (2013)

[2] Hai, C.M., Murphy, R.A.: Cross-bridge phosphorylation and regulation of latch state in smooth muscle. American Journal of Physiology - Cell Physiology 254(1), C99– C106 (1988)

[3] Murtada, S.I., Kroon, M., Holzapfel, G.A.: A calcium-driven mechanochemical model for prediction of force generation in smooth muscle. Biomechanics and Modeling in Mechanobiology 9(6), 749–762 (2010)

[4] Miehe, C.: A micro-macro approach to rubber-like materials. Part I: the non-affine micro-sphere model of rubber elasticity. Journal of the Mechanics and Physics of Solids 52(11), 2617–2660 (2004)

[5] Holzapfel, G.A., Ogden, R.W.: Elasticity of biopolymer filaments. Acta Biomaterialia 9(7), 7320–7325 (2013)

The potential of *Ganoderma lucidum* to develop cosmeceutical formulations behind its nutritional value

O. Taofiq[1,2,3,*], S.A. Heleno[1,3], L. Barros[1,3], R. C. Calhelha[1], M.J Alves[1], A.M. González-Paramás[2], M.F. Barreiro[3], I.C.F.R. Ferreira[1]
[1]Mountain Research Centre (CIMO), ESA, Bragança Polytechnic Institute, Bragança, Portugal;
[2]GIP- USAL, Unidad de Nutrición y Bromatología, Faculty of Pharmacy, University of Salamanca, Salamanca, Spain;
[3]Laboratory of Separation and Reaction Engineering – Laboratory of Catalysis and Materials (LSRE-LCM), Bragança Polytechnic Institute, Bragança, Portugal.
*taofiq.oludemi@ipb.pt

Keywords: *Ganoderma lucidum;* Nutritional composition; Bioactive compounds; Cosmeceuticals

There is a renewed interest in the discovery of novel bioactive extracts and compounds from natural sources for several industrial purposes (medicinal, drug discovery, food, nutraceuticals and cosmeceuticals). In particular, mushrooms have well reported nutritional and bioactive composition and have been utilised as food, as well as in the design of nutraceuticals and cosmeceuticals (Taofiq et al., 2016).

Ganoderma lucidum (Curtis) P. Karst. is one of the most widely known medicinal mushrooms because of its well reported bioactive, nutritional and chemical composition, including different compounds (e.g., phenolics and triterpenoids) that have been responsible for the overall health promoting benefit associated with their consumption (Zhao et al., 2016).

In the present work, *G. ludicum* samples were characterized in terms of nutritional and chemical composition (macronutrientes such as proteins, fat and total carbohydrates, total terpenoids and polysaccharides, energetic value, sodium chloride, free sugars, fatty acids and tocopherols). Thereafter, this mushroom species was used to obtain Soxhlet ethanolic extracts that were evaluated for their bioactive properties (antioxidant, anti-inflammatory, antityrosinase, cytotoxic and antimicrobial activities) and compounds (phenolic compounds and triterpenoids). Finally, the obtained extracts were incorporated in a cosmetic base cream (100 mg of extract per gram of base cream) and the bioactive properties of the final formulations were also tested.

G. lucidum proved to be a good source of carbohydrates (88.4 ± 02 g/100 g dw) and proteins (6.72 ± 0.04 g/100 g dw), presenting a low fat (2.50 ± 0.02 g/100 g dw) and caloric contribution (201 ± 3 g/100 g dw). Fructose was the only free sugar found and linoleic acid was the major fatty acid and tocopherol (141 ± 7 μg/100 g dw) being α and δ isoforms. Terpenoid, triterpenoid and polysaccharide contents were 27.2 ± 0.7 mg equiv. linalol/g dw, 5.6 ± 0.5 mg equiv. ursolic acid/g dw and 15.4 ± 0.2 mg equiv. starch/g dw, respectively.

After HPLC-DAD-ESI/MS analysis, the Soxhlet ethanolic extract revealed the presence of 26 triterpenic acids, being ganoderic acid H one of the most abundant compounds, and three phenolic acids (protocatechuic, *p*-hydroxibenzoic and syringic acids). It also showed high antioxidant (EC_{50} 0.73 ± 0.01 and 0.15 ± 0.01 mg/mL for radical scavenging activity and reducing power, respectively), antityrosinase (EC_{50} 2.81± 0.01 mg/mL), cytotoxic (cell lines: MCF7- GI_{50} 61 ± 4 μg/mL; NCI-H460- 64 ± 3; HepG2- 68.44 ± 0.08 μg/mL; Hela- 73 ± 2 μg/mL) and antimicrobial

(MICs up to 10 mg/mL against *Escherichia coli*, *Enterococcus faecalis*, methicillin-sensitive *Staphylococcus aureus* and methicillin-resistant *S. aureus*) activities. The extract did not show cytotoxicity for non-tumor cells (GI_{50} > 400 µg/mL).

The cosmeceutical formulation prepared with the extract still presented antioxidant, anti-tyrosinase and antimicrobial activities while the colour parameters using the *L*a*b** system were 70.3 ± 0.6, 12.1 ± 0.5, 32.9 ± 0.9, respectively, suggesting that the lightness of the cosmeceutical formulation was closely followed by its yellowness. The formulation presented a pH of 4.61± 0.02, which is considered a favourable pH in cosmeceutical's design.

Overall, behind the important nutritional value of *G*. *lucidum* mushroom that can be important for nutraceutical's development, its ethanolic extract showed several bioactive properties ideal to be explored in the development of cosmeceutical formulations.

Acknowledgements

The authors are grateful to the Foundation for Science and Technology (FCT, Portugal) and FEDER under Programme PT2020 for financial support to CIMO (UID/AGR/00690/2013) and L. Barros grant (SFRH/BPD/107855/2015) S.A.Heleno grant (SFRH/BPD/101413/2014). This work was also financially supported by: Project POCI-01-0145-FEDER-006984 – Associate Laboratory LSRE-LCM funded by FEDER through COMPETE2020 - Programa Operacional Competitividade e Internacionalização (POCI) – and by national funds through FCT and project NORTE-01-0145-FEDER-000006, supported by Norte Portugal Regional Operational Programme (NORTE 2020), under the Portugal 2020 Partnership Agreement, through the European Regional Development Fund (ERDF).

References

Taofiq, O., González-Paramás, A. M., Martins, A., Barreiro, M. F., & Ferreira, I. C. F. R. (2016). Mushrooms extracts and compounds in cosmetics, cosmeceuticals and nutricosmetics-A review. Industrial Crops and Products, 90, 38–48. https://doi.org/10.1016/j.indcrop.2016.06.012

Zhao, X. R., Zhang, B. J., Deng, S., Zhang, H. L., Huang, S. S., Huo, X. K., Wang, C., Liu, F., Ma, X. C. (2016). Isolation and identification of oxygenated lanostane-type triterpenoids from the fungus *Ganoderma lucidum*. Phytochemistry Letters, 16, 87–91. https://doi.org/10.1016/j.phytol.2016.03.007

Chemical changes in heat-treated *Eucalyptus urophylla* wood

Túlio A.S. Vieira[1,2*], Sónia A.C. Carabineiro[1], Paulo F. Trugilho[2],
Rodrigo Simetti[2], Breno Assis Loureiro[2]
[1] Lab. Catalysis & Materials (LCM), Associate Lab. LSRE/LCM, Faculty of Engineering, University of Porto, Portugal
[2] Science and Technology of Wood, Forest Sciences Department, UFLA - Federal University of Lavras, MG, Brazil
*tuliovieira19@hotmail.com

Keywords: Lignin, Holocellulose, Extractives.

Abstract

A thermal treatment of wood aims to change its chemical properties, resulting in improved dimensional stability and more resistance to degrading agents. This study aimed to evaluate the chemical changes produced in wood when treated between 140 °C and 250 °C. Above 220 °C, an increase in the amount of lignin and extractives was found, along with a decrease in the amount of holocellulose. The amount of carbon increased with temperature increase, while the amounts of hydrogen and oxygen decreased with temperature increase.

Introduction

The thermorretification is a thermal process that uses temperatures between 160 and 250 °C. It degrades mainly the polyoses of wood (Brito et al. 2008). However, the lignin and cellulose structures also show some changes (Tumen et al. 2010). This process improves the dimensional stability and biological resistance, reducing hygroscopicity and mechanical resistance of the material (Araújo et al. 2012). The purpose of this research was to evaluate the chemical changes produced in the *Eucalyptus urophylla* wood, thermorretified at different temperatures.

Materials and Methods

In this work, wood samples of the MN-463 clone (natural hybrid of *Eucalyptus urophylla*) were used. The materials were dried in an oven for 24h and thermorretified at 140, 160, 180, 200, 220 and 250 °C for 3 h, in air and atmospheric pressure. Elemental analyses were carried out to determine the amount of carbon (C), hydrogen (H), nitrogen (N) and sulphur (S). The amount of oxygen (O) was obtained by subtraction of the previous values from 100(%). The amount of extractives was determined according to the TAPPI 204 om-88 regulation. The amount of insoluble lignin was determined by the modified Klason method (Gomide, Demuner; 1986). A reading of the Klason filtered (above) was made in a spectrophotometer (Goldischimid; 1971) to determine the soluble lignin. The total lignin was the sum of the former two. The amount of holocellulose was determined by subtracting from 100(%) the sum of total lignin and extractives.

Discussion

Table 1 shows the results obtained for the amounts of carbon, hydrogen, nitrogen, sulphur, oxygen, extractives, lignin and holocellulose present in wood, at different temperatures. Only treatments carried out at 220 and 250 °C showed a change in the composition. The amounts of extractives and lignin increased at those temperatures, while the amount of holocellulose decreased. That is related to the thermal stability of the components present in the structure of the wood, since hemicelluloses degrade at temperatures above 200 °C, originating substances soluble in ethanol/toluene (Brito et al. 2008).

Regarding the elemental composition, the increase in the amount of carbon and reduction of the amount of oxygen and hydrogen are explained by the larger amount of hydroxylic groups present in holocellulose. Lower amount of nitrogen and sulphur were found, but lignin, the most resistance to the degradation process, showed a larger amount of carbon in its structure (Zanuncio et al. 2014).

The reduction in the amount of holocellulose with temperature increase is linked to the reduction of OH- groups (responsible for the hygroscopicity of wood). This leads to a decrease in capacity of wood to absorb moisture (Brito et al. 2008).

Table 1. Chemical and elemental composition of heat treat treated *Eucalyptus urophylla* wood. The average values with the same letter (a-d in the columns) do not show significant changes in Tukey test (p>0,05). Values in parenthesis display the coefficient of variation.

	C (%)	H (%)	N (%)	S (%)	O (%)	Extractives (%)	Lignin (%)	Holocellulose (%)
Blank	47,43 d (2,55)	5,80 ab (2,30)	1,09 ab (3,83)	0,00	45,67 A (2,89)	3,82 b (1,54)	24,75 c (3,25)	71,43 a (1,21)
140	48,70 cd (2,06)	5,98 ab (2,11)	1,05 a (4,36)	<0,01	44,27 A (2,61)	3,43 b (0,93)	23,95 c (4,06)	72,62 a (1,38)
160	50,27 cd (3,13)	6,03 a (2,62)	1,09 ab (4,22)	<0,01	42,61 Ab (4,15)	3,76 b (8,09)	25,01 c (5,12)	71,23 a (1,64)
180	50,95 bc (1,63)	5,54 bc (2,08)	0,96 b (0,00)	<0,01	42,55 Ab (2,21)	3,28 b (15,50)	23,03 c (1,28)	73,69 a (0,33)
200	51,26 bc (1,73)	5,18 c (6,17)	1,07 ab (4,60)	0,00	42,48 Ab (2,68)	3,58 b (2,63)	24,3 c (9,63)	72,12 a (3,13)
220	54,19 b (0,65)	5,14 c (0,57)	1,07 ab (3,24)	0,00	39,60 Bc (0,91)	5,06 a (2,51)	32,31 b (1,47)	62,63 b (0,96)
250	58,16 a (3,22)	4,66 d (3,32)	1,10 a (6,36)	0,00	36,07 C (5,67)	4,59 a (8,34)	41,06 a (3,75)	54,34 c (2,82)

Conclusions

The increase in thermorretification temperature increased the amounts of lignin, extractives and carbon, and the reduction of the amounts of holocellulose, hydrogen and oxygen.

Acknowledgements

TASV is grateful to EBWplus/Erasmus Mundus grant n°2014-0982. SACC thanks Fundação para a Ciência e Tecnologia (FCT) for financial support (IF/01381/2013/CP1160/CT0007, Investigador FCT), with financing from the European Social Fund and the Human Potential Operational Program. This work was supported by Project POCI-01-0145-FEDER-006984 – Associate Lab. LSRE-LCM funded by FEDER through COMPETE2020 – POCI – and by national funds through FCT.

References

Brito, J. O., F. G. Silva, M. M. Leão, and G. Almeida. 2008. Bioresource Technology 99 (18): 8545–48. doi:10.1016/j.biortech.2008.03.069.

Araújo, S.O., B.R. Vital, Z.M.S.H. Mendonza,T.A.S. Vieira, A.C.O. Carneiro. 2012. Scientia Forestalis. 40, 327-336.

Goldschimid, O. Ultraviolet spectra.1971. In: Sarkanen, K. V.; Ludwig, C. H. Lignins: occurrence, formation, structure and reactions. New York: John Wiley & Sons p.241-298.

Gomide, J. L.; Demuner, B. J. 1986. O Papel, v.47, n.1, p.36-38.

Tumen, I., D. Aydemir, G. Gunduz, B. Uner, and H. Cetin. 2010. BioResources 5: 1936–44.

Zanuncio, A. J. V., J. R. C. Nobre, J. P. Motta, and P. F. Trugilho. 2014. Revista Árvore 38 (4): 765–70.

Liquid-liquid extraction of biomolecules in biodegradable ATPS: phase equilibria and partitioning

Kamila Wysoczanska, Eugénia A. Macedo*

Laboratory of Separation and Reaction Engineering – Laboratory of Catalysis and Materials (LSRE-LCM), Faculty of Engineering, University of Porto, Rua Dr. Roberto Frias, 4200-465 Porto, Portugal

*eamacedo@fe.up.pt

Keywords: ATPS, partitioning, phase equilibria, biomolecules

Abstract

Aqueous two-phase partitioning is a separation technique, with very low environmental impact, considered as an accurate and very adequate methodology for purification of biomolecules. For optimal separation, however, it is of crucial importance to know the biomolecules' partitioning behaviour, and which parameters are relevant, regardless of scale – laboratorial or industrial. The limited comprehension of the molecular mechanisms behind the solute partitioning has narrowed the incorporation of aqueous two-phase systems (ATPS) at a large industrial scale. In order to fully understand the phenomena that rule partitioning, as well as to obtain the full set of extraction information that relates to it, a high number of complex and time consuming experiments and calculations are needed.

So far, studies have been conducted on the two major types of ATPS: polymer + polymer, polymer + salt, and it has been proven that these systems are highly suitable for the gentle separation of many biocompounds. However, ATPS formed by a polymer and a salt are usually more adopted due to the larger difference in densities, higher selectivity, lower viscosity, and the lower cost of salts compared to polymers.

The main goal of this work is to study (1) the liquid-liquid phase equilibria and (2) the partitioning of different biomolecules in ATPS that contain biodegradable components, polyethylene glycol (PEG) and organic salts (citrates, tartrates) [1], [2]. PEG was chosen as it has many advantages: low toxicity, biodegradability, low volatility, and infrequent occurrence of unwanted side reactions. Considering that PEG of higher molecular weight possesses also a higher density, and this can be not very convenient at an industrial level, several PEG with different molecular weights were chosen for the experiments. Due to the fact that citrates and tartrates, when combined with an inexpensive PEG polymer, present high heterogeneous regions on biphasic diagrams, a lower salt concentration may be used to obtain two immiscible phases. This leads to smaller consumption of salts and a lower cost of a highly pure chemical.

The binodal curves and tie-lines were obtained experimentally. The fitting of the binodal curves was achieved by means of Merchuk equation, and the reliability of the tie-lines was determined by Othmer–Tobias and Bancroft equations. The partitioning coefficients of biomolecules were measured on the systems that presented the highest efficiency in terms of liquid-liquid equilibrium (LLE). Partitioning of amino acids was evaluated using the relative hydrophobicity of the equilibrium phases.

References

[1] Wysoczanska, Kamila, and Eugénia A. Macedo. 2016. "Influence of the Molecular Weight of PEG on the Polymer/Salt Phase Diagrams of Aqueous Two-Phase Systems". Journal of Chemical & Engineering Data, 61(12), 4229-4235. doi: 10.1021/acs.jced.6b00591.

[2] Wysoczanska, Kamila, and Eugénia A. Macedo. 2016. "Effect of molecular weight of polyethylene glycol on the partitioning of DNP-amino acids: PEG (4000, 6000) with sodium citrate at 298.15 K". Fluid Phase Equilibria, 428, 84-91. doi: 10.1016/j.fluid.2016.07.009.

Biofilm formation by cyanobacterium *Leptolyngbya mycoidea* LEGE 06118: surface effect

M. J. Romeu[1*], P. Alves[1], J. Morais[2], V. Ramos[2], V. Vasconcelos[2,3] and F. J. Mergulhão[1]

[1]LEPABE, Department of Chemical Engineering, Faculty of Engineering, University of Porto, Porto, Portugal;
[2]CIIMAR, Interdisciplinary Centre of Marine and Environmental Research, University of Porto, Porto, Portugal;
[3]Faculty of Sciences, University of Porto, Porto, Portugal
*mariaromeu@fe.up.pt

Keywords: biofouling, hydrodynamic conditions, glass, *Leptolyngbya mycoidea*, marine cyanobacteria, perspex

Biofouling is an ongoing concern in marine applications such as aquaculture nets, offshore oil platforms and ship hulls, leading to material deterioration and surface corrosion (Salta 2013). Moreover, the build-up of biofouling on ship hulls leads to high economic losses (Schultz 2011). Cyanobacteria are early surface colonizers which promote the onset of surface macrofouling by invertebrate larvae, mussels, seaweeds and barnacles (Mieszkin 2012). Although the economic and environmental impact of biofouling on immersed abiotic surfaces is widely recognised, there is still a lack of knowledge about the influence of surface properties on the attachment and biofilm formation of cyanobacteria. Therefore, the main goal of this work was evaluate the effect of two different surfaces (glass and perspex) on the biofilm formation behaviour of a filamentous cyanobacterium isolated from a tidal puddle in south of Portugal, during a three week period and in controlled hydrodynamic conditions (Romeu 2016). The chosen surfaces represent commonly submerged artificial surfaces (such as boat hulls), aquaria and aquaculture tanks (Sekar 2004; Satheesh and Wesley 2010).

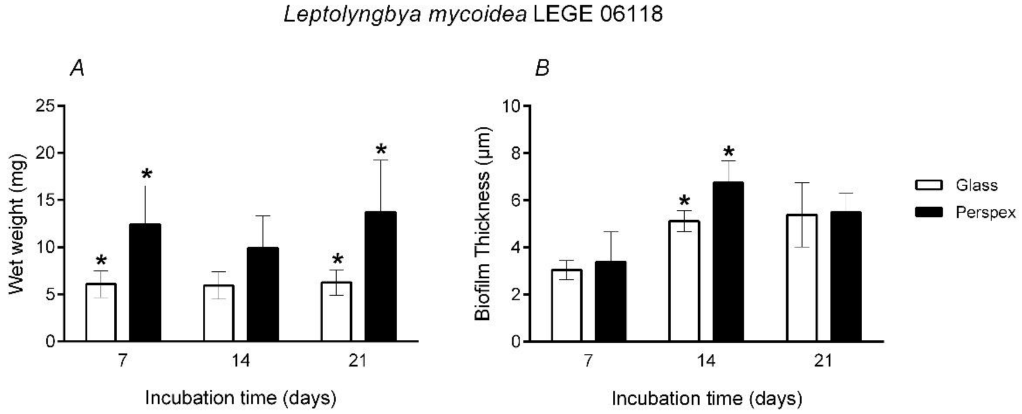

Figure 1. Evaluation of cyanobacterial biofilm development. The parameters analysed refer to wet weight (A) and biofilm thickness (B) of filamentous cyanobacterium *Leptolyngbya mycoidea* LEGE 06118 in two different surfaces (glass and perspex) during 21 days. Bars represent the average of wet weight and biofilm thickness values and standard deviations obtained from 3 individual coupons for each sampling day. Symbol (*) indicates statistically different values ($p < 0.1$) comparing the two surfaces. Adapted from Romeu 2016.

Strain identification was previously performed based on morphological features and 16S rRNA gene sequencing and the position of this strain on a phylogenetic tree was established (Romeu 2016). The surfaces were characterized according their hydrophobicity by contact angle measurement and results show that higher biofilm formation occurred in the most hydrophobic surface (perspex) as thicker biofilms were obtained and their wet weight was on average 50% higher than in hydrophilic surface (glass) (Figure 1). Biofilm morphology was further analysed by conventional and 3D microscopy (Figure 2), where a higher amount of filaments is visible on perspex when compared to the glass surface.

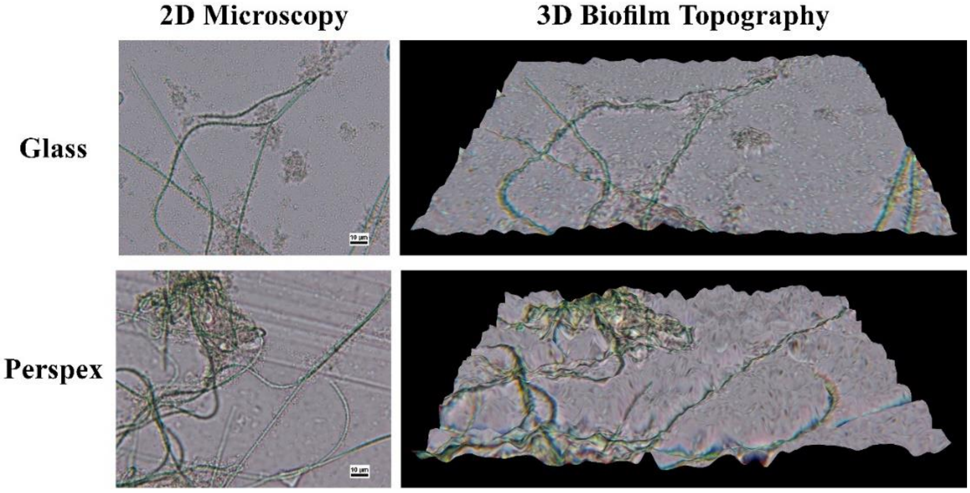

Figure 2. 2D microscopy and 3D cyanobacterial biofilm topography. Representative images of *Leptolyngbya mycoidea* LEGE 06118 biofilm formed after 21 days on glass and perspex coupons (scale bars = 10 µm). Adapted from Romeu 2016.

References

Mieszkin, S., P. Martin-Tanchereau, M. E. Callow, and J. A. Callow. 2012. “Effect of Bacterial Biofilms Formed on Fouling-Release Coatings from Natural Seawater and *Cobetia Marina*, on the Adhesion of Two Marine Algae.” *Biofouling* 28 (9): 953–68. doi:10.1080/08927014.2012.723696.

Romeu, Maria João, Patrícia Alves, João Morais, Vítor Ramos, Vítor Vasconcelos and Filipe Mergulhão. 2016. "Biofilm Formation by a Cyanobacterium Strain Belonging to a Distinct *Leptolyngbya* phylotype: Surface Effect". In Biofilms: Characterization, Applications and Recent Advances, 153-174. New York: Nova Science Publishers.

Salta, M., J. A. Wharton, Y. Blache, K. R. Stokes, and J. F. Briand. 2013. “Marine Biofilms on Artificial Surfaces: Structure and Dynamics.” *Environmental Microbiology* 15 (11): 2879–93. doi:10.1111/1462-2920.12186.

Satheesh, S. and S. G. Wesley. 2010. “Biofilm Development on Acrylic Coupons during the Initial 24 Hour Period of Submersion in a Tropical Coastal Environment.” *Oceanological and Hydrobiological Studies* 39 (1): 27–38. doi:10.2478/v10009-010-0012-x.

Schultz, M. P., J. A. Bendick, E. R. Holm, and W. M. Hertel. 2011. “Economic Impact of Biofouling on a Naval Surface Ship.” *Biofouling* 27 (1): 87–98. doi:10.1080/08927014.2010.542809.

Sekar, R., V. P. Venugopalan, K. K. Satpathy, K. V. K. Nair, and V. N. R. Rao. 2004. “Laboratory Studies on Adhesion of Microalgae to Hard Substrates.” *Hydrobiologia* 512: 109–16. doi:10.1023/B:HYDR.0000020315.40349.38.

Evaluation of bacterial adhesion to biomedical surfaces in controlled hydrodynamic conditions

P. M. Alves [1*], J. M. R. Moreira[1] and F.J. Mergulhão[1]
[1] LEPABE, Department of Chemical Engineering, Faculty of Engineering, University of Porto, Porto, Portugal
*up201510029@fe.up.pt

Keywords: Bacterial adhesion, *Escherichia coli*, Parallel plate flow chamber, PDMS, hydrodynamic conditions

Microorganisms attach to surfaces, such as biomedical devices and form biological communities called biofilms (Neoh 2017). *Escherichia coli* is responsible for about 80% of urinary tract infections (UTIs) (Shunmugaperumal 2010). The complex process of biofilm formation depends on multiple factors, such as the properties of the catheter material, hydrodynamics, physical and chemical properties of the liquid in contact with the surface and bacterial cells (Donlan 2002). Parallel plate flow chambers (PPFCs) have been used for the study of dynamic biofilms enabling a better understanding of the factors affecting the initial bacterial adhesion (Moreira et al. 2014). In the present study, the adhesion of *E. coli* under defined flow rates was monitored in a PPFC using polydimethylsiloxane (PDMS), a type of silicone, as a model surface. Silicone has been widely used in biomedical devices like contact lenses, breast implants and catheters (Kaali 2011). The shear stress range covered in this study was previously determined by computational fluid dynamics (Moreira 2014) and the values used were between 0.005 and 0.056 Pa. This is a 1 log range covering shear stress values that can be found in the human body particularly in the urinary (bladder and urethra), circulatory (veins) and reproductive (uterus) systems (Nauman 2007). The results show that *E. coli* adhesion decreases with shear stress particularly at low flow rates (until 5 mL s^{-1}) and after that the decrease is subtler. Increasing the flow rate increases the shear stress which can make the adhesion process more difficult. On the other hand, increased flow rates also facilitate mass transport and therefore the number of cells arriving at the surface (which can be beneficial for initial attachment). The results presented in this study indicate that the relative importance of these two factors changes in the tested range with the negative impact of the shear forces being predominant at the lower flow rates tested.

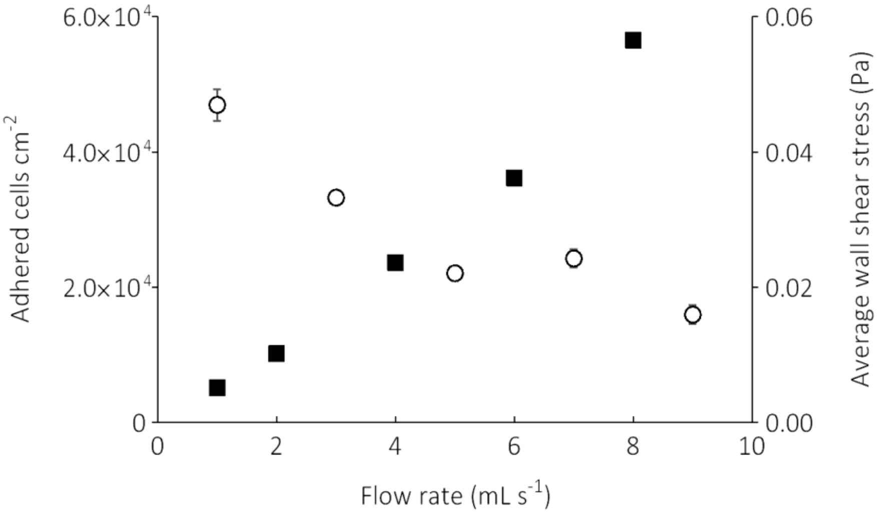

Figure 1. Initial adhesion rates (opened circles) for *Escherichia coli* on the bottom plate in a parallel plate flow chamber and average wall shear stress (squares) for each flow rate (mL s^{-1}) determined by computational fluid dynamics applied on the PDMS surfaces.

References

Donlan, Rodney M. 2002. "Biofilms: microbial life on surfaces." *Emerg Infect Dis* 8 (9). Accessed 2 March, 2017. doi:10.3201/eid0809.020063.

Kaali, Peter, Emma Strömberg, and Sigbritt Karlsson. 2011. *Prevention of biofilm associated infections and degradation of polymeric materials used in biomedical applications*: INTECH Open Access Publisher.

Moreira, JMR, JDP Araújo, JM Miranda, M Simões, LF Melo, and FJ Mergulhão. 2014. "The effects of surface properties on Escherichia coli adhesion are modulated by shear stress." *Colloids and Surfaces B: Biointerfaces* 123:1-7. Accessed 2 March, 2017. doi: 10.1016/j.colsurfb.2014.08.016.

Nauman, Eric A, C Mark Ott, Ed Sander, Don L Tucker, Duane Pierson, James W Wilson, and Cheryl A Nickerson. 2007. "Novel quantitative biosystem for modeling physiological fluid shear stress on cells." *Applied and environmental microbiology* 73 (3):699-705. Accessed 2 March, 2017. doi: 10.1128/AEM.02428-06.

Neoh, Koon Gee, Min Li, En-Tang Kang, Edmund Chiong, and Paul Anantharajah Tambyah. 2017. "Surface modification strategies for combating catheter-related complications: recent advances and challenges." *Journal of Materials Chemistry B*. Accessed 2 March, 2017. doi: 10.1039/C6TB03280J.

Shunmugaperumal, Tamilvanan. 2010. *Biofilm eradication and prevention: a pharmaceutical approach to medical device infections*: John Wiley & Sons.

Tarragon extract as a functional ingredient for development of new pizza dough

Andreia Ribeiro[1,3,*], Madalena M. Dias[1], Maria Filomena Barreiro[2], Isabel C.F.R. Ferreira[3]

[1]Laboratory of Separation and Reaction Engineering – Laboratory of Catalysis and Materials (LSRE-LCM), Faculty of Engineering, University of Porto, Portugal;

[2]Laboratory of Separation and Reaction Engineering – Laboratory of Catalysis and Materials (LSRE-LCM), Bragança Polytechnic Institute, Bragança, Portugal;

[3]Mountain Research Centre (CIMO), ESA, Ploytechnic Institute of Bragança, Campus Santa Apolónia, 1172, 5300-253, Bragança, Portugal

[*] asribeiro@fe.up.pt

Keywords: Tarragon extract, Phenolic Compounds, Antioxidant, Antimicriobial, Functional ingredient, Pizza dough.

Introduction

Plants are used in various fields due their sensory, nutritional and medicinal properties, and aromatic plants can be used as functional food ingredients to enhance organoleptic properties and/or to replace the salt. Additionally, their large amount of bioactive compounds, namely phenolic compounds (PC), can contribute to food preservation, promote human health (Costa et al., 2015), and provide bioactive effects. Tarragon, *Artemisia dracunculus* L., usually known for its pleasant spicy aroma, is widely used in food preparations (Hassanzadeh et al., 2016). In this work, a lyophilized hydroethanolic tarragon extract was characterized in terms of PC and bioactive properties, such as antioxidant, antimicrobial and cytotoxic activities and further used to develop functional foods namely by its incorporation in pizza dough.

Materials and Methods

Dried tarragon was kindly offered by "Cantinho das Aromáticas" (Vila Nova de Gaia, Portugal). The extract was obtained by maceration using 1 g of the powdered sample and 30 mL of an ethanol:water mixture (80:20, *v/v*). The PC were analyzed by HPLC-DAD-MS and the antioxidant activity by DPPH radical scavenging activity, reducing power (RP), inhibition of β-carotene bleaching and lipid peroxidation inhibition. The cytotoxic properties were evaluated in human tumor cell lines (breast, cervical, hepatocellular and non-small lung carcinoma) and in non-tumor cells (porcine liver primary cell culture) by the sulforhodamine B colorimetric assay. Antibacterial and antifungal activities were evaluated against 11 bacteria and 8 fungi species. Pizza dough was prepared using 250 mg of tarragon extract per 125 g of fresh or baked dough. For each type of pizza dough, two controls (one without the extract and another with 250 mg of ascorbic acid (E300), a commonly used commercial antioxidant) were prepared. The PC profile and the antioxidant activity (DPPH and RP) of the final products were assessed immediately after preparation and after 5 days of storage at 4˚C. More details are provided in Ribeiro et al. (2016).

Discussion

Eight PC were identified and quantified in the hydroethanolic tarragon extract: 7 phenolic acids and 1 flavonoid. However, a ferulic acid hexoside was the most abundant molecule, followed by rutin and 5-O-caffeoylquinic acid, and represent 33.7±0.3, 31.90±0.03 and 23.8±0.1 mg/g of the extract, respectively. In terms of antioxidant properties, the tarragon extract revealed different EC_{50} values (concentration responsible for 50% of antioxidant activity) in the performed assays; the highest potential of the extract was found as a reducing agent (155±1 μg/mL). The tarragon extract also demonstrated ability to inhibit the growth of tumor cell lines, mostly the cervical carcinoma cell line (HeLa), and the extract did not show any toxicity for non-tumor cells. The extract showed a broad antimicrobial activity against microorganisms with relevance for public health and food contamination. Methicillin resistant *Staphylococcus aureus* (MRSA), *Listeria monocytogenes*, *Pseudomonas aeruginosa* and *Escherichia coli* were the most sensitive bacteria, while *Aspergillus fumigatus*, *Trichoderma viride*, *Penicillium funiculosum*, *Penicillium ochrochloron* and *Penicillium verrucosum* the most susceptible fungi.

After incorporation of the extract in fresh and backed pizza dough, the amounts of PC were monitored. Both fresh and baked dough incorporated with the tarragon extract present similar profiles as the extract itself, mainly in terms of ferulic acid and rutin. As expected, the controls did not revealed PC. In terms of antioxidant properties, the dough incorporated with E300 showed the highest antioxidant capacity. However, the dough supplemented with the tarragon extract displayed improved capacity comparatively with the control and the various molecules present in the extract may have synergistic effects with other antioxidants and can contribute to other bioactive effects.

Conclusion

Tarragon extract can be considered as a potential food additive, preventing food spoilage and contamination, replacing synthetic additives widely used in the food sector. Further studies with the tarragon hydroethanolic extract are needed in order to understand its complete role and also to define the best conditions to be used. This work complements a similar potential of the rosemary extract, already allowed in Europe, as a natural antioxidant for the food industry.

Acknowledgements

POCI-01-0145-FEDER-006984 (LA LSRE-LCM), funded by FEDER, through POCI-COMPETE2020 and FCT; Project NORTE-01-0145-FEDER-000006, funded by NORTE2020 under the PT2020, through ERDF; FCT and ERDF under PT2020 for financial support to CIMO (UID/AGR/00690/2013). Andreia Ribeiro acknowledges her PhD fellowship funded by Project NORTE-08-5369-FSE-000028, supported by N2020, under PT2020, through ESF.

References

Costa, D. C., Costa, H. S., Albuquerque, T. G., Ramos, F., Castilho, M. C., & Sanches-Silva, A. (2015). Advances in phenolic compounds analysis of aromatic plants and their potential applications. Trends in Food Science & Technology, 45, 336–354.

Hassanzadeh, M. K., Najaran, Z. T., Nasery, M., & Emami, S. A. (2016). Tarragon (Artemisia dracunculus L.) oils in essential oils in food preservation, flavor and safety (Vol. 92, pp. 813–817). Academic Press.

Ribeiro, A., Barros, L., Calhelha, R.C., Carocho, M., Ćirić, A., Sokovic, M., Dias, M.M., Santos-Buelga, C., Barreiro, M.F. & Ferreira, I.C.F.R. (2016). Tarragon phenolic extract as a functional ingrediente for pizza dough: Comparative performance with ascorbic acid (E300). Journal of Functional Foods, 26, 268-278.

Oligoetherols and Polyurethane Foams with silicon atoms

E.Chmiel[1*], J. Lubczak[1]
[1]Department of Chemistry, Faculty of Organic Chemistry, Rzeszów University of Technology, Rzeszów, Poland
*chmielewelina@gmail.com

Keywords: polyurethane foams, non flammable polyurethane foams, environmentally friendly polyurethane foams, reduced flammability, oligoetherols, silicon, glycidol, ethylene carbonate, dichlorodimethylsilane,.

Method of preparation of the oligoetherol containing silicon atoms in their structure is presented. This compound is useful substrate for obtaining polyurethane foams of enhanced thermal stability, lower flammability and good mechanical strength. The physical properties of the foams have been examined.

Classic rigid polyurethane foams are flammable and have low thermal resistance, which restrict their use. The attempts to improve their properties are nowadays the matter of interest. One of the methods to improve their thermal stability is introduction of phosphorus, chlorine, boron, or silicon elements into their structure. This can be achieved both by chemical incorporation of these elements into the appropriate oligoetherols or polyurethane precursor (urethane oligomer) or addition of substances containing these elements into foaming composition. The oligoetherols with silicon elements are not often substrates for polyurethane foams. Introduction of silicon-containing fillers into foaming compositions improves the thermal stability of polyurethane foams (PUF). Moreover, silicone components are ecologically friendly and combustion of such materials is not accompanied by corrosive smokes. It has been discovered that addition of small amount of reactive silicon compounds resulted in considerable increase of thermal stability and decrease of flammability of PUFs. This is probably related to lower percentage of oxidizable elements in foam. Moreover, in case of flaming the silicone oxide in the PUF surface forms a heat insulator layer.

We are looking for simple synthetic method of oligoetherol suitable for obtaining thermally resistance polyurethane foams with decreased flammability. Therefore we have tested dichlorodimethylsilane (silicon source) as potencial flame retardant. In our work we obtained oligoetherols containing silicon and we use them to synthesize polyurethanes foams. The method of synthesis of oligoetherols was elaborated based upon hydroxyalkylation of oligosiloksanodiol with glycidol and then ethylene carbonate. To obtain semi-product (oligosiloskanodiol), dichlorodimethylsilane was dripped in water for 5 hours. The reaction was carried out for 12 hours at room temperature. Oligosiloksanodiol reacts with glycidol with triethylamine as catalyst at 180 °C, and with ethylene carbonate in presence of potassium carbonate at 135 °C. The density of oligoetherols was determined by pycnometer, the viscosity was studied using Höppler viscosimeter (type BHZ, prod. Prüfgeratewerk, Germany) and surface tension was determined using ring detachment method. Elemental analysis for C, H, N, were done with EA 1108, Carlo-Erba analyzer. The ^{1}H-NMR spectra of products were recorded at 500 MHz Bruker UltraShield in DMSO-d_6 with hexamethyldisiloxane as internal standard. IR spectra were registered on ALPHA FT-IR BRUKER spectrometer spectrometer in KBr pellets or ATR technique.

The oligoetherols obtained from such three-component reaction were suitable to obtain polyurethane foams. Foaming of oligoetherols was performed at 500 cm^3 cups at room temperature. The foams were prepared from 10 g of oligoetherol, to which 0,5 g of surfactant (Silicon 5340, pure, Houdry Hülls, USA) and 2,0 g of triethylamine (pure, Fluka, Switzerland) as catalyst and water (4%) were added. After the homogenization the diphenylmethane 4,4'-diisocyanate was added. The commercial isocyanate containing 30% of tri-functional isocyanates was used (Merck, Germany). The mixture was vigorously stirred until creaming began. The samples for further studies were cut off the obtained foams.

The apparent density, water uptake, dimensional stability in temperature 150 °C, heat conductance coefficient, heat capacity, and compressive strength of PUFs with flame retardants were measured. Thermal resistance of modified foams was determined both by static and dynamic methods. In static method the foams were heated at 150, 175 and 200 °C with continuous measurement of mass loss and determination of mechanical properties before and after heat exposure. Flammability of foams was determined by oxygen index and horizontal test according to norm.

Table 1. Thermal stability, compressive strength and flame properties of foams.

Foam	Mass loss in %wt. after exposition in 30 days	Compressive strength (MPa)	Oxygen inndex	Flame zone [mm]	Flame rate (mm/s)	Mass loss upon flaming (% mas.)
unexposed	-	0,2054	20,2	150	1,64	64,15
thermal exposure at 150°C	9,99	0,3220	22,6	Non-flammable in flame source		
thermal exposure at 175°C	27,7	0,2650	31,0	Non-flammable in flame source		
thermal exposure at 200°C	43,2	0,2550	54,7	Non-flammable in flame source		

Obtained polyurethane foams have properties comparable with classic, rigid PUFs except their enhanced thermal resistance and mechanical strength. They also stand long term heating at 200°C. Thermal exposure of synthesized PUFs resulted in increase of compressive strength of the PUFs. Obtained polyurethane foams are combustible (flame zone 1,64 (mm/s), oxygen index 20,2 (%)), but the flammability is lower than classic polyurethane foams (flame zone 6,2 (mm/s), oxygen index 21-22 (%)). All PUFs showed decrease of flammability after thermal exposure; they burn only in flame contact and flaming ceased after removal of flame source, which might be useful feature for practical purposes.

References

Chattopadhyay D.K., Webster C.: Progress in Polymer Sci., Vol.34, (1068), 2009. doi: 10.1016/j.progpolymsci.2009.06.002.

Pusztai E., Kenyó Cs., Nagy J., Wagner Ö., eXPRESS Polymer Letters Vol.7, No.5 (456), 2013, doi: 10.3144/expresspolymlett.2013.42.

Terraza C. A., Tagle L. H., Leiva A., Poblete L., Concha F.: J. Appl. Polym. Sci., 109, (303), 2008. http://dx.doi.org/10.4067/S0717-97072011000400027.

Nucleic Acid Mimics (NAMs) delivery into live bacteria mediated by nanovehicles

L. Moreira[1*], N. Guimarães[1,2,3], J. A. Loureiro[1], M. Carmo Pereira[1] and N. F. Azevedo[1]

[1]LEPABE, Department of Chemical Engineering, Faculty of Engineering, University of Porto, Porto, Portugal;
[2]I3S, Instituto de Investigação e Inovação em Saúde, Universidade do Porto, Porto, Portugal;
[3]Institute of Molecular Pathology and Immunology of the University of Porto (IPATIMUP), University of Porto, Porto, Portugal
[*]luismoreira@fe.up.pt

Keywords: Nucleic acid mimics (NAMs), Cationic liposomes, Fluorescence *in situ* Hybridization (FISH)

Nucleic acid mimics (NAMs) have been widely applied in living systems mostly due to their higher biological stability and improved kinetics characteristics for hybridization in comparison with DNA or RNA (Jepsen 2004). Currently, locked nucleic acids (LNA) and 2'-O-Methyl-RNA (2'OMe) oligonucleotides have emerged as a suitable tool to upgrade the imaging modalities at research, diagnosis and therapeutic levels. However, internalization of large molecules into live cells, without strongly affecting cellular viability, has always been challenging. The challenge is even greater when cells are small and very selective biological membranes, in which is the case of bacteria (Good 2000). Permeabilization methods currently used for internalization of oligonucleotides into bacteria require specific equipment and time-consuming optimization procedures or toxic chemical treatments, which strongly affect bacterial viability. These issues have encouraged conjugation of NAMs to non-toxic nanoparticle carriers, which are also well-known cellular permeabilizers. Between them, liposomes, especially those which have cationic lipids in their formulations, have demonstrated the ability to entrap and deliver oligonucleotides (Semple 2001) into both mammalian and bacterial cells. In contrast with classical formulations (negative and neutral charged), cationic liposomes formed by positive charged 1,2-dioleoyl-3-trimethylammonium-propane (DOTAP) and fusogenic neutral 1,2-dioleoyl-sn-glycero-3-phosphoethanolamine (DOPE) lipids yield very fluidic vesicles with higher ability to fuse with Gram-negative bacterial membranes (Ma 2013) and deliver oligonucleotides into cytoplasmic space where they interact with endogenous nucleic acids. Thus, the main goal of this work was to assess the ability of cationic liposomes to transport LNA/2'OMe oligonucleotides through the membrane of Gram-negative *Escherichia coli* bacterium, targeting the mRNA expressed by *acpP* gene (an essential gene for bacterium survival), toward the development of a strategy for antisense therapy. Results have shown higher performance of liposome-encapsulated NAMs for detection of *Escherichia coli*, in comparison with worldwide used standard Fluorescence *in situ* Hybridization (FISH) (Figure 1), which proves the concept of this innovative strategy.

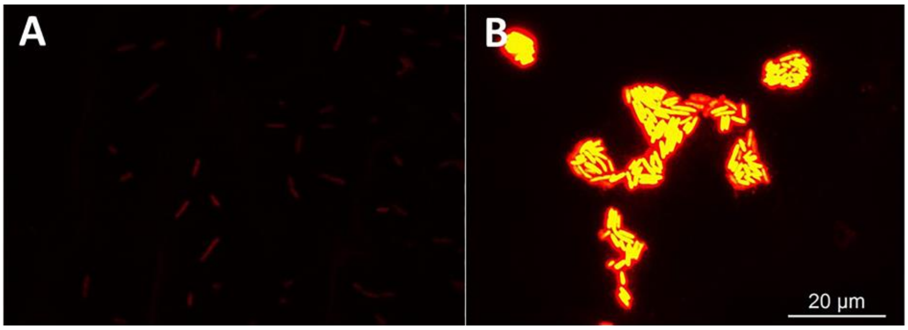

Figure 1. FISH detection of *Escherichia coli* ATCC 25922 by standard protocol (A) and liposomal delivery protocol (B).

Acknowledgements

This work was the result of the project:

(i) POCI-01-0145-FEDER-006939 (Laboratory for Process Engineering, Environment, Biotechnology and Energy – UID/EQU/00511/2013) funded by the European Regional Development Fund (ERDF), through COMPETE2020 - Programa Operacional Competitividade e Internacionalização (POCI) and by national funds, through FCT - Fundação para a Ciência e a Tecnologia, (ii) NORTE-01-0145-FEDER-000005 – LEPABE-2-ECO-INNOVATION, supported by North Portugal Regional Operational Programme (NORTE 2020), under the Portugal 2020 Partnership Agreement, through the European Regional Development Fund (ERDF), (iii) PhD fellowship NORTE-08-5369-FSE-000028 and (iv) Post-Doctoral fellowship SFRH/BPD/78846/2011.

References

Good, L., R. Sandberg, O. Larsson, P.E. Nielsen and C. Wahlestedt. 2000. “Antisense PNA effects in Escherichia coli are limited by the outer-membrane LPS layer”. Microbiology 146: 2665-2670. doi: 10.1099/00221287-146-10-2665.

Jepsen, J.S., M.D. Sørensen and J. Wengel. 2004. “Locked Nucleic Acid: A Potent Nucleic Acid Analog in Therapeutics and Biotechnology”. Oligonucleotides 14: 130-146. doi: 10.1089/1545457041526317.

Ma, Y., Z. Wang, W. Zhao, T. Lu, R. Wang, Q. Mei and T. Chen. 2013. “Enhanced bactericidal potency of nanoliposomes by modification of the fusion activity between liposomes and bacterium”. International Journal of Nanomedicine 8: 2351-2360. doi: 10.2147/IJN.S42617.

Semple, S.C., S.K. Klimuk, T.O. Harasym, N.D. Santos, S.M. Ansell, K.F. Wong, N. Maurer, H. Stark, P.R. Cullis, M.J. Hope, P. Scherrer. 2001. “Efficient encapsulation of antisense oligonucleotides in lipid vesicles using ionizable aminolipids: formation of novel small multilamellar vesicle structures”. Biochimica et Biophysica Acta 1510(1-2): 152-166. doi: 10.1016/S0005-2736(00)00343-6.

Platinum-group elements in Portuguese aquatic systems: the (un)known data and future research

C. E. Monteiro[1,2*], M. C. Santos[1], A. Cobelo-Garcia[3] and M. Caetano[2]
[1]Centro de Química Estrutural, Instituto Superior Técnico – Universidade de Lisboa, Portugal;
[2]Instituto Português do Mar e da Atmosfera IPMA, Lisboa, Portugal;
[3]Bioxeoquímica Mariña, Instituto de Investigacións Mariñas IIM-CSIC, Vigo, Spain.
*cessmonteiro@gmail.com

Keywords: Platinum, Rhodium, Portuguese estuaries, Sediments, Waters.

Abstract

Platinum-group elements (PGE) are emergent contaminants in the environment, having wide technological applications which range from automobile industry to medicine. These elements are severely depleted in the Earth's crust (< 0.50 ng g^{-1}), but the exploitation of these elements has increased over the past years. Only the automobile industry is responsible for approximately 50 % of global demand (Johnson 2016). In addition, automobile catalytic converters used to reduce emissions of hazardous pollutants, carbon monoxide and nitrogen oxides, are thought to be the main source of anthropogenic emissions of PGE due to their degradation and abrasion. As a consequence, this results in the widespread and increase of PGE in different environmental compartments (Zereini and Wiseman 2015). Among these, estuaries are transition areas between the land and the ocean that can be greatly impacted with anthropogenic pressures. Therefore, the Tagus and Douro estuaries are ideal settings for PGE studies due to surrounding highly urbanised and industrialised areas with considerably high traffic, as well adjacent to the Atlantic Ocean. Furthermore, these two estuaries have very different hydrodynamic controls, which may affect distribution and fate of PGE at a regional scale.

The quantification of PGE in environmental matrices has been additionally a challenge over the past years. Several analytical techniques have been proposed to quantify PGE in different matrices, such ICP-MS or AAS. However, due to their elevated costs and time of analysis, these techniques are not frequently used for routine analysis. Voltammetry has been pointed out as a suitable technique for PGE determination due to fast analysis and less expensive procedure. Platinum and Rh can be simultaneously determined by Adsorptive Cathodic Stripping Voltammetry (AdCSV). Though ill-defined peaks from voltammograms are observed at the ultra-trace range of concentrations, leading to inexact measurements of both element peaks and inaccurate quantification of their concentrations. To overcome this drawback, the use of second derivative signal transformation of the voltammograms increases the accuracy of the determinations (Monteiro et al., submitted). Thus, this combination makes the technique suitable for monitoring purposes.

This work presents the first data on the pathways of Pt and Rh in Portuguese estuaries (SW Europe). It is aimed to assess Pt and Rh concentrations in different environmental matrices, as well as to evaluate their sources and fate at regional scale. Spatial distribution of Pt and Rh in sediments from the Tagus estuary was evaluated for the first time in an estuarine system. Superficial sediments (< 5-cm depth) were collected in 57 stations inside the estuary. These were acid digested and analysed for Pt and Rh by AdCSV using the second derivative transformation in a single scan. Data were also compared with other interpretative parameters. Concentrations

of Pt and Rh were in general below 1.0 and 0.50 ng g^{-1}, respectively. However, some samples showed increased levels up to 6.5 ng Pt g^{-1} in the lower estuary and 1.5 ng Rh g^{-1} in the upper estuary. The ratios Pt/Rh determined were similar to those of typical catalytic converters values (4.0 – 9.0; Rauch and Peucker-Ehrenbrink 2015), with some higher values found in some samples which suggest other pathways of entrance into the Tagus estuary. The lower estuary can be considered an area of moderate deposition of both PGE, which corresponds to the area between two motorway bridges with high traffic.

In addition to the sediments, samples from a waste water treatment plant (WWTP) in Lisbon were also collected before and during the first heavy rainfall after a long period of dryness. Water samples from the WWTP showed a markedly increase of dissolved Pt concentrations, ranging from 10.0 ±0.3 ng L^{-1} to 25 ± 2 ng L^{-1} during the rainfall, while in the dry period Pt levels were lower and ranged from 5.0 ± 0.7 ng L^{-1} to 17 ± 2 ng L^{-1}. Contrarily, Rh concentrations remained constant between the two periods, with values around 0.3 ± 0.1 ng L^{-1}. These results evidence the important role of heavy rainfall periods on PGE flushing, in particular Pt, from urban areas to the surrounding aquatic systems. The impacts of periodic flushing of PGE to estuaries through the WWTP or other drainage channels remain unclear.

Furthermore, the hydrodynamic regime of an estuary, in particular the tidal forcing and currents, may have a key role on the transport of these emerging contaminants to other remote areas, such as the natural reserve park in the case of Tagus estuary and/or export them towards the coastal area. The potential export of PGE towards the coastal area has been assessed by the total amount of Pt and Rh (dissolved + particulate) using samples collected on a monthly basis in three Portuguese systems during ebb tide: Tagus, Douro and Ria de Aveiro. The first two systems are estuaries with very distinct hydrodynamics regime. Moreover, the coastal lagoon system of Ria de Aveiro is also hydrodynamically different. Accordingly, understanding the distribution of Pt and Rh on different systems will allow to reckon the fate and possible impacts caused by the increase of emergent contaminants such as PGE.

This study is funded by the Portuguese Foundation for Science and Technology (FCT) through the PhD grant funding CEM (SFRH/BD/111087/2015), project UID/QUI/001002013 and COST Action TD1407 - NOTICE.

References

Johnson, Matthey. 2016. “Platinum Group Metals Market Report - November.” http://www.platinum.matthey.com/documents/new-item/pgm market reports/pgm_market_report_november_2016.pdf.

Monteiro, Carlos Eduardo, Antonio Cobelo-Garcia, Miguel Caetano, and Margarida Correia dos Santos. n.d. “Improved Voltammetric Method for Simultaneous Determination of Pt and Rh Using Mathematical Signal Transformation – Application to Environmental Samples.” Submitted to *Talanta*, under review.

Rauch, Sebastien, and Bernhard Peucker-Ehrenbrink. 2015. “Sources of Platinum Group Elements in the Environment.” In *Platinum Metals in the Environment*, 3–17. Springer.

Zereini, Fathi, and Clare L.S. Wiseman. 2015. *Platinum Metals in the Environment*. Edited by Fathi Zereini and Clare L.S. Wiseman. Environmental Science and Engineering. Berlin, Heidelberg: Springer Berlin Heidelberg. doi:10.1007/978-3-662-44559-4.

Hydroquinone degradation by Fenton process: a new application for the bubble column reactor

V. N. Lima[1*], C. S. D. Rodrigues[1] and Luis M. Madeira[1]
[1]LEPABE, Engineering Department Chemical, Faculty of Engineering University of Porto, Porto, Portugal;
*vanessa.nlima@gmail.com

Keywords: AOP. Bubble column reactor. Fenton process. Organic compounds. TOC removal.

The application of advanced oxidation processes (AOPs) for organic compounds degradation has increased in recent years. New perspectives for these processes include, for example, the use of different types of reactors. In this sense, this study proposes the treatment of hydroquinone (HQ), one intermediate compound generated in the oxidation of other organics (e.g., benzene and phenol), by the Fenton process in a bubble column reactor (BCR). This application has never been reported in the literature. The experiments carried out in the BCR aimed evaluating the influence of the H_2O_2 dose and catalyst (dissolved Fe^{2+}) concentration, air flow rate, initial pH and temperature in the HQ degradation and mineralization (total organic carbon – TOC – removal). The HQ was completely degraded after 5 min and it was reached ~42% of TOC removal after 4 h of reaction. The acute toxicity was null in the final effluent.

Introduction

The bubble column reactor (BCR) is a multiphase device with industrial importance for processes as hydrogenation, polymerization and oxidation, with easy maintenance and more effective for processes where mass transference is critical. For environmental applications, it was reported the use of BCRs by different AOPs, namely ozonation for the treatment of liquid effluents (Shah et al. 1982) and UV/H_2O_2 for the treatment of gas streams (Liu et al. 2010). However, it was never reported the application of the Fenton process, a classic AOP, in a BCR for liquid effluents treatment. This study aims to evaluate the possibility of employing the Fenton process in a BCR for HQ degradation, a compound reported as intermediate of the degradation of organics as benzene (Ito et al. 1988) and phenol (Bielicka-Daszkiewicz et al. 2004). Few studies report HQ degradation by AOPs, and it is expected that application of the Fenton process can ensure good degradation results.

Experimental

The Fenton process was carried out in a BCR (V = ~10 L, H = 1.40 m and ø = 9.8 cm) with a gas dispersion plate with 9 holes (ø = 0.5 mm); the jacketed column is connected to a thermostatic bath for temperature control. The installation had one pump (Agua medic, Mistral 2000) for feeding compressed air, which promotes the mixing inside the column, and two rotameters which allow the control of the air flow rate, in range of 1 to 5 mL/min (Figure 1). The BCR was fed with a given volume of the HQ solution (100 mg/L) and after stabilizing the temperature the initial pH was adjusted with H_2SO_4 1 M. Then, the catalyst ($FeSO_4.7H_2O$) was dissolved and subsequently the H_2O_2 (30% m/v) added, this instant corresponding to the one when the reaction started (t = 0). After certain periods of time samples were collected for measuring the

HQ and organics content (by HPLC) and TOC (in a Shimadzu TOC-L apparatus) after stopping the homogeneous reaction in the sampling flasks (with excess of Na_2SO_3). At the end of the reaction it was measured the effluent inhibition towards *vibrio fischeri* (in a Microtox apparatus).

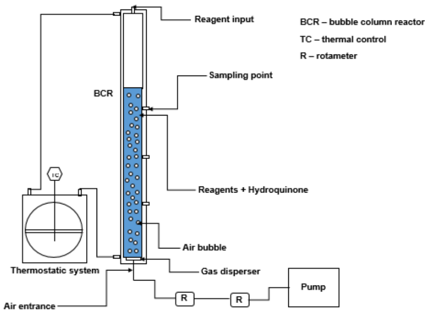

Figure 1. Schematic diagram of the experimental set-up.

Results and Discussion

In this work it was evaluated the effect of the air flow rate (1 to 5 mL/min), reaction temperature (15 to 70 °C), initial pH (3 to 7), H_2O_2 dose (0.25 to 1.50 g/L) and catalyst concentration (30 to 120 mg/L). The HQ removal was complete in all runs carried out (in most cases after only a few minutes) and the acute toxicity of the effluent was in all cases reduced from 100% (in the sample with 100 mg/L of the HQ) to 0%, demonstrating that the treatment was effective in the reduction of the effluent toxicity. The air flow rate did not influence the efficiency of the Fenton process, although providing an efficient internal mixing in the BCR (assessed by sampling at different column heights). The maximum TOC removal (~42 %) was obtained when using the following conditions: T = 22-24 °C; pH = 3; $[H_2O_2]$ = 0.50 g/L and $[Fe^{2+}]$ = 45 mg/L.

Conclusions and perspectives

The application of the Fenton process in a BCR was studied for the first time and proved to be effective for treating an HQ-containing effluent. Considering the good performance of the Fenton reaction obtained in this type of reactor, in a future work it will be evaluated the degradation of organic compounds present in the gas stream by this process in a BCR.

Acknowledgments

VL is grateful to the Brazil National Council of Technological and Scientific Development (CNPq) for her PhD grant (process 201859/2015-7).

References

Bielicka-Daszkiewicz, Katarzyna, Magdalena Dębicka, and Adam Voelkel. 2004. "Comparison of Three Derivatization Ways in the Separation of Phenol and Hydroquinone from Water Samples." *Journal of Chromatography A*. Vol. 1052, 233–236.

Ito, Sotaro, Atsutaka Kunai, Hiroshi Okada, and Kazuo Sasaki. 1988. "Direct Conversion of Benzene to Hydroquinone. Cooperative Action of copper(I) Ion and Dioxygen." *The Journal of Organic Chemistry* 53 (2): 296–300.

Liu, Yangxian, Jun Zhang, Changdong Sheng, Yongchun Zhang, and Liang Zhao. 2010. "Simultaneous Removal of NO and SO2 from Coal-Fired Flue Gas by UV/H2O2 Advanced Oxidation Process." *Chemical Engineering Journal* 162 (3): 1006–1011.

Shah, Y. T., B. G. Kelkar, S. P. Godbole, and W.-D. Deckwer. 1982. "Design Parameters Estimations for Bubble Column Reactors." *AIChE Journal*, no. 3: 353–379.

Is our daily routine reflected in the vegetables we eat?

S. Ramos[1], V. Homem[1*] and L. Santos[1]
[1]LEPABE — Laboratory for Process Engineering, Environment, Biotechnology and Energy, Faculty of Engineering,
University of Porto, Rua Dr. Roberto Frias, 4200-465 Porto, Portugal
[*]vhomem@fe.up.pt

Keywords: emerging contaminants, synthetic musks, UV-filters, WWTPs, PCPs, agriculture, vegetables

People say that we are what we eat, but is our daily routine somehow involved in what we eat? Most people's daily routine includes the use of toiletries, like perfumes, lotions, shampoos, deodorants, sunscreens, but also, for household maintenance it is common the use of products like detergents, washing powders, fabric softeners or even air fresheners. Incorporated in these products are different classes of compounds frequently designated by personal care products (PCPs)(Alvarez-Rivera et al. 2013). Due to their massive use, continuous input and persistence in the environment, PCPs are now considered emerging pollutants and have raised concern in the scientific community. Within PCPs, synthetic musks (fragrance fixatives) and UV-filters (sunscreen active agents) are examples of compounds commonly used in cosmetics and toiletries (Pedrouzo et al. 2011). Although, the use of some of these compounds have been restricted or prohibited, they are still largely used. They are considered environmentally persistent contaminants that can bioaccumulate and are suspected to be hormone disruptors. An obvious endpoint for these compounds, are the wastewater treatment plants (WWTPs). However, conventional WWTPs are not completely efficient in their removal and/or degradation. Therefore, parent compounds and degradation products are discharged through effluents into surface waters (mostly hydrophilic compounds) or sorb into sludge (lipophilic ones). They have already been detected in wastewater effluents and sewage sludge and their transfer to crops has also been described (Homem et al. 2015; Ramos et al. 2015). So, sludge-amended soils can be considered a way for the introduction of musks (SMCs) and UV-filters (UVFs) into the food chain through the uptake of crops (Prosser and Sibley 2015). So far, the lack of information regarding uptake analysis by different crop plants in sludge/compost-amended soils in real fields, has prevented the development of a real risk analysis studies. Therefore, the main goal of this study is to present the current state of the art on this theme, focusing on the levels found of SMCs and UVFs in sludge and sludge-amended soils and the uptake of those PCPs by vegetables after crop fertilization with sludge/compost. Some questions related to the analytical methodologies used to determine SMCs and UVFs in those different environmental matrices will be answered.

References

Alvarez-Rivera, G., M. Lores, M. Llompart, and C. Garcia-Jares. 2013. "Cosmetics and Toiletries: Chromatography." In *Reference Module in Chemistry, Molecular Sciences and Chemical Engineering*. Elsevier. doi:10.1016/B978-0-12-409547-2.05839-X.

Homem, Vera, Avelino Silva, Nuno Ratola, Lúcia Santos, and Arminda Alves. 2015. "Long Lasting Perfume E A Review of Synthetic Musks in WWTPs." *Journal of Environmental Management* 149: 168–92. doi:10.1016/j.jenvman.2014.10.008.

Pedrouzo, Marta, Francesc Borrull, Rosa Maria Marcé, and Eva Pocurull. 2011. "Analytical Methods for Personal-Care Products in Environmental Waters." *TrAC - Trends in Analytical Chemistry* 30 (5): 749–60. doi:10.1016/j.trac.2011.01.009.

Prosser, R. S., and P. K. Sibley. 2015. "Human Health Risk Assessment of Pharmaceuticals and Personal Care Products in Plant Tissue due to Biosolids and Manure Amendments, and Wastewater Irrigation." *Environment International* 75. Elsevier Ltd: 223–33. doi:10.1016/j.envint.2014.11.020.

Ramos, Sara, Vera Homem, Arminda Alves, and Lúcia Santos. 2015. "A Review of Organic UV-Filters in Wastewater Treatment Plants." *Environment International* 86 (October): 24–44. doi:10.1016/j.envint.2015.10.004.

Acknowledgements

This work was the result of the project: (i) POCI-01-0145-FEDER-006939 (Laboratory for Process Engineering, Environment, Biotechnology and Energy – UID/EQU/00511/2013) funded by the European Regional Development Fund (ERDF), through COMPETE2020 - Programa Operacional Competitividade e Internacionalização (POCI) and by national funds, through FCT - Fundação para a Ciência e a Tecnologia; (ii) NORTE-01-0145-FEDER-000005 – LEPABE-2-ECO-INNOVATION, supported by North Portugal Regional Operational Programme (NORTE 2020), under the Portugal 2020 Partnership Agreement, through the European Regional Development Fund (ERDF); (iii) Post-doctoral Grant SFRH/BPD/76974/2011 - Vera Homem; (iv) Doctoral Grant SFRH/BD/110831/2015 – Sara Ramos.

Sweet potato ethanol upgrade using quicklime

Joab Silva, Manuel F. Almeida, Conceição Alvim-Ferraz, Joana M. Dias
LEPABE, Faculty of Engineering, University of Porto, Porto, Portugal, Portugal;
joab@uft.edu.br, mfa@fe.up.pt , aferraz@fe.up.pt e jmdias@fe.up.pt

Keywords: Bioethanol, sweet potato, upgrade, quicklime.

Sweet potato ethanol might be a sustainable alternative to diversify the energy matrix throughout the world. To ensure its use, after production, bioethanol must be upgraded (>99 °GL). In the present study, quicklime was evaluated as a low cost material, to upgrade sweet potato bioethanol from a pilot scale plant, with an initial purity of 88 and 94 °GL. Experiments included the distillation of bioethanol under fixed conditions (78 °C, 600 mbar, 30 rpm and 1 h in a rotary evaporator) and varying CaO concentration (0.13, 0.20, 0.27, 0.33 and 0.40 g mL^{-1}). The highest purity obtained was 99.4 °GL, using the highest concentration of CaO (0.40 g mL^{-1}) with the ethanol initial grade of 94 °GL.

Introduction

Currently, biofuels are an important renewable source of energy and with growing investment prospects for the next decade. Bioethanol accounted for 74% of world production in 2015, followed by biodiesel with 22% and HVO (Hydrotreated Vegetable Oil) with 4% (REN 2016). Bioethanol is produced mainly by corn, sugarcane and sugar beet, but the sweet potato is a promising alternative source due to high alcohol productivities, of 10 467 L/ha (Silveira et al. 2007), when compared to those obtained from corn, of 4 250 L/ha (Dunn et al. 2013), and sugarcane, of 7 224 L/ha (Urquiaga, Alves, and Boodey 2005). To obtain anhydrous ethanol, it is necessary to use processes and reagents that break the azeotrope (Ethanol:Water), such as ethylene glycol and glycerol, which can obtain purity values above 98 °GL (Navarrete-Contreras et al. 2014). Quicklime is a low cost material and can be a viable and sustainable alternative in the purification of bioethanol. Thus, the present work aims to study the effect of quicklime concentration on the purification of sweet potato bioethanol.

Materials and Methods

Sweet potato bioethanol was obtained in a small production plant with a capacity of 3 000 L/day (Palmas-TO/Brazil), from which a mean yield of 161.4 L/t and a minimum purity of 88.0 °GL (or Vol.%) were obtained, according to previously established operating conditions (Silveira et al. 2007). The alcohol with lower grade was subjected to distillation in a rotary evaporator (Heidolph) under fixed conditions (76 °C, 600 mbar, 30 rpm, 1 h) to reach the maximum purity of 94.0 °GL, and these two alcohol grades were further studied.

The purity (°GL) of the bioethanol was determined using a densitometer (Gay-Lussac/ALLA) according to NBR-5992 (ABNT 2008). CaO was obtained from calcination of calcium hydroxide (Quimirraia) at 850 °C using a furnace (Salfor) according to NBR 6473 (ABNT 2003). For sweet potato bioethanol upgrading, samples of 150 mL of alcohol (88.0 and 94.0 °GL) were used under fixed conditions of the rotary evaporator (78 °C, 600 mbar, 30 rpm, 1 h) varying the CaO concentrations (0.13, 0.20, 0.27, 0.33 and 0.40 g mL^{-1}) on the basis of the stoichiometry hydration reaction of CaO. Experiments were performed in duplicate.

Results and Discussion

Figure 1 shows that ethanol purity was directly proportional to calcium oxide concentration, within the range studied (0.13 – 0.40 g mL^{-1}). The highest purity, of 99.4 ± 0.1 °GL was obtained using a CaO concentration of 0.40 g mL^{-1}, starting from the 94.0 °GL product. This value is very close (± 1%) to all presented standards about ethanol, being slightly higher (+ 1%) than that obtained by Navarrete-Contreras et al (2014). using ethylene glycol (98.4 °GL). Note that no reflux or distillation stages were used for distillation, making this process simpler.

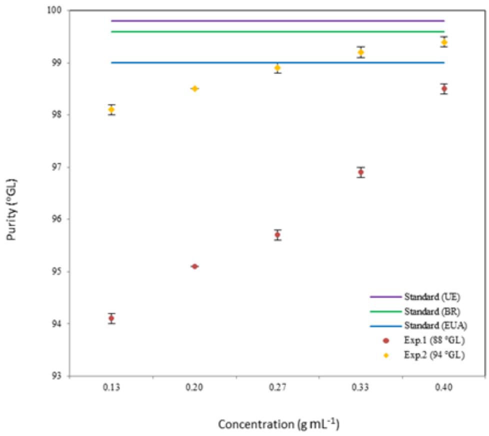

Figure 1: Purities obtained from bioethanol (88.0 and 94.0 °GL) with different concentrations of CaO and comparison with grades on BR-ANP.7 (2011), EUA-ASTM.D4806 and UE-EN15376 (Force 2007) .

Conclusions

The use of a low cost reagent – quicklime – for bioethanol upgrading was studied. The purity increased when CaO concentration increased, and it was shown to be possible obtaining the highest purity of 99.4 °GL using 0.40 g mL^{-1} of CaO, a grade very close (± 1%) to that from the existing standards in USA, Brazil and Europe.

References

ABNT. 2003. Normativa ABNT/NBR 6473: "Cal virgem e cal hidratada - Análise química". Rio de Janeiro, 2003.

ABNT. 2008. Associação Brasileira de Normas Técnicas, "NBR 5992: Álcool etílico e suas misturas com água - Determinação da massa especifica e teor alcoólico - Método de densítometro de vidro". Rio de Janeiro, 2008.

ANP. 2011. Agência Nacional de Petróleo, Gás Natural e Biocombustíveis (ANP), "Resolução ANP Nº 7, DE 9.2.2011. Diário Oficial da União, 10 de fev.2011.

Dunn, Jennifer B., Steffen Mueller, Ho-young Kwon, and Michael Q. Wang. 2013. "Land-use change and greenhouse gas emissions from corn and cellulosic ethanol." Biotechnology for Biofuels 6:1-13. doi: 10.1186/1754-6834-6-51.

Force, Tripartite Task. 2007. White paper on internationally compatible biofuel standards. In Tripartite Task Force Brazil, European Union & United State of America.

Navarrete-Contreras, S, M Sánchez-Ibarra, F O Barroso-Muñoz, S Hernández, and A J Castro-Montoya. 2014. "Use of glycerol as entrainer in the dehydration of bioethanol using extractive batch distillation: Simulation and experimental studies." Chemical Engineering and Processing: Process Intensification 77:38-41. doi: http://dx.doi.org/10.1016/j.cep.2014.01.003.

REN. 2016. Renewables 2016 Global Status Report. In Ren21, edited by REN Secretariat. France: Ren21.

Silveira, MA, CMG André, TCl Alvim, LE Dias, IB Tavares, WR Santana, and FR Souza. 2007. "A cultura da batata-doce como fonte de matéria-prima para a produção de etanol. Palmas, Universidade Federal do Tocantins. 45p." Boletim Técnico.

Urquiaga, Segundo, Bruno José Rodrigues Alves, and Roberto Michael Boodey. 2005. "Produção de biocombustíveis A questão do balanço energético." Revista de política agrícola 14 (1):42-46.

Arsenic removal from contaminated water by adsorption on iron-coated *Sargassum muticum*

B. Vieira, R. Boaventura, C. Botelho, S. Santos and A. Pintor*
Laboratory of Separation and Reaction Engineering – Laboratory of Catalysis and Materials (LSRE-LCM), Department of Chemical Engineering, Faculty of Engineering, University of Porto, Porto, Portugal
*ampintor@fe.up.pt

Keywords: Adsorption, Arsenic, Seaweeds, Iron-coating, Water, Coagulation/Flocculation.

Arsenic is a toxic and carcinogenic semi-metal. Its presence in water bodies and drinking water supplies is due to natural deposits but also to mining, industrial and agricultural practices. The goal of the present study was the evaluation of an alternative process for removing this element from water, based on adsorption on *Sargassum muticum* seaweed, after being coated with iron (50 mg-Fe/g).

As it can be seen in Figure 1(a), the iron-coated *S. muticum* is viable for the removal of arsenic from water. In the pH range 2-7, adsorption of As(V) was independent of pH, while As(III) uptake increased with pH, reaching a maximum level at pH 7. Similarly, iron leaching from the adsorbent decreased with increasing pH, due to the higher solubility of iron hydroxides in acidic medium. Under studied conditions, the percentage of iron loss varied between 2% (pH 7, As(V)) and 27% (pH 2, As(III)).

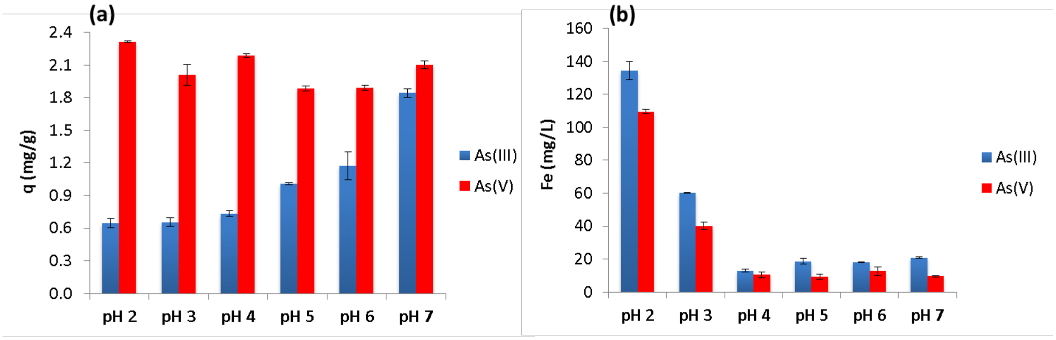

Figure 1. pH effect on: (a) As(III) and As(V) adsorbed amounts (q, mg/g) and on (b) iron leached by the adsorbent. Arsenic initial concentrations=25 mg/L, contact time=4h, 20°C, adsorbent dosage 10.0 g/L.

Adsorption kinetics (Figure 2) and equilibrium were studied for As(III) and As(V). Kinetics was especially well described by pseudo-second order model. Langmuir model fitted to equilibrium data indicated maximum adsorption capacities of 4.2 mg/g for As(III) and 7.3 mg/g for As(V), at pH 7 and 20°C. These values compare favourably to other similar adsorbents in the literature (Ungureanu et al. 2015). The proposed adsorption mechanism is based on the assumption that As(V) was the adsorbed As species, with the oxidation of As(III) to As(V) before uptake by the adsorbent, and Fe(III) reduction to Fe(II). This was supported by the following observations: (i) the speciation of As and Fe in aqueous solution after adsorption (obtained using voltammetric techniques and colorimetric methods) indicated the presence of As(V) and Fe(II); (ii) a higher adsorption capacity was obtained for As(V), when compared to As(III); (iii) higher iron leaching in As(III) adsorption tests (Figures 1(b) and 2), caused by higher dissolution of iron due to the reduction of Fe(III) to Fe(II), increasing its soluble concentration and (iv) no difference was observed between the infrared spectra of loaded-adsorbents, obtained when As(III) or As(V) were used as adsorbates.

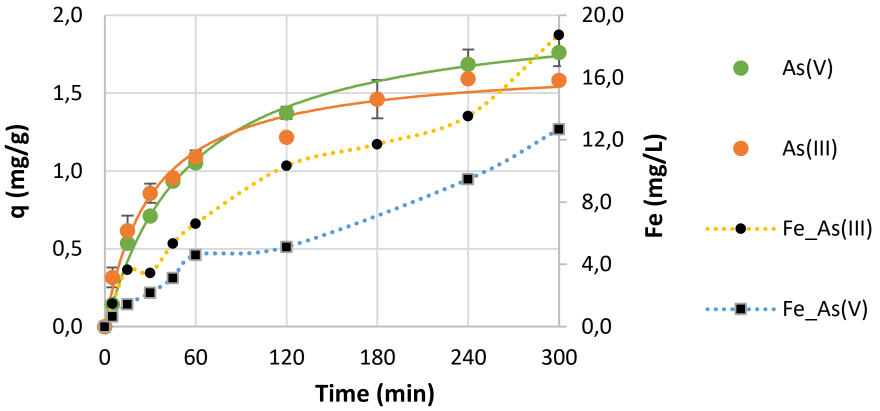

Figure 2. Iron leaching on the As(III) and As(V) samples as a function of time (As initial concentration=25 mg/L, pH=7, 20°C, adsorbent dosage 10 g/L).

The performance of As adsorption on the iron-coated *S. muticum* was compared to coagulation/flocculation (coagulant: 12 g/L $Fe_2(SO_4)_3$), in the treatment of a groundwater sample, contaminated with As(III). Both processes provided practically 100% of arsenite removal, leading at best to final As concentrations of 13 µg/L, after the adsorption and precipitation assays, and 15 µg/L, after the coagulation/flocculation process (Table 1).

Table 1. Treatment of the As-contaminated water (2.5 mg As/L): As removal percentages and final As and Fe concentrations obtained by adsorption and coagulation/flocculation in optimal conditions.

	As (µg/L)	As removal (%)	Fe (mg/L)
Adsorption at pH 4	42	67	123
Adsorption at pH 4 + precipitation at pH 6	14	99.5	1.6
Adsorption at pH 4 + precipitation at pH 8	13	99.5	1.9
Coagulation/Flocculation at pH 9	15	99.4	<0.5

Adsorption on the iron-coated *S. muticum* seems to be an interesting alternative treatment for the removal of arsenic from water, with environmental advantages over other technologies: low amount of sludge, possibility of algae regeneration and posterior utilization, and alternative management option for dead algae. Further studies are necessary to prove the proposed adsorption mechanism and to try to minimize iron leaching to the solution.

Acknowledgements

This work was financially supported by: Project POCI-01-0145-FEDER-006984 – Associate Laboratory LSRE-LCM funded by FEDER through COMPETE2020 – Programa Operacional Competitividade e Internacionalização (POCI) – and by national funds through FCT – Fundação para a Ciência e a Tecnologia.

References

Ungureanu, Gabriela, Sílvia Santos, Rui Boaventura, and Cidália Botelho. 2015. "Arsenic and antimony in water and wastewater: Overview of removal techniques with special reference to latest advances in adsorption". Journal of Environmental Management 151: 326-342.

Highest methane production from sugarcane vinasse with filter cake in thermophilic UASB reactors

Valciney Gomes de Barros[1], Rose Maria Duda[2] and Roberto Alves de Oliveira[1*]

[1]Laboratory of Environmental Sanitation, Department of Rural Engineering, Faculty of Agricultural and Veterinary Sciences, Univ Estadual Paulista, Jaboticabal, SP, Brazil.
[2]Faculty of Technology – Fatec, Jaboticabal, SP, Brazil;
*raoder@fcav.unesp.br

Keywords: organic loading rate, methanogenic archaea, alkalinity and nutrient supplementation.

Introduction

For each one liter of sugarcane bioethanol distilled generates 10 to 14 L of vinasse, a byproduct that can be used as a fertilizer. It has a high energetic potential that can be converted into a readily usable form, such as biogas, mostly made up of methane. The availability of nutrients, different configurations of anaerobic reactor and operational strategies are important issues for achieving stability in the production of methane and quality biodigested vinasse. These issues must be solved before widespread production of biogas from vinasse can be implemented. The use of the filter cake in the vinasse for a two-stage process with reactors in series could solve many of these issues. We use a thermophilic anaerobic treatment because the vinasse leaves the distillation process with high temperatures. Currently there is no established technology for using filter cake in vinasse anaerobic digestion reactors. The purpose of our study was to evaluate the thermophilic anaerobic conversion of vinasse in upflow anaerobic sludge blanket (UASB) reactors, in two stages, with high organic loading rate (OLR) to obtain high methane production. For this, the OLR was increasing from 5 to 55 g totalCOD (L d)$^{-1}$, with supplementation of alkalinity and nutrients through the filter cake and effluent recirculation.

Material and methods

The sugarcane vinasse influent used was from distillation of hydrous ethanol to feed the UASB reactors installed in series (Reactor 1 (R1) and Reactor 2(R2)), with volumes of 12.1 L (R1) and 5.6 L (R2), maintained in the range (54 to 56 °C). The amount of filter cake used per liter of vinasse was based on the COD:N:P ratio of 350:5:1 recommended for anaerobic digestion (Chernicharo 2007).

Table 1. Operating conditions of UASB reactors in two stages (R1 and R2), thermophilic vinasse treatment.

Days in operation	1 to 110	110 to 170	171 to 230	231 to 310	311 to 380	381 to 460
Organic loading rate (R1) (g tCOD (L d)$^{-1}$)	8	18	28	32	45	37
Organic loading rate (R2) (g tCOD (L d)$^{-1}$)	13	26	30	38	49	55
Hydraulic retention time	R1 (24h) and R2 (11 h)				R1 (17h) and R2 (8 h)	
Source of N and P	Filter Cake					
Alkalinity Soure	Recirculation of the R2 effluent					

After 340 days of operation, quantitative real-time PCR (qPCR) was conducted with DNA samples isolated from the reactor sludge, three samples of R1 and three of R2. This procedure was performed in order to verify if there are significant differences in the quantification of the microorganisms along the height of the reactors digestion chamber.

Results and discussion

OLR gradually increased during the 460 days of processing. The values increased from 8 to 45 g tCOD (L d)$^{-1}$ in R1 and 13 to 55 g tCOD (L d)$^{-1}$ in R2. Total volatile acids (TVA) and partial alkalinity (PA) values increased with OLR, TVA values ranged from 1472 to 5095 mg L^{-1} in R1 and 1456 to 4605 mg L^{-1} in R2, AP values were 1584 to 3327 mg L^{-1} in R1 and 1517 to 3877 mg L^{-1} in R2. The system displayed operational stability and satisfactory buffering capacity during the experimental period, as demonstrated by the increase in both values of PA and of TVA. The highest COD removal efficiency was 60%, similar to the values obtained by Fuess et al. (2017).

The methane production in the anaerobic digestion of vinasse is extremely important to make the technology application feasible. High volumetric methane production was obtained in this work, reaching levels up to 4.1 L CH_4 L^{-1} d^{-1} d^{-1} in R1 and 1.4 L CH_4 L^{-1} d^{-1} in R2. The methane concentrations in biogas varied between 49 to 65% in R1, and 49 to 79% in R2, the highest concentrations of methane in the biogas occurred in R2 suggesting high hydrolytic and acidogenic activity in R1, with higher TVA concentrations.

Quantification of microorganisms indicated a balance between domains archaea and bacteria, with ($3x10^9$ and $2x10^9$ copies/g in R1 and R2, respectively) and archaea ($4x10^8$ to $7x10^8$ copies/g in R1, $2x10^8$ copies/g to $5x10^8$ in R2). In order for the stability in the anaerobic reactors to occur, the archaea concentration must be higher then or close to the bacteria levels. At these levels, the archaea can efficiently use the substrates produced by the bacteria, since these microorganisms have low growth rate.

The use of filter cake and recirculation of the effluent under thermophilic conditions allowed us to reach high OLR. We observed adequate nutrients availability for anaerobic digestion of vinasse in the system influent.

Conclusion

This study demonstrates high methane production from vinasse. Both sugar clarification filter cake and effluent recirculation was important to elevate organic loading rates (OLR) up to 45 and 49 g tCOD (Ld)$^{-1}$ in R1 and R2. Under these conditions in stability, the amounts of bacteria and archaea in the sludge were balanced. The configuration of the reactors in series contributed to the increase of the anaerobic conversion from vinasse to methane and the process stability.

References

Carlos Augusto de Lemos Chernicharo. 2007. *Reatores Anaeróbios*. 2nd ed. Belo Horizonte: DESA/UFMG; 2007. www.iwapublishing.com.

Lucas Tadeu Fuess, Luma Sayuri Mazine Kiyuna, Antônio Djalma Nunes Ferraz, Gabriela Felix Persinoti, Fabio Marcio Squina, Marcelo Loureiro Garcia, Marcelo Zaiat. 2017. “Thermophilic Two-Phase Anaerobic Digestion Using an Innovative Fixed-Bed Reactor for Enhanced Organic Matter Removal and Bioenergy Recovery from Sugarcane Vinasse.” *Applied Energy* 189. Elsevier Ltd: 480–91. doi:10.1016/j.apenergy.2016.12.071.

Environmental mobility of antibiotics: A global human health treat

Isabel Carvalho*, Paula Penêda, Joana Teixeira and Lúcia Santos
LEPABE - Laboratory for Process Engineering, Environment, Biotechnology and Energy, Faculty of Engineering, University of Porto, Rua Dr. Roberto Frias, 4200-465 Porto, Portugal
*isabelc@fe.up.pt

Keywords: antibiotics, environment, mobility, water, soils, vegetables, QuEChERS, HPLC-DAD

Antibiotics are chemotherapeutic agents that inhibit or prevent the growth of microorganisms and, more recently, they have been recognized as an emerging class of environmental pollutants. These compounds are used in veterinary and human medicine on a large scale, therefore a significant quantity of pharmaceuticals is continuously spreading into environment (Carvalho and Santos 2016).

The excretion rate of veterinary antibiotics is dependent of the administrated substance, the application form, the animal species and the duration of the treatment. Nevertheless, its absorption is incomplete being estimated that 90% of the initial dose is eliminated in a non-metabolized way or as active metabolites (Tasho and Cho 2016).

The excrements reached the environment as result of the ineffective treatment in wastewater treatment plants since they are not prepared to remove this type of contaminants. The contaminated effluents (liquids or solids) could achieve the natural watercourses or the agricultural soils owed to their use as irrigation water or fertilizer. From the soil, antibiotics could disseminate to groundwater or through metabolic processes they could be accumulated by vegetables and plants (Thiele-Bruhn 2003).

As a result of this diffusion through aquatic (e.g. superficial and groundwater) and terrestrial environments (e.g. soil and vegetables matrices), it is promoted the development and dissemination of antibiotic resistance bacteria, which is becoming one of the most crucial problems concerning about public health.

The antibiotics selected for this work are metronidazole, sulfamethoxazole and trimethoprim due to the increment of their presence in environment because of their significant use on veterinary and human medicine. The interest of studying sulfamethoxazole and trimethoprim simultaneity is on account of their synergetic effect.

Studies in this area report a wide variety of extraction methods which, more recently, include QuEChERS (Quick, Easy, Cheap, Effective, Rugged and Safe). This technique is becoming one of the most applied methodologies to extract a broad range of contaminants that are present in solid samples, such as soil and vegetables matrices (Bruzzoniti et al. 2014).

This study focus on the above-mentioned antibiotics and on development, optimization and validation of a combined instrumental method using QuEChERS as extraction methodology and HPLC-DAD (High Performance Liquid Chromatography – Diode Array Detector) as analytical technique. In order to get an overview of the behaviour of these contaminants in soil and vegetables it was study their distribution in real matrices (soils and vegetables) with pre-established conditions.

This study may be relevant for future works once there is no legislation for this specific class of contaminants. Moreover, their concentrations in environment have tendency to increase accounting the population growth. In addition, accumulation of these contaminants in environment could contaminate food resources and they also could represent a potential issue for public health.

References

Bruzzoniti, Maria Concetta, Leonardo Checchini, Rosa Maria De Carlo, Serena Orlandini, Luca Rivoira, and Massimo Del Bubba. 2014. "QuEChERS Sample Preparation for the Determination of Pesticides and Other Organic Residues in Environmental Matrices: A Critical Review." *Analytical and Bioanalytical Chemistry* 406 (17): 4089–4116. doi:10.1007/s00216-014-7798-4.

Carvalho, Isabel T., and Lúcia Santos. 2016. "Antibiotics in the Aquatic Environments: A Review of the European Scenario." *Environment International* 94: 736–57. doi:10.1016/j.envint.2016.06.025.

Tasho, Reep Pandi, and Jae Yong Cho. 2016. "Veterinary Antibiotics in Animal Waste, Its Distribution in Soil and Uptake by Plants: A Review." *The Science of the Total Environment* 563–564: 366–76. doi:10.1016/j.scitotenv.2016.04.140.

Thiele-Bruhn, Sören. 2003. "Pharmaceutical Antibiotic Compounds in Soils - A Review." *Journal of Plant Nutrition and Soil Science* 166 (2): 145–67. doi:10.1002/jpln.200390023.

Selective photocatalytic oxidation of alcohols to aldehydes using exfoliated g-C_3N_4

M. J. Lima*, A. M. T. Silva, C. G. Silva and J. L. Faria
Laboratory of Separation and Reaction Engineering – Laboratory of Catalysis and Materials (LSRE–LCM), Faculty of Engineering University of Porto, Porto, Portugal
*mj.lima@.up.pt

Keywords: Carbon nitride, g-C_3N_4, selective photocatalysis, green chemistry, selective oxidation, benzyl alcohol, benzaldehyde.

Aromatic aldehydes are compounds widely employed in industry as building block for several chemical processes, like in fragrances and pharmaceuticals production. Normally, their synthesis at industrial scale requires the use of homogeneous catalysts, organic solvents, and severe conditions of temperature and pressure. Photocatalysis is considered an environmentally friendly alternative, since light is used for catalyst activation and the process may occur under ambient temperature and pressure, thus decreasing the harsh conditions used in typical industrial organic synthesis.

In the domain of semi-conductive carbon materials with photocatalytic activity, carbon nitrides (C_3N_4), and specifically graphitic carbon nitride (g-C_3N_4), attracted the attention of the scientific community due to its benign chemical composition (mostly composed by C and N, and a minor percentage of H) and the capacity of being effectively activated by visible light excitation.

One of the main bottlenecks of g-C_3N_4 is the low surface area which is may play a crucial rolein specific reactions. Similarly to graphene, g-C_3N_4 layers can be separated and etched into g-C_3N_4 nanosheets by thermal, physical and chemical methods (Figure 1), normally resulting in an increase in the surface area and consequently in the photocatalytic activity in comparison to the bulk catalyst (Han et al. 2015).

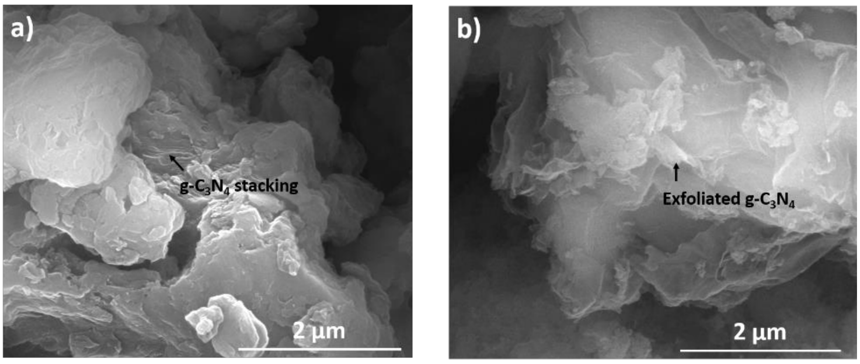

Figure 1. SEM images of bulk g-C_3N_4 (a) and thermal post-treated g-C_3N_4 (b).

In the present work, the selective photocatalytic conversion of alcohols to aldehydes was studied using environmental-friendly conditions using water as solvent, metal-free catalysts, natural pH, ambient temperature and pressure, and light emitting diodes (LEDs) as highly-efficient and low cost radiation sources.

The exfoliated g-C_3N_4 material was obtained by thermal treatment of bulk g-C_3N_4 to produce few layered nanosheets, which were then subjected to ultra-sonication. The resulting exfoliated catalyst was then used for the selective oxidation of a set of benzylic alcohols to the corresponding aldehydes (Figure 2).

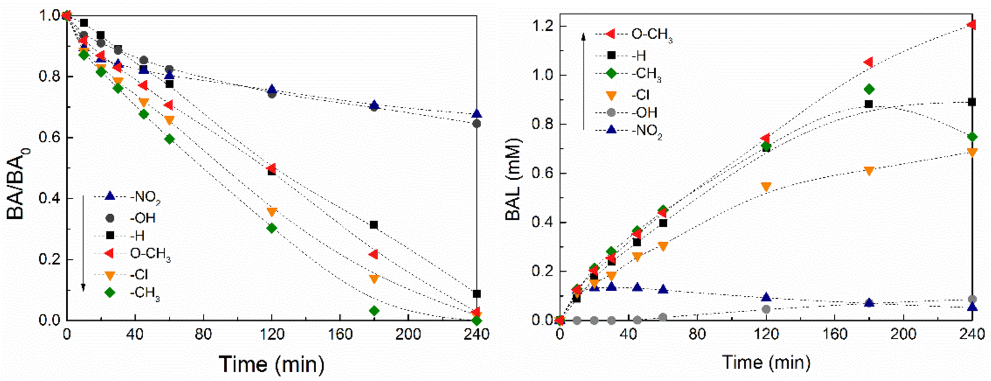

Figure 2. Photocatalytic oxidation of a set of aromatic alcohols to the respective aldehydes. Experimental conditions: 0.5 g L^{-1} catalyst, $[BA]_0$ = 1.5 mM, V_i = 50 mL, LED_λ = 392 nm.

The best performing systems were those using benzyl alcohol (-H), 4-methoxy benzyl alcohol (O-CH_3) and 4-methyl benzyl alcohol (-CH_3). The results indicate that the photocatalytic activity is greatly influenced by the nature of the substituent in the *para* position (Xu et al. 2017), the conversion being enhanced by the presence of electron-donating groups. A maximum of 76% of yield with 78% selectivity was obtained for the production of 4-methoxy benzaldehyde under the selected conditions.

Acknowledgments

This work was financially supported by Project POCI-01-0145-FEDER-006984 – Associate Laboratory LSRE-LCM funded by FEDER through COMPETE2020 - Programa Operacional Competitividade e Internacionalização (POCI) – and by national funds through FCT - Fundação para a Ciência e a Tecnologia. M.J. Lima gratefully acknowledges her Ph.D. scholarship (PD/BD/52623/2014) from FCT. AMTS and CGS acknowledge the FCT Investigator Programme (IF/01501/2013 and IF/00514/2014, respectively) with financing from the European Social Fund and the Human Potential Operational Programme.

References

Han, Qing, Fei Zhao, Chuangang Hu, Lingxiao Lv, Zhipan Zhang, Nan Chen, and Liangti Qu. 2015. "Facile production of ultrathin graphitic carbon nitride nanoplatelets for efficient visible-light water splitting." Nano Research 8 (5):1718-1728. doi: 10.1007/s12274-014-0675-9.

Xu, Yong, Zi-Cheng Fu, Shuang Cao, Yong Chen, and Wen-Fu Fu. 2017. "Highly selective oxidation of sulfides on a CdS/C_3N_4 catalyst with dioxygen under visible-light irradiation."Catalysis Science & Technology 7 (3):587-595. doi: 10.1039/C6CY01568A.

Photocatalytic synthesis of aromatic aldehydes using ZnO-based catalysts and energy-efficient light sources

R. A. Fernandes, M. J. Sampaio, J. L. Faria and C.G. Silva*
Laboratory of Separation and Reaction Engineering – Laboratory of Catalysis and Materials (LSRE-LCM), Department of Chemical Engineering, Faculty of Engineering, University of Porto, Rua Dr. Roberto Frias s/n, 4200-465 Porto, Portugal
*cgsilva@fe.up.pt

Keywords: photocatalysis, zinc oxide, synthesis, aromatic aldehydes

Heterogeneous photocatalysis has been established as a promising alternative to traditional thermal catalytic processes used in the synthesis of organic compounds. It presents advantages as the possible use of aqueous solvents, room temperature, atmospheric pressure and energy-efficient light sources (Di Paola et al. 2015). Aromatic aldehydes, as vanillin, are compounds with several industrial applications, which make their production processes an interesting research line (Augugliaro et al. 2012).

In this work, zinc oxide (ZnO) synthetized by chemical vapor deposition (CVD) was combined with different amounts of carbon nanofibers (CNF) to form hybrid photocatalysts. SEM micrographs of ZnO reveal a tetrapod-like morphology (Figure 1a). The typical morphology of CNF/ZnO composites can be observed in Figure 1b, with CNF surrounding the ZnO tetrapods.

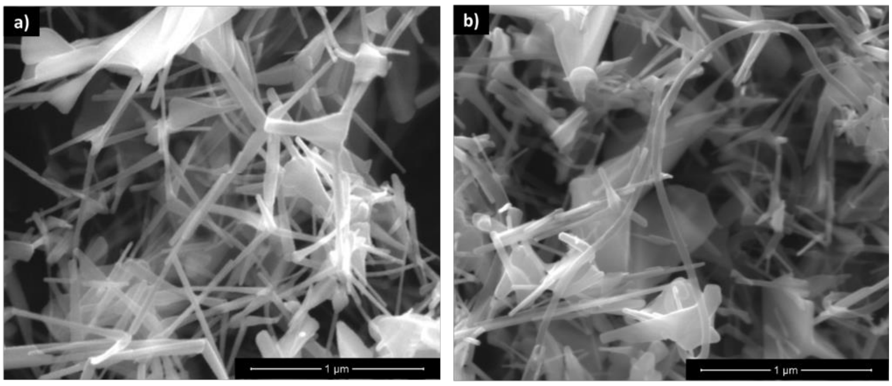

Figure 1. SEM micrographs of ZnO (a) and CNF/ZnO hybrid (b) materials.

The presence of CNF contributes to an increase in the surface area of the catalysts, as compared to neat ZnO. Although the band-gap of the ZnO-based materials is not significantly changed by the presence of the carbon phase, the photoluminescence of the material undergoes a dramatically decrease. This may be indicative of a decrease in the electron/hole recombination mechanism.

The efficiency of the photocatalytic materials was assessed for the synthesis of vanillin (V) through oxidation of vanillyl alcohol (VA) in aqueous media under UV-LED irradiation, by monitoring the conversion (C), yield (Y) and selectivity (S), following the concentrations of the reagents and products by high performance liquid chromatography (HPLC).

The effect of a carbon phase was assessed by increasing the CNF content of the photocatalytic material from 5, to 10, to 15 and to 20 wt. % with relation to the metal oxide. The photocatalytic performance of the hybrid catalysts was compared against the results obtained with neat ZnO in the same reaction (Figure 2a). The best results were obtained with the material containing 10 wt.% of CNF, reaching 50% of VA conversion and 20% yield of V (corresponding to S = 40%).

Finally, ZnO and the best performing hybrid catalyst were tested in the conversion of other aromatic alcohols (anisyl alcohol and piperonyl alcohol) into the respective aldehydes (anisaldehyde (A) and piperonal (P), Figure 2b).

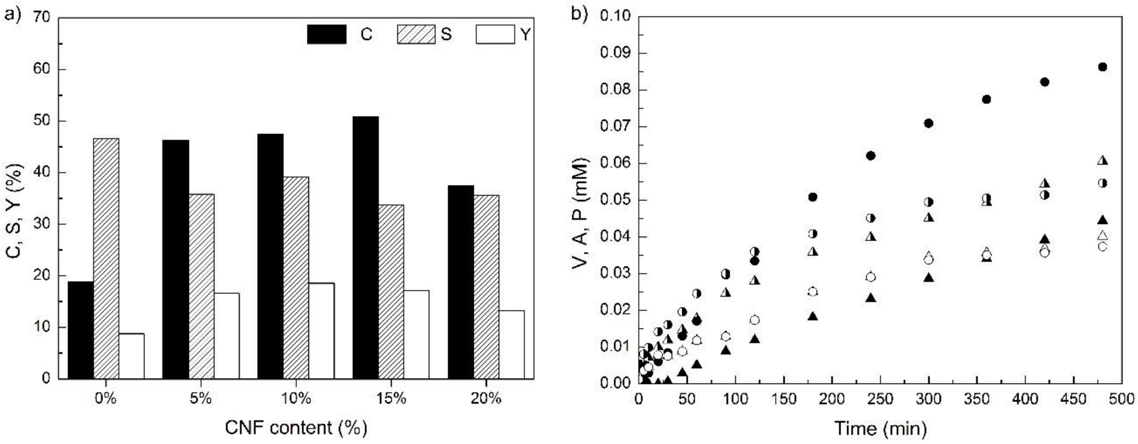

Figure 2. C, S and Y towards V production using different contents of CNF (a). Photocatalytic production of aromatic aldehydes (V, solid; A, semi-solid; P, open) by ZnO (circles) and 10%CNF/ZnO (triangles) (b).

The results show that the relative efficiency of ZnO and CNF/ZnO depends on the target reaction. The synergetic effect promoted by the presence of the carbon phase is more evident for the production of vanillin.

Acknowledgments

This work was financially supported by Project POCI-01-0145-FEDER-006984 – Associate Laboratory LSRE-LCM funded by FEDER through COMPETE2020 - Programa Operacional Competitividade e Internacionalização (POCI) – and by national funds through FCT - Fundação para a Ciência e a Tecnologia. R.A.F. acknowledges the PhD fellowship funded by Project NORTE-08- 5369-FSE-000028, supported by Norte Portugal Regional Operational Programme (NORTE 2020), under the PORTUGAL 2020 Partnership Agreement, through the European Social Fund (ESF). C.G.S. acknowledge the FCT Investigator Programme (IF/00514/2014) with financing from the European Social Fund and the Human Potential Operational Programme.

References

Augugliaro, Vincenzo, Giovanni Camera-Roda, Vittorio Loddo, Giovanni Palmisano, Leonardo Palmisano, Francesco Parrino, and Maria Angela Puma. 2012. “Synthesis of Vanillin in Water by TiO_2 Photocatalysis”. Applied Catalysis B: Environmental 111–112: 555–61. doi: 10.1016/j.apcatb.2011.11.007.

Paola, Agatino Di, Marianna Bellardita, Bartolomeo Megna, Francesco Parrino, and Leonardo Palmisano. 2015. “Photocatalytic Oxidation of Trans-Ferulic Acid to Vanillin on TiO_2 and WO_3-Loaded TiO_2 Catalysts”. Catalysis Today 252: 195–200. doi: 10.1016/j.cattod.2014.09.012.

Adsorption behaviour of MIL-100(Fe) under vapour water

M.P. Silva[1*], A.M. Ribeiro[1], C.G. Silva[1], J. Faria[1], J.M. Loureiro[1], J.-S. Chang[2], A.E. Rodrigues[1] and A. Ferreira[1]

[1] Laboratory of Separation and Reaction Engineering - Laboratory of Catalysis and Materials (LA / LSRE-LCM), Associate Laboratory LSRE/LCM, Faculty of Engineering University of Porto, Portugal

[2] Catalysis Center for Nanocatalysts, Korea Research Institute of Chemical Technology (KRICT), Jang-dong 100, Yuseong, Daejeon, Korea

*mpsilva@fe.up.pt

Keywords: MIL-100(Fe), adsorption, water.

MIL-100(Fe) is a material which presents great potential for water extraction by adsorption processes. Water vapour presented isotherms type VI and the adsorbed amount was of approximately 35.0 mol.kg^{-1} at 283 K for $p/p_0 = 0.93$. DRIFT spectra showed an upward trend proving the continuous water adsorption until reaching equilibrium after 120 min.

Introduction

Extraction of water (H_2O) from atmospheric air by adsorption base technologies is a method for H_2O production. Some Metal Organic Frameworks (MOFs) show a great potential in H_2O adsorption, being stable under H_2O adsorption/desorption cycles. This study evaluates the MOF MIL-100(Fe) potential as adsorbent for adsorption based atmospheric H_2O extraction processes.

Materials and Methods

Granulates of MIL-100(Fe) (Figure 1) were synthesized at the KRICT (Seo et al. 2012, Yoon et al. 2010) and prepared accordingly with procedure presented in Ribeiro et al. (2013).

Figure 1. MIL-100(Fe) granulates as provided by KRICT.

Adsorption equilibrium isotherms were assessed by means of a gravimetric system using a Rubotherm magnetic suspension balance in batch mode. While, diffuse reflectance infrared Fourier transform (DRIFT) spectra measurements were conducted using a Jasco FT/IR-6800 spectrometer equipped with a DiffusIR™ diffuse reflection.

Discussion

The H_2O equilibrium adsorption isotherms present type VI isotherm (Figure 2).

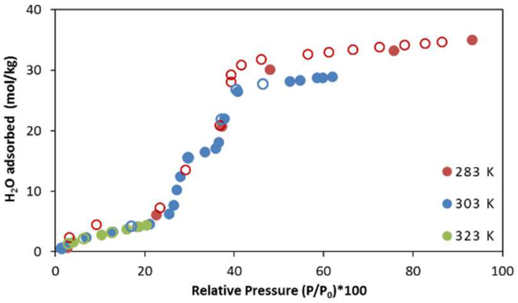

Figure 2. H_2O vapour adsorption–desorption isotherms on MIL-100(Fe) at 283, 303 and 323 K (filled symbol: adsorption, open symbol: desorption).

H_2O adsorption spectra (Figure 3) were obtained after feeding a continuous stream of helium saturated in H_2O at room temperature. Adsorption equilibrium for these feed conditions was achieved about 120 min after the inlet of the moist stream.

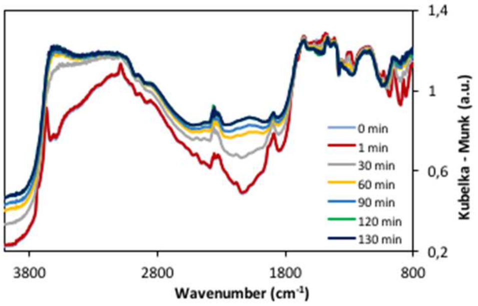

Figure 3. DRIFT spectra during water saturation of MIL-100(Fe).

Conclusions

H_2O isotherms present a Type VI isotherm shape, not being visible any hysteresis. Regarding DRIFT spectra, in the range 4000-1750 cm^{-1} a gradual rise of bands and peaks is visible due to H_2O adsorption on the material.

References

Ribeiro, Ana M., Marta C. Campo, Guler Narin, João C. Santos, Alexandre Ferreira, Jong-San Chang, Young Kyu Hwang, You-Kyong Seo, U. Hwang Lee, José M. Loureiro, and Alírio E. Rodrigues. 2013. "Pressure swing adsorption process for the separation of nitrogen and propylene with a MOF adsorbent MIL-100(Fe)." *Separation and Purification Technology* no. 110:101-111. doi: http://dx.doi.org/10.1016/j.seppur.2013.03.009.

Seo, You-Kyong, Ji Woong Yoon, Ji Sun Lee, U. Hwang Lee, Young Kyu Hwang, Chul-Ho Jun, Patricia Horcajada, Christian Serre, and Jong-San Chang. 2012. "Large scale fluorine-free synthesis of hierarchically porous iron(III) trimesate MIL-100(Fe) with a zeolite MTN topology." *Microporous and Mesoporous Materials* no. 157:137-145. doi: http://dx.doi.org/10.1016/j.micromeso.2012.02.027.

Yoon, J. W., Y. K. Seo, Y. K. Hwang, J. S. Chang, H. Leclerc, S. Wuttke, P. Bazin, A. Vimont, M. Daturi, E. Bloch, P. L. Llewellyn, C. Serre, P. Horcajada, J. M. Greneche, A. E. Rodrigues, and G. Ferey. 2010. "Controlled reducibility of a metal-organic framework with coordinatively unsaturated sites for preferential gas sorption." *Angew Chem Int Ed Engl* no. 49 (34):5949-52. doi: 10.1002/anie.201001230.

Identification of microorganisms with high cell viability for winery wastewater treatment in Microbial Fuel Cells

Francisco Ramalhosa[1], Joana Vilas Boas[1], Vânia Oliveira[1], Manuel Simões[2], Alexandra Rodrigues Pinto[1*]
[1]CEFT, Department of Chemical Engineering, Faculty of Engineering University of Porto, Porto, Portugal;
[2]LEPABE, Department of Chemical Engineering University of Porto, Porto, Portugal
*apinto@fe.up.pt

Keywords: Microbial fuel cell, winery wastewater treatment, synthetic winery wastewater, cell viability.

Abstract

Microbial Fuel Cells (MFCs) are bio-electrochemical systems capable of transforming the organic matter into electricity, by using microorganisms that perform the oxidation of the organic matter and transfer the electrons produced, directly or through mediators, to the anode, under anaerobic conditions. Winery wastewaters have a chemical composition that allows its treatment by biological processes. In this context, MFCs seem to be a good option to perform that since, unlike the traditional wastewater treatment technologies (such as anaerobic digestion), do not need high electrical energy inputs. Therefore, this work intended to evaluate the viability of seven different microorganisms (Acetobacter aceti, Gluconobacter oxydans, Saccharomyces cerevisiae, Zygosaccharomyces bailii, Zygosaccharomyces rouxii, Bacillus cereus and Escherichia coli) in a synthetic winery wastewater, in order to identify the two microorganisms with higher growth rate and study their performance in a single-chamber MFC. The microorganisms were chosen due to their adaptive behaviour in wine wastewater conditions.

Introduction

Microbial Fuel cells (MFCs) are a sustainable way to produce energy since they combine the electricity generation and the wastewater treatment. MFCs are seen as very promising alternative to the traditional wastewater treatment facilities, which require a higher input of energy. Usually MFCs are composed by an anode, an external circuit, a cathode and a semipermeable membrane that separates de anode and the cathode sides. At the anode occurs the oxidation of the organic matter and the extracellular transference of electrons and protons by the microorganisms, under anaerobic conditions. The external circuit is responsible for the transference of electrons from the anode to the cathode. At the cathode the electrons are released and transferred to a final electron acceptor, with high reducing potential (such as oxygen), producing water. The semipermeable membrane facilitates the protons transfer to the cathode and allows the operation of the MFC with different pH conditions on both sides.

Winery industries worldwide produce billion of litters of wine every year and consequently high quantities of winery wastewaters (WW) must to be treat before being disposal. Bustamante et al. 2005, studied the composition of eight Spanish winery effluents and conclude that in those effluents existed reasonable percentages of nitrogen, heavy metals, polyphenols and nutrients.

According to Malandra et al. 2003, most of the winery wastewaters have a high organic charge with an average chemical oxygen demand (COD) between 800 and 12 800 $mg\,O_2/L$, considerable ratios of organic acids (acid acetic, acid tartaric, acid propionic) alcohols (ethanol, propanol, glycerol), esters and an acid pH between 3 and 4. In general, the concentrations of these different compounds in the WW exceeds the limits established for their application in irrigation water to agriculture. In order to avoid environmental issues related with the WW disposal, biological winery wastewater treatments, such as anaerobic digestion and activated sludge reactors, are crucial to allow the use of these effluents in agricultural soils as fertilizers, however this kind of treatments represent high costs to the winery industry. For that reason, founding new lower cost technologies is assumed as a major concern. In this context, the use of MFCs to accomplish this treatment, a technology without high energy necessities, appears as an attractive idea for this sector. Nonetheless, until now, only a few studies have reported the winery wastewater treatment with MFCs and in those studies only Acetobacter aceti, Gluconobacter roseus and activated sludge were used as anodic inoculum (Rengasamy, et al. 2011). In this work, Acetobacter aceti, Gluconobacter oxydans, Saccharomyces cerevisiae, Zygosaccharomyces bailii, Zygosaccharomyces rouxii, Bacillus cereus and Escherichia coli were analysed thru its cell viability in a synthetic winery wastewater (SWW). These microorganisms were chosen based on the fact that they are very resistant and therefore can survive in the wine effluent conditions. Among these seven microorganisms, the two that presented a high adaptation to the SWW were selected and properly characterized, thru its growth phase curve, with the objective of being further used in a single-chamber MFC (SCMFC). The cell performance was evaluated in terms of the power density achieved, the biofilm formation and the COD removal rate.

Materials and Methods

The seven microorganisms were inoculated as single cultures in 60 mL of SWW (Malandra et al. 2003) at ambient temperature during 72 hours. The microorganisms were cultivated by the plating method in a PCA medium at 28 oC and different periods of time (0 h, 2 h, 24 h, 48 h and 72 h of the inoculation). The Colony Forming Units (CFU) counting was made according to the different microorganism's growth cycles. For B. cereus, the CFU counting was made after 16 hours, for E. coli after 24 hours, for A. aceti, G. oxydans, S. cerevisiae and Z. bailii after 48 hours and for Z. rouxii after 72 hours. The OD600nm, optical density, was also measured in the spectrophotometer for each culture.

References

Rengasamy, K. and Berchmans, S., "Simultaneous degradation of bad wine and electricity generation with the aid of the coexisting biocatalysts Acetobacter aceti and Gluconobacter roseus". Bioresource Technology 104:388–393. doi:10.1016/j.biortech.2011.10.092 .

Malandra L., Wolfaardt G., Zietsman A., Viljoen-Bloom M. 2003. "Microbiology of a biological contactor for winery wastewater treatment". Water Research 37:4125-4134. doi: 10.1016/S0043-1354(03)00339-7.

Bustamante M.A., Paredes C., Moral R., Moreno-Caselles J., Pérez-Espinosa A. and Pérez-Murcia M.D. 2005. "Uses of winery and distillery effluents in agriculture: characterisation of nutrient and hazardous components". Water Science and Technology, 51:145-151.

Emulsification using the NETmix technology for production of microcapsules

Ana C. G. Moreira[1], Madalena M. Dias[1], José C. B. Lopes[1]

[1]Laboratory of Separation and Reaction Engineering – Laboratory of Catalysis and Materials (LSRE-LCM), Faculty of Engineering, University of Porto, Portugal (acmoreira@fe.up.pt)

Keywords: NETmix reactor, oil-in-water emulsion, resin, oleic active principle

1. Introduction

Microencapsulation is a technique which allows an active principle, the core, to be covered by an external material, a membrane. Microcapsules usually present a spherical shape with size between 1 and 1000 µm (Bansode et al. 2010). This size is controlled by the mixing quality achieved in one of the most important steps for microencapsulation, emulsification. Emulsions can be of different types (double emulsion, oil-in-water or water-in-oil) and are usually obtained using typical mechanical stirrers, ultrasonication or homogenizers (Santos 2011). The goal of the present work is to obtain an oil-in-water emulsion using the NETmix technology (Laranjeira et al. 2011, Laranjeira et al. 2009, Lopes et al. 2005). NETmix consists of a network of interconnected chambers and channels: chambers operate as mixing zones while channels behave as a plug flow. Above a critical Reynolds number (circa 150) the system evolves to a self-sustained oscillatory laminar flow regime inducing local strong laminar mixing. The NETmix reactor allows continuous production where the mixture is obtained in a few seconds and using different injection schemes for the reactants may result in different mixing properties. The Reynolds number is easily controllable by changing the flow rate of the reactants. The obtained emulsions can be used in the production of microcapsules of resin with an oleic core through polycondensation reaction for textile applications.

Materials and Methods

The emulsion was obtained on a Lab-scale NETmix comprising 8 input and output chambers, by mixing two solutions: an aqueous solution of resin (A) and an oleic active principle (B). It was tested at Reynolds number of 200 and injection scheme with alternated inputs of reactants A and B.

The morphology of emulsion was characterized by optical microscopy and scanning electronic microscopy (SEM), and the diameter distribution was analyzed by laser diffraction.

2. Discussion

In the emulsion obtained from NETmix, the droplets of oil are dispersed on an aqueous solution that contains the membrane built from the resin. Optical microscopy shows droplets of oil with a regular and spherical shape (Figure 1a). Through SEM imaging, it is possible to observe some small microcapsules (Figure 1b). It is believed that membranes are already formed in this step, encapsulating the oil (Figure 1a). However, a curing process may be required in order to consolidate the membranes, resulting in more stable microcapsules. Using Laser Diffraction, the volume particle size distribution of the emulsion is obtained, with an observed mean microcapsules diameter of 65 µm (Figure 1c). The observed size by optical microscopy matches with the mean diameter obtained from laser diffraction. However, SEM imaging does not corroborate with this observation. A possible explanation is that once the first microcapsules are produced during the emulsification step, these are not stable enough to keep their physical consistency when dried. This is why the larger microcapsules tend to break after drying, while the smaller, which are more stable, keep their shape intact.

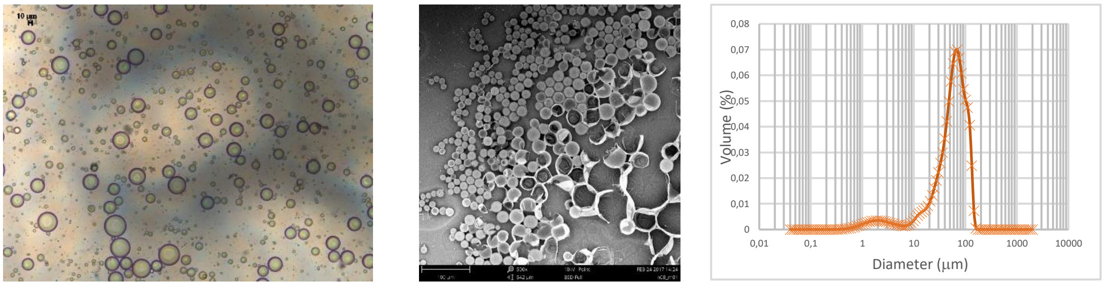

(a) (b) (c)

Figure 1: (a) Optical microscopy (x500) image of emulsion; **(b)** SEM image (x100) of dried emulsion; **(c)** Volume particle size distribution of emulsion.

3. Conclusions

The key step of microencapsulation techniques, emulsification, is performed in a continuous process, using the NETmix reactor. An oil-in-water emulsion was produced with mean diameter around 65 µm and optical microscopy of emulsion confirms their spherical shape. SEM imaging shows that in this step, possibly some microcapsules are produced, however these are not stable.

The produced emulsion allows the production of melamine-formaldehyde microcapsules with an oleic active principle. However, in the future, the process must be optimized for example decreasing the mean diameter of emulsion by increasing the Reynolds number.

Acknowledgements

LA LSRE-LCM, POCI-01-0145-FEDER-006984, funded by FEDER, through COMPETE2020 and FCT; Project TexBioPro, POCI-01-0247-FEDER-003472, funded by FEDER, through COMPETE 2020, under PT2020.

References

Bansode, S.S., Banarjee, S.K., Gaikwad, D.D., Jadhav, S.L., and Thorat, R.M. 2010. "Microencapsulation: A review." *International Journal of Pharmaceutical Sciences Review and Research* 1 (2):38-43.

Laranjeira, P.E., Martins, A.A., Lopes, J.C.B., and Dias, M.M. 2009. "NETmix®, a new type of static mixer: Modeling, simulation, macromixing, and micromixing characterization." *AIChE* 55 (9):2226-2243.

Laranjeira, P.E., Martins, A.A., Nunes, M.I., Lopes, J.C.B., and Dias, M.M. 2011. "NETmix®, a new type of static mixer: Experimental characterization and model validation." *AIChE* 57 (4):1020-1032.

Lopes, J.C.B., Laranjeira, P.E.M.d.S.d.C., Dias, M.M., and Martins, A.A.A. 2005. Network mixer and related mixing process.

Santos, F.R.A.d. 2011. "Emulsões múltiplas: formulação, caracterização, estabilidade e aplicações."Master Thesis, Faculdade de Ciências da Saúde, Universidade Fernando Pessoa.

Use of Green Public Procurement for Acquiring Copy Paper and Graph Paper

Inês A. M. C. V. Carvalho[1*] and Patrícia A. S. Reis[1**]
[1]Master students in Environmental Engineering, Faculty of Engineering University of Porto, Porto, Portugal;
*up201007733@fe.up.pt
**patricia.reis.1495@gmail.com

Keywords: Green Public Procurement, European Commission, criteria, paper, virgin fibers, environmental impacts, sustainability

Abstract

This paper outlines the use of public procurement for the acquisition of copy paper and graphic paper in Europe. The main objective of this work is to carry out a global vision of Green Public Procurement (GPP) and what they imply, that is, the criteria underlying them. In order to achieve this objective, the paper starts with a description of what the GPP is, the sectoral groups covered by them and the applicable criteria. Is also made an analysis of the technical specifications that meet the GPP criteria for the purchase of copy paper and graphic paper. Finally, four case studies are evaluated from four European Community Member Countries: Bulgaria, Spain, Hungary and Italy. An important result of this study is that the GPP process, contrary to what can be interpreted, does not imply necessarily an increase in costs in the procurement process of products and/or services by the public administrations of each country.

Introduction

Green Public Procurement (GPP) is a process whereby public entities seek to purchase products and services which, when compared to products and services with the same function but not purchased through GPP, have a reduced environmental impact throughout their life. [1]

The Green Public Procurement criteria of the European Union (EU) are developed to facilitate the inclusion of green requirements in public tender documents. Although the EU GPP criteria aim at a good balance between environmental performance, cost considerations, market availability and easy verification, contracting authorities may choose, according to their needs and ambition, all or only requirements in their tender documents. [2]

In this way, the European Commission has defined a specific set of twenty one groups of products and services. The copy paper and graph paper is one of them. [3]

For the groups described, a collection of criteria was proposed, and these were created with the main objective of promoting the acceptance of GPPs by contracting entities. According to the "Uptake of Green Public Procurement in the EU27" report, there are two types of criteria used in GPP. On the one hand, we have the fundamental criteria, which translate into criteria that can be appropriate for any contracting entity that is concerned with and addresses key environmental impacts across Europe; these criteria have been designed to avoid possible additional checks and increased costs. On the other hand, there are complementary criteria, which are intended for contracting entities whose objective is to acquire the best environmental products on the market. These criteria may already require additional checks and possibly a slight increase in cost. In essence, what distinguishes the two types of criteria for EPC is the level of ambition of the contracting authority. [3]

Case studies results

Case studies were analyzed in four countries: Bulgaria, Spain, Hungary and Italy. After analyzing the case studies, the results were:

- Bulgaria - 100% recycled paper in the Bulgarian Ministry of Environment

The Ministry of the Environment carried out a pre-purchase analysis of the market prices of recycled and non-recycled paper for printers, and it was revealed that both have an approximate cost, and recycled paper meets all the required technical characteristics. As a successful outcome of the GPPs, the Ministry proposed to the Central Purchasing Body (CPB) in Bulgaria to purchase 100% recycled paper. [4]

- Spain - Eco-shopping in Badalona schools

Based on the information obtained after the analysis of the acquisitions, six individual GPP Action Plans were prepared in Spain. Currently, in Badalona, is being created a network of green schools, which aims to monitor the application of a guide for ecological purchasing. [1]

- Hungary - Centralized procurement of greener office supplies

In Hungary, the estimated value of Green Public Procurement for office supplies was HUF 4.4 billion, or EUR 14.5 million over 18 months. The framework entered force on January 31, 2011 and public entities have since acquired about 980 million HUF, which is 3.2 million euros in products and/or services. [5]

- Italy - Purchase of paper for the local governments of Lombardy

The value of the GPP is approximately 5.5 million euros over a period of 18 months. The allocation of the table results in the possibility for the 1600 public entities in the Lombardy region to be able to acquire paper of various sizes and qualities from a high ecological supplier in their production operations. [6]

References

[1] *Green Public Procurement - A collection of good practices*. (n.d.). https://doi.org/10.2779/93178

[2] *Copying and Graphic Paper - Background Product Report*. (2008). Bruxelas. Retrieved from http://ec.europa.eu/environment/gpp/pdf/toolkit/paper_GPP_background_report.pdf

[3] Renda, A., Pelkmans, J., Egenhofer, C., Schrefler, L., Luchetta, G., Selçuki, C., … Zirnhelt Brussels, A.-C. (2012). THE UPTAKE OF GREEN PUBLIC PROCUREMENT IN THE EU27 Centre for European Policy Studies (CEPS) College of Europe (core team). Retrieved from http://ec.europa.eu/environment/gpp/pdf/CEPS-CoE-GPP MAIN REPORT.pdf

[4] GPP Case Studies_100% recycled paper for Bulgaria's Environment Ministry. (n.d.). Retrieved from http://ec.europa.eu/environment/gpp/pdf/news_alert/Issue5_Case_Study12_Bulgaria_paper.pdf

[5] Centralised procurement of greener office supplies. (n.d.). Retrieved from http://ec.europa.eu/environment/gpp/pdf/news_alert/Issue16_Case_Study37_Hungary_supplies.pdf

[6] Carpineti, L., & Masiello, G. (n.d.). GPP In Practice Paper purchasing for Lombardy local governments. Retrieved from http://ec.europa.eu/environment/gpp/pdf/news_alert/Issue6_GPP_Example15_Lombardy_Paper_Framework.pdf

Coupling bioelectrochemical systems and redox flow batteries for sustainable energy production and storage

M.S.S. Santos[1,2,3*], L. Peixoto,[2] C. Dias-Ferreira[3],M.M. Alves[2], A. Mendes[1]
[1]LEPABE, Chemical Engineering Dpt., Faculty of Engineering University of Porto, Porto, Portugal;
[2]Centre of Biological Engineering, University of Minho, Braga, Portugal;
[3]Research Centre for Natural Resources, Environment and Society (CERNAS) / College of Agriculture, Polytechnic Institute of Coimbra, Bencanta 3045-601 Coimbra, Portugal;
[*]marciasofiasantos@hotmail.com

Keywords: Bioelectrochemical systems, redox flow batteries, electroactive bacteria, quinones

Abstract:

Different technologies use different types of renewable energy sources (solar, wind, hydraulic) that are capable to compete with fossil fuels responsible for carbon dioxide emissions with strong impact in global warming (deLlano-Paz *et al.,* 2015). Electrochemical systems are designed to produce sustainable energy, conversion, conservation and energy storage (Badwal *et al.,* 2014). They are also designed to produce different chemical compounds and fuels (e.g. chlorine and aluminium)(Botte 2014).

Bioelectrochemical systems (BES) are systems capable to convert chemical energy into electricity through the degradation of different sources of organic compounds with electrogenic microorganisms as biocatalyst (Bajracharya *et al.,* 2016). These systems are also able to produce fuels or chemical compounds with different types of electroactive bacteria and different system's configurations. The ability of microorganisms to form biofilms in electrode surfaces allows the transport of electrons from the oxidation of carbon sources to be captured by a terminal electron acceptor (Kracke, Vassilev, and Krömer 2015). BES systems were successfully applied in small, on site applications in autonomous systems, but the bioelectrochemical energy produced was not stored (Peixoto 2012). Coupling a BES with a redox flow battery has potential to assemble innovative energy production and storage devices.

Redox flow batteries (RFB) are electrochemical energy converting systems able to transform and store chemical energy in electricity. Redox chemical species (in soluble form) are introduced in external tanks of a fuel cell with a recirculation system that is used to generate energy (Pan and Wang 2015). The chemical and physical properties of the redox chemical species (e.g. solubility), redox potentials, and materials used (carbon electrodes, membranes, etc) are mainly responsible for the high-energy conversion and storage in RFB. These systems are considered suitable for large-scale applications (Perry and Weber 2016).

The aim of this work is the development of a system that couples BES and RFB in a disruptive way to produce and store bioelectrochemical energy. For this new technology a BES system using electroactive microorganisms that degrade simple carbon sources will be used to charge redox chemical species. Quinones compounds are being studied in BES for the conversion to

their reduced form. In the RFB this organic redox chemical species will be used for electrochemical energy conversion and storage in the form of electricity.

References:

Badwal, Sukhvinder P S, Sarbjit S Giddey, Christopher Munnings, Anand I Bhatt, and Anthony F Hollenkamp. 2014. “Emerging Electrochemical Energy Conversion and Storage Technologies.” Frontiers in Chemistry 2: 79. doi:10.3389/fchem.2014.00079.

Bajracharya, Suman, Mohita Sharma, Gunda Mohanakrishna, Xochitl Dominguez Benneton, David P.B.T.B. B T B Strik, Priyangshu M. Sarma, and Deepak Pant. 2016. “An Overview on Emerging Bioelectrochemical Systems (BESs): Technology for Sustainable Electricity, Waste Remediation, Resource Recovery, Chemical Production and beyond.” Renewable Energy 98 (March). Elsevier Ltd: 153–70. doi:10.1016/j.renene.2016.03.002.

Botte, Gerardine G. 2014. “Electrochemical Manufacturing in the Chemical Industry.” The Electrochemical Society Interface Fall (c): 49–50. doi:10.1149/2.F04143if.

deLlano-Paz, Fernando, Anxo Calvo-Silvosa, Susana Iglesias Antelo, and Isabel Soares. 2015. “The European Low-Carbon Mix for 2030: The Role of Renewable Energy Sources in an Environmentally and Socially Efficient Approach.” Renewable and Sustainable Energy Reviews 48. Elsevier: 49–61. doi:10.1016/j.rser.2015.03.032.

Kracke, Frauke, Igor Vassilev, and Jens O. Krömer. 2015. “Microbial Electron Transport and Energy Conservation - The Foundation for Optimizing Bioelectrochemical Systems.” Frontiers in Microbiology 6 (JUN): 1–18. doi:10.3389/fmicb.2015.00575.

Pan, Feng, and Qing Wang. 2015. “Redox Species of Redox Flow Batteries: A Review.” Molecules 20 (11): 20499–517. doi:10.3390/molecules201119711.

Peixoto, Luciana. 2012. “Microbial Fuel Cells for Autonomous Systems : Kinetics and Technological Advances in Wastewater Treatment and Sensor Applications.” University of Minho. http://hdl.handle.net/1822/20786.

Perry, Mike L., and Adam Z. Weber. 2016. “Advanced Redox-Flow Batteries: A Perspective.” Journal of The Electrochemical Society 163 (1). The Electrochemical Society: A5064–67. doi:10.1149/2.0101601jes.

Droplet-based microfluidic platform for protein crystallization

J. Ferreira[1,2*], F. Castro[1,3], F. Rocha[1] and S. Kuhn[2]
[1]LEPABE – Laboratory for Process Engineering, Environment, Biotechnology & Energy, Chemical Engineering Dpt., Faculty of Engineering of the University of Porto, Porto, Portugal;
[2]Department of Chemical Engineering, KU Leuven, Leuven, Belgium;
[3]CEB – Centre of Biological Engineering, Biological Engineering Dpt., University of Minho, Campus de Gualtar, Braga, Portugal.
*eq11028@fe.up.pt

Keywords: Microfluidics, droplet, protein crystallization.

Introduction

The main focus of protein crystallization has been in the production of high-quality protein crystals for 3D structure determination by X-ray diffraction. However, this is a complex and multiparametric process, involving thermodynamic and kinetic features, as well as the optimization of several variables, where there is not an accurate theory to substitute for empirical approaches (Giegé and McPherson 2006). In this context, droplet-based microfluidics allows the generation of hundreds of droplets, each one acting as a microreactor, enabling thus to perform high-throughput screening of protein crystallization experiments under identical conditions.

The main goal of the present work is to develop an easy-to-use and cheap droplet-based microreactor for protein crystallization. The first part of the study aims at obtaining a broad range of droplet size by testing different flow rate ratios between the dispersed and the continuous phases (Q_d/Q_c). To study the regime of droplet formation, a range of low values of the Capillary number (Ca) was studied ($Ca < 2 \times 10^{-4}$). This part covers also a numerical study with CFD (Computational Fluid Dynamics) for the prediction of the droplet size. In a second part, it is intended to perform multiple microbatch lysozyme trials to study the influence of the droplet size on the nucleation mechanism.

Materials and Methods

The experimental set-up consists of a flow-focusing geometry coupled to a 1 mm diameter Teflon tube fixed by an acrylic plate, which is jacketed to control the temperature. Droplets were generated at the intersection between the continuous (silicon oil 1 cSt) and dispersed (aqueous solution) phases. Droplet size measurements were then conducted by image analysis. Microbatch lysozyme crystallization trials were carried out by mixing an egg white lysozyme ($60\ \mathrm{mg \cdot ml^{-1}}$) and a precipitant agent (sodium chloride 6% (w/v)) in a *T*-junction before the intersection between the continuous and dispersed phases. Both solutions were prepared in a 0.2 M phosphate buffer adjusted to pH 4.7. After approximately 20 h, the formed crystals were counted by microscopy. Afterwards, nucleation rates were determined using the double pulse technique (Galkin and Vekilov 1999). Regarding the numerical study, 2D numerical simulations were performed using a FEM platform together with the Level-Set (LS) technique to capture the dynamic shape of the fluid interface between the two liquid phases.

Results and Discussion

According to Figure 1, the developed droplet-based platform enabled to produce uniform and stable droplets with a very good frequency (up to 250 droplets per assay). It also allowed a large flexibility regarding the generated droplet volume (range of 0.9 - 18 µl). Figure 1 also shows a slight deviation between the numerical and the experimental results, probably due to the 2D geometry used in the simulations, which limits the prediction of the droplet curvature effects and the complex flow topology inside the droplet.

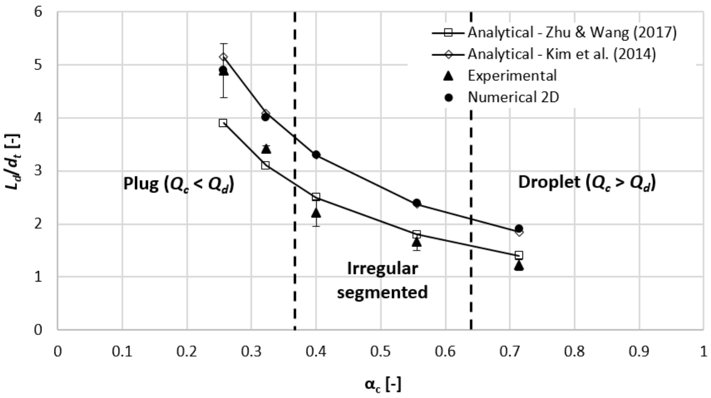

Figure 1. Scaled lengths of the dispersed phase (L_d) by Teflon tube diameter (d_t) as a function of the continuous fluid volumetric flow ratio (α_c) for squeezing flow regime and transition lines between regimes [The error bars are standard deviations from three independent experiments].

Lastly, correlations reported by Zhu and Wang (Zhu and Wang 2017) and Kim *et al.* (Kim et al. 2014) are in good agreement with experimental and numerical results, respectively (Figure 1). As to the lysozyme nucleation study, crystallization trials are currently being performed for further estimation of both the nucleation rate and induction time.

Acknowledgments

This work was financially supported by: Project POCI-01-0145-FEDER-006939 (Laboratory for Process Engineering, Environment, Biotechnology and Energy – LEPABE) funded by FEDER funds through COMPETE2020 - Programa Operacional Competitividade e Internacionalização (POCI) – and by national funds through FCT - Fundação para a Ciência e a Tecnologia; post-doctoral Fellowship [SFRH/BPD/96132/2013], and Fonds Wetenschappelijk Onderzoek (FWO).

References

Galkin, O, and P. G. Vekilov. 1999. “Direct Determination of the Nucleation Rates of Protein Crystals.” *The Journal of Physical: Chemistry B* 103 (49): 10965–71. Accessed 24 March, 2017. doi:10.1021/jp992786x.

Giegé, Richard, and Alexander McPherson. 2006. “Chapter: Crystallization – General Methods (Ch. 4.1).” In *International Tables of Crystallography, Vol. F, Crystallography of Biological Macromolecules*, edited by E. Arnold, D. M. Himmel, and M. G. Rossmann, 2nd edition, 81–93. John Wiley & Sons.

Kim, N., M. C. Murphy, S. A. Soper, and D. E. Nikitopoulos. 2014. “Liquid-Liquid Segmented Flows in Polycarbonate Microchannels with Cross-Sectional Expansions.” *International Journal of Multiphase Flow* 58. Elsevier Ltd: 83–96. Accessed 24 March, 2017. doi:10.1016/j.ijmultiphaseflow.2013.09.002.

Zhu, P., and L. Wang. 2017. “Passive and Active Droplet Generation with Microfluidics: A Review.” *Lab on a Chip* 17. Royal Society of Chemistry: 34–75. Accessed 24 March, 2017.doi:10.1039/C6LC01018K.

Laminaria sp. and *Fucus spiralis* marine macroalgae as potential biomass sources for biorefinery processing

C.Filote[1,2*], S.Santos[1], I.Volf[2] and C. Botelho[1]

[1]*LSRE-Laboratory of Separation and Reaction Engineering, Associate Laboratory LSRE/LCM, Faculdade de Engenharia da Universidade do Porto, Portugal*

[2]*"Gheorghe Asachi" Technical University of Iasi, Faculty of Chemical Engineering and Environmental Protection, Romania*

*catalina.filote@gmail.com

Keywords: macroalgae, biorefinery, ultrasounds assisted extraction, polyphenols.

The purpose of the present work is to determine the potential of brown marine macroalgae *Laminaria sp.* and *Fucus spiralis* collected from the northern coast of Portugal to be used in a biorefinery context to obtain valorizable compounds. The biorefinery approach is recommended for the simultaneous production of biofuels, bioenergy and value-added co-products for successful, efficient and cost-effective valorization of macroalgae biomass (Trivedi et al., 2015). Apart from alginate which is already commercially extractable, other known brown algae polysaccharides have shown important bioactive properties and industrial applications.

The studied macroalgae were firstly washed with distilled water to remove impurities, sand and epiphytes and afterwards dried in the oven at 50° C. Chemical characterization tests performed with the dry biomass revealed a relatively high content of polysaccharides for all the tested algae, 28±2% for *Laminaria sp.* and 16.3±0.7% for *Fucus spiralis*. To determine the total polyphenolic content (TPC), an ultrasounds-assisted extraction (UAE) was performed in optimal conditions previously established: 70% ethanol, at 40° C, for 45 minutes extraction time (Lazar et al., 2016). Also, the use of ultrasounds and ethanol-water mixture as solvent are known to improve the polyphenols extraction yield and reduce the duration of the process (Kadam et al., 2015). The highest TPC values were generated at 40° C, 1.5±0.1 mg GAE g^{-1} for *Laminaria sp.* and 13.0±0.1 mg GAE g^{-1} for *Fucus spiralis*. The results obtained from the characterization tests are presented in table 1.

Table 1. Characterization of selected macroalgae.

	Humidity %	Ash %	Total polysaccharides %	TPC (mg GAE g^{-1})
Laminaria sp.	9.1±0.1	16.8±0.5	28±2	1.5±0.1
Fucus spiralis	11.5±0.7	22.5±0.9	16.3±0.7	13.0±0.1

The present work demonstrates that *Laminaria sp.* and *Fucus spiralis* can be used as important and valuable biomass sources to obtain polysaccharides and polyphenols. Even more, the use of innovative extraction methods such as ultrasounds can be successfully applied to generate better extraction products and yield. Based on the composition of the macroalgae biomass, a biorefinery flow sheet with sequential extraction steps was proposed for an efficient and sustainable processing (Figure 1).

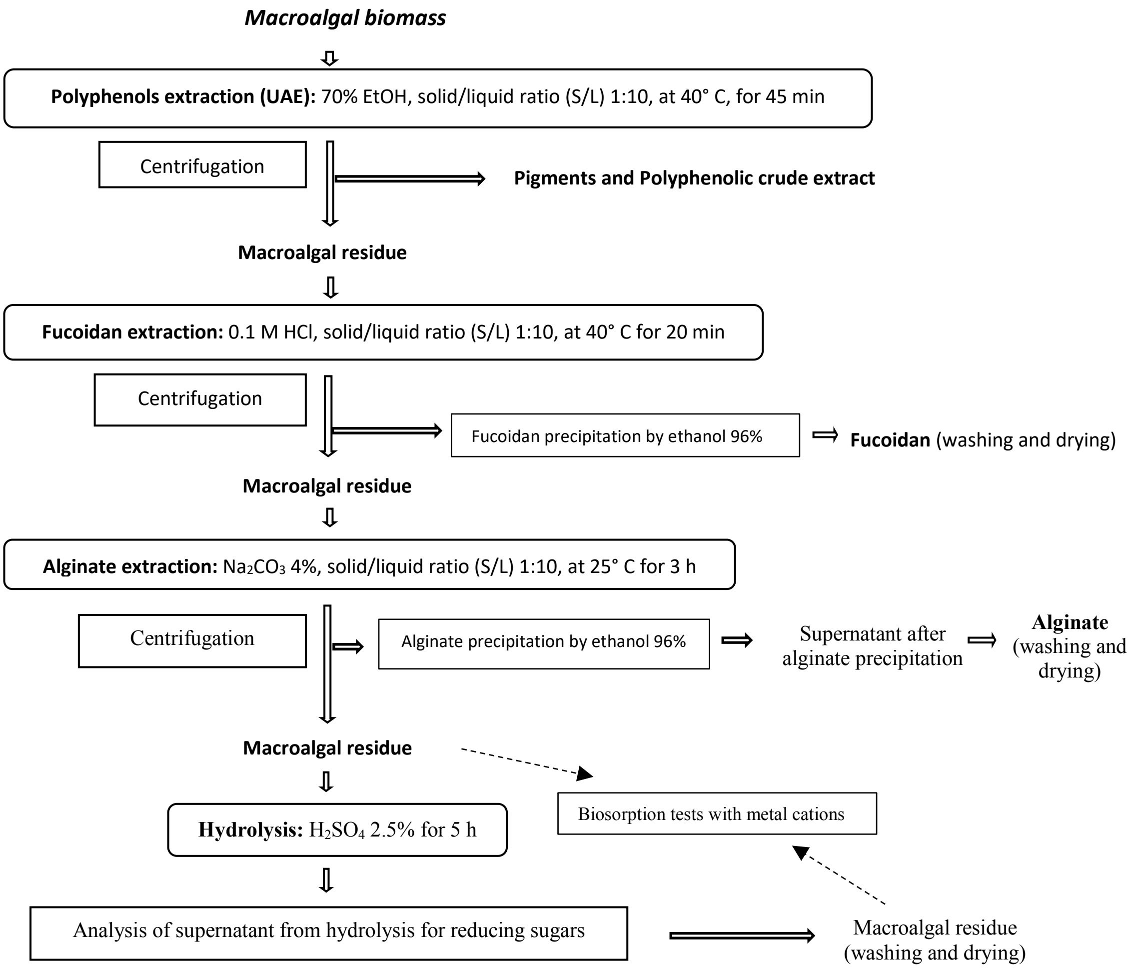

Figure 1. Proposed biorefinery flow sheet for *Laminaria sp.* and *Fucus spiralis*.

References

Lazar, L., A. Talmaciu, I. Volf, V.I. Popa. 2016. "Kinetic modeling of the ultrasounds-assisted extraction of polyphenols from *Picea abies* bark". Ultrasonics Sonochemistry 32: 191-197.

Kadam, S.U., B.K. Tiwari, T.J. Smyth, C.P. O’Donnell. 2015. "Optimization of ultrasound assisted extraction of bioactive components from brown seaweed *Ascophyllum nodosum* using response surface methodology". Ultrasonics Sonochemistry 23: 308-316.

Trivedi, J., M. Aila, D.P. Bangwal, S. Kaul, M.O. Garg. 2015. "Algae based biorefinery - How to make sense?". Renewable and Sustainable Energy Reviews 47: 295-307.

Acknowledgements

This work was financially supported by: Project POCI-01-0145-FEDER-006984 – Associate Laboratory LSRE-LCM funded by FEDER through COMPETE2020 – Programa Operacional Competitividade e Internacionalização (POCI) – and by national funds through FCT - Fundação para a Ciência e a Tecnologia. C. Filote acknowledges her Erasmus+ scholarship for a traineeship at FEUP (Portugal).

Description of Household Waste in the Northeast Region of Brazil: Case Study in Juazeiro do Norte, Ceará.

Anny Kariny Feitosa[1], Júlia Elisabete Barden[2], Odorico Konrad[2], Manuel Arlindo Amador de Matos[3], Diogo Appel Colvero[4]

[1]Doctoral Student in Environment and Development, Univates, Lajeado, Brazil, Researcher CAPES/PSDE/Process N.º 88881.135779/2016-1; [2]Teacher-researcher in Univates, Av. Avelino Talini, 171 - Universitário, Lajeado – RS, Brazil; [3]Department of Environment and Planning, University of Aveiro, Aveiro, Portugal, Aveiro, Portugal; [4]Department of Environment and Planning, University of Aveiro, Aveiro, Portugal, - Researcher Brazilian National Council for Scientific and Technological Development (CNPq), File N.º 207172/2014-5.

*akfeitosa@hotmail.com

Keywords: Solid Waste, Gravimetric Characterization, Variability.

The study aimed the description of household waste collected in the city of Juazeiro do Norte, CE, in the northeast region of Brazil. 473 door-to-door waste samples were collected, comprising 53 households registered, and the gravimetric composition of household waste was performed. In total, 797.58 kg. Was a prevalence of organic waste in the collected, with average of 58.49%. The total amount of recyclable materials corresponds to 18,21% of the total waste generated.

1. Introduction

The study aimed the description of household waste collected in the city of Juazeiro do Norte, CE, in the northeast region of Brazil. To know the quantities and composition of urban solid waste is essential to draw up assertive strategies of waste management (KARAK et al., 2012), as well as for the planning of education programs which can contribute to the reduction of waste generation, collection organization, as well as better disposal alternatives (KONRAD et al., 2015).

2. Materials and Methods

In the periods of 20-24 June and 15-19 August, 2016, 473 door-to-door waste samples were collected, comprising 53 households registered by simple random sampling in the city of Juazeiro do Norte. In total, 797.58 kg of waste were sampled and the gravimetric composition of household waste was performed, according a sampling procedure done in Konrad et al. (2010).

3. Discussion

Based on the data obtained, the description of household waste collected are shown in Table 1, below:

Table 1. Description of household waste in Juazeiro do Norte. *Source*: the authors.

Waste type	June (%)	August (%)	Average (%)
Organic waste	58.29	58.68	58.49
Plastic film	5.53	5.08	5.31

Rigid plastic	3.44	2.40	2.92
Polyethylene terephthalate (PET)	1.30	1.20	1.25
Paper/Newspaper	2.02	2.74	2.38
Cardboard	2.85	2.76	2.81
Composite packing (ECAL)	0.64	0.47	0.56
Glass	1.02	2.57	1.80
Metal	1.25	0.82	1.04
Styrofoam	0.15	0.26	0.21
Metalized plastic packaging	0.57	0.56	0.57
Diapers	10.39	10.85	10.62
Toilet paper	3.57	3.27	3.42
Rags/textiles	2.88	2.52	2.70
Wood	0.23	0.21	0.22
Rubber	0.15	0.49	0.32
Special waste	0.35	0.22	0.29
Construction and demolition waste	0.16	1.34	0.75
“Mela” - Recyclable rubber	0.26	0.01	0.14
Refuse	4.95	3.55	4.25
Total	100	100	100

According to Table 1, there was a prevalence of organic waste in the collected, with average of 58.51%. The following materials and percentages average were identified as recyclable potential: plastic film (5.31%), rigid plastic (2.92%), PET (1.25%), paper/newspaper (2.38%), cardboard (2,81%), ECAL (0,56%), glass (1.80%), metal (1.04%) and “Mela” (0.14%). The total amount of recyclable materials corresponds to 18.21% of the total waste generated, in the present study.

4. Conclusions

From this study, it was possible to know the composition of household waste collected in the city of Juazeiro do Norte, CE, contributing to the improvement of aspects related to the dimensioning of the structure necessary for the solid waste management in the municipal scope.

References

Karak, T.; Bhagat, R. M.; Bhattacharyya, P. Municipal solid waste generation, composition, and management: The World Scenario. “Critical Reviews Environmental Science and Technology”, v. 42, n. 15, p. 1509-1630, 2012.

Konrad, O.; Silva, G. R.; Konrad, A. C.; Hasan, C.; Marder, M. Schmeier, N. P. Geração per Capita de Resíduos Sólidos Domésticos na Zona Urbana de Municípios do Vale do Taquari – RS. “Revista Educação Ambiental”. Número, v. 53, Ano XIV., set./nov. 2015.

Konrad, O.; Casaril, C. E.; Schmitz, M. Estudo dos resíduos sólidos domésticos de Lajeado/RS pela caracterização gravimétrica. “Destaques Acadêmicos”, v. 4, p.57-62, 2010.

Catalytic Hydrolysis of $NaBH_4$ for Hydrogen synthesis: Study of recyclability of by-product $NaBO_2$

D. L. Silva[1], H. X. Nunes[1], C. M. Rangel[2], A. M. F. R. Pinto[1,*]
[1]CEFT – Transport Phenomena Research Center, Chemical Engineering Dpt., Faculty of Engineering University of Porto, Porto, Portugal;
[2]Solar Energy Unit, LNEG – Nacional Laboratory of Energy and Geology, Lisboa, Portugal
*apinto@fe.up.pt

Keywords: Hydrogen, hydrolysis of sodium borohydride, recyclability of sodium metaborate, mechano-chemical process, electrochemical process

Hydrogen, with an energy content of 142 MJ/kg (gaseous state), is one of the most promising alternatives to fossil fuels ("Fuels - Higher Calorific Values" 2017). Nevertheless, it is not found in its pure form in the planet and it is not easy to store under safe conditions, since it is lighter than air and flammable. Chemical hydrides, for example sodium borohydride, are able to safely store H_2. In theory, $NaBH_4$ is composed of 10,8% hydrogen and, when reacting with water, releases 4 moles of H_2 per mole of $NaBH_4$, as shown in Equation 1.

$$NaBH_4+(2+x)H_2O \rightarrow NaBO_2.x\ H_2O+4H_2+\text{heat} \tag{1}$$

In Equation 1, x represents the hydration factor. This reaction itself, although exothermic, requires a catalyst to lower the high activation energy of the reaction. Among different catalysts studied, an improved nickel-ruthenium based powdered one was selected to use in the experiments reported. Sodium hydroxide and additives are used in the hydrolysis reaction too. NaOH acts as an inhibitor in the hydrogen formation, stabilizing the sodium borohydride solution and avoiding spontaneous hydrolysis (Demirci 2015). The additives have different tasks, such as: the rearrangement of the $NaBH_4$'s structure, lowering the energy of the B-H bonds, for example, carboxymethylcellulose, CMC; to promote the reactants-catalyst contact, since it decreases the mass transfer limitations, increasing the H_2 generation yield and generation rate, for example, sodium dodecyl sulfate, SDS.

Hydrogen production through hydrolysis of $NaBH_4$ has great advantages for portable applications. However, for the development of an H_2-PEMFC system for energy production, necessary some barriers must be overcome namely the recycling of by-product $NaBO_2$. This can be achieved with the processes i) Brown and Schlesinger-reduction with reducing agents; ii) Bayer or mechano-chemical and iii) electrochemical. The mechano-chemical and the electrochemical processes are the ones who may be adaptable for small portable applications since they do not require high pressure and temperature but are still in development. The recyclability of $NaBO_2$ to $NaBH_4$ via mechano-chemical and electrochemical processes were carried out.

The hydrolysis of $NaBH_4$ with water was performed in a batch reactor, made in stainless steel, with conical bottom geometry (internal volume of 229 mL). Three different reactant solutions were prepared with the following mass percentages: 1) 13% $NaBH_4$, 7% NaOH; 2) 10% $NaBH_4$, 7% NaOH; 3) 10% $NaBH_4$; 7% NaOH; 1% CMC. In the set of experiments performed, a mass of catalyst/mass $NaBH_4$ ratio of 0,4 g/g was used. The reaction was performed under uncontrolled room temperature. The data were monitored and recorded with a data acquisition system using *LabView* software.

Produced and commercialized $NaBO_2$ were needed for the sodium borohydride regeneration. In the mechano-chemical process, the Retsch MM200 vibratory mill was employed to support the mixture of $NaBO_2$ with magnesium hydride, MgH_2, obtaining $NaBH_4$ and MgO, that can be recycled back to MgH_2. For the electrochemical process, an electrochemical cell will be used for reduction of $NaBO_2$ at 25°C, as represented in the Equations 2a to 2c, (Pereira 2015).

Cathode: $NaBO_2+6H_2O+8e^- \rightarrow NaBH_4+8OH^- (E_0 = -1{,}24V)$ (2a)

Anode: $8OH^- \rightarrow 2O_2 + 4H_2O + 8e^- (E_0 = 0{,}40V)$ (2b)

Global: $NaBO_2 + 2H_2O \rightarrow NaBH_4 + 2O_2$ (2c)

Hydrogen yields between 90 and 100% and generation rates up to 14 $L.min^{-1}gcat^{-1}$ were obtained.

In the recycling mechano-chemical process, results obtained in the literature present high yields (higher than 80%) for $NaBH_4$ production, depending on the ball mill reactor used, the reaction time, the temperature and pressure and the isolation of the reactor, to avoid H_2 leak to the exterior. Previous experiences on the vibratory mill were inconclusive, since, after 5 minutes, the reaction needed to be stopped due to hydrogen leak that could damage the reactor (Pereira 2015). However, with the proper adaptation, the same yields obtained in the literature mentioned above are expected to be observed. Unlike the mechano-chemical reaction, the only by-product in the electrochemical process is O_2. However, this process has a high-energy consumption (the Gibbs standard reaction energy is -269,7 kJ.mol-1), which requires alternatives to the direct formation of $NaBH_4$ from $NaBO_2$.

References

Demirci, Umit B. 2015. “The Hydrogen Cycle with the Hydrolysis of Sodium Borohydride: A Statistical Approach for Highlighting the Scientific/technical Issues to Prioritize in the Field.” International Journal of Hydrogen Energy 40 (6). Elsevier Ltd: 2673–91. doi:10.1016/j.ijhydene.2014.12.067.

“Fuels - Higher Calorific Values.” 2017. Accessed February 13. http://www.engineeringtoolbox.com/fuels-higher-calorific-values-d_169.html.

Pereira, Ana. 2015. “Mestrado Integrado Em Engenharia Química Reciclabilidade Do Metaborato de Sódio a Borohidreto de Sódio Com Vista À Produção de Hydrogénio Para Células de Combustível Do Tipo PEM (Proton Exchange Membrane).”

Proposal for MSW management facility in a Goiás State municipality, Brazil

Diogo Appel Colvero[1*], Ana Paula Duarte Gomes[2], Luís António da Cruz Tarelho[2], Manuel Arlindo Amador de Matos[2] and Anny Kariny Feitosa[3]

[1]Department of Environment and Planning, University of Aveiro, Aveiro, Portugal - Researcher Brazilian National Council for Scientific and Technological Development (CNPq), File No. 207172/2014-5; [2]Department of Environment and Planning, University of Aveiro, Aveiro, Portugal; [3]Univates, Lajeado, Brazil - Researcher CAPES/PSDE/Process No. 88881.135779/2016-1

*diogocolvero@ua.pt

Keywords: Municipal solid waste (MSW), centre of mass, shared MSW management facility, Goiás State.

This study aims to propose the host municipality (HM) for a future municipal solid waste management facility (MSWMF) in the micro-region of Iporá, Goiás State, Brazil. For the purpose, the mass geometry methodology was chosen. The proposed MSWMF to serve the micro-region of Iporá will be in the Israelândia municipality and will serve 10 municipalities.

1. Introduction

The Goiás State municipalities, Brazil, have difficulty in managing properly their municipal solid waste (MSW). In accordance to the Goiás Environment Secretariat, of the 246 municipalities in Goiás, only 15 have licensed landfills (SECIMA/GO, 2015). Therefore, the study identified appropriate areas for an MSW management facility in a region of Goiás. This MSWMF should preferably serve two or more municipalities and will need to be optimized in terms of location, so that MSW transportation costs can be minimized (Chen e Lo, 2016). So, in view of the need for MSW treatment and disposal technologies in Goiás, this study aims to propose a host municipality for the future MSWMF in the micro-region of Iporá, Goiás State.

2. Materials and Methods

The Goiás State is located in Brazil and it is divided into 18 micro-regions. One of the micro-regions is Iporá, which includes 10 municipalities. In 2015 there were 65 447 inhabitants in this region and approximately 12 963 tons of MSW were produced (IBGE, 2016). Concerning the study, firstly it was essential to learn about availability, subject to approval and restricted areas for MSW treatment and disposal facilities installation in the micro-region of Iporá. In order to make a selection of free or restricted areas for the installation of landfills in the micro-region of Iporá, five legal documents of Goiás State and Brazil were used as a reference to define which geographic and environmental aspects should be considered. A geographic information system application, (ESRI, version 10.3.1), was used to locate and identify suitable areas for landfill construction, as in the studies of Gbanie *et al.* (2013). Once the available areas for landfill installation were identified, the second HM criterion was established: geographic location. To find the optimal location, the mass geometry methodology was chosen. For the purpose of finding the desired centre of mass – CM (Pereira *et al.*, 2013; Russo, 2003) it was used the x and y coordinates and the MSW production (t/day) of each municipality that is part of the region. The maximum distance between the HM and the other municipalities must be of 25 km (Chen and Lo, 2016). Municipalities that are over 25 km from a HM must send their MSW to a transfer station (TS).

3. Discussion

The founded results indicate that in the micro-region of Iporá, 33% of its area is suitable for MSW treatment facilities. Therefore, the proposed MSWMF serve the municipalities of the micro-region of Iporá as shown in Figure 1. This option was chosen by taking into account the CM of the Iporá micro-region. This facility will be in the Israelândia municipality and will serve all the 10 municipalities of Iporá micro-region.

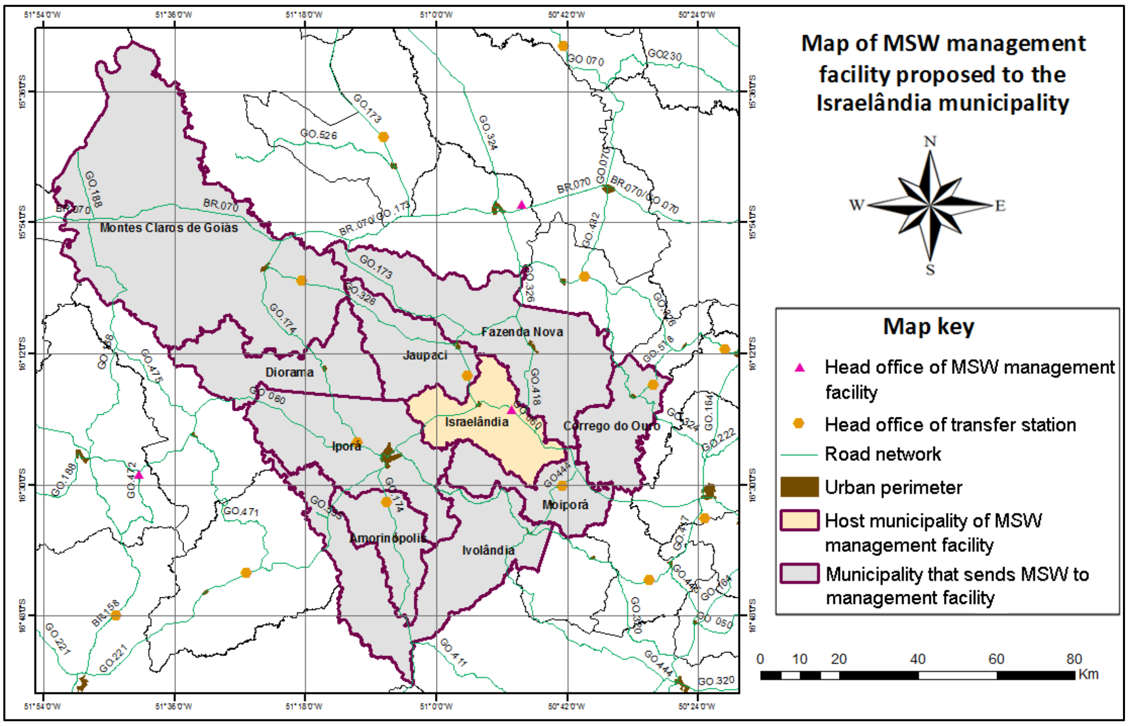

Figure 1. MSW management facility proposed to the micro-region of Iporá.

4. Conclusions

About 67% of the micro-region of Iporá is restricted for location of municipal waste treatment facilities. The delimitation of free or subject to approval areas, combined with the waste production mass centre methodology, pointed approximately the most suitable location for MSWMF facility to be in Israelândia municipality, situated in the micro-region of Iporá.

References

Chen, Y.-C., & Lo, S.-L. 2016. Evaluation of greenhouse gas emissions for several municipal solid waste management strategies. Journal of Cleaner Production, 113, 606–612.

Gbanie, S. P., Tengbe, P. B., Momoh, J. S., Medo, J., & Kabba, V. T. S. 2013. Modelling landfill location using Geographic Information Systems (GIS) and Multi-Criteria Decision Analysis (MCDA): Case study Bo, Southern Sierra Leone. Applied Geography, 36, 3–12.

IBGE – Instituto Brasileiro de Geografia e Estatística. 2016. Cidades@Goiás.

Pereira, C. D., Franco, D., & Castilhos Jr., A. B. de. 2013. Implantação de Estação de Transferência de Resíduos Sólidos Urbanos utilizando Tecnologia SIG. Revista Brasileira de Ciências Ambientais, (ISSN Impresso 1808-4524 / ISSN Eletrônico: 2176-9478), 71–84.

Russo, M. A. T. 2003. Tratamento de resíduos sólidos. Universidade de Coimbra, 196 p.

SECIMA/GO – Secretaria de Meio Ambiente, Recursos Hídricos, Infraestrutura, Cidades e Assuntos Metropolitanos. 2015. Nota técnica – aterros sanitários. Goiânia, GO, Brasil.

Sustainability of microalgae biofuel production

Branco-Vieira, M.[1,2*], San-Martin, S.[3], Agurto, C[3], Freitas, M.A.V.[2], Caetano, N.S.[1,4].

[1]LEPABE, Chemical Engineering Dpt., Faculty of Engineering University of Porto, Porto, Portugal;
[2] Energy Planning Program, COPPE, Federal University of Rio de Janeiro, Rio de Janeiro, Brazil;
[3]Biotechnology Centre, Concepción University, Concepción, Chile.
[4]School of Engineering, Polytechnic Institute of Porto, Porto, Portugal
[*]monique.branco@fe.up.pt

Keywords: microalgae, biofuel, LCA, biorefinery.

Microalgae are sunlight-driven cell factories that convert carbon dioxide into potential biofuels, foods, feed, and high-value bio-actives (Mata, Martins, and Caetano 2010). Compared with traditional crops, they have a high areal productivity, a relatively high oil and protein content, and do not depend on arable land and freshwater (Demirbas 2011). Nowadays, there is a strong interest in lipid production using microalgae. Microalgae are theoretically capable of producing much more lipids than any conventional crops and are, therefore, attractive as a potential source of biodiesel. The evaluation of carbon footprint and environmental impact of algal biofuels have currently been performed using mostly theoretical data and process assumptions (Campbell, Beer, and Batten 2011; Collet et al. 2014). A gap exists for a thorough and methodical study of algal biodiesel production based on actual process data (Bradley, Maga, and Antón 2015).

This study will be focusing on the analysis of environmental impacts from microalgae biofuels production using a biorefinery approach. Thereunto, it will be considered the microalgae culture systems performed in photobioreactors at Portugal industries and Latin America pilot plants, localized at Chile and Brazil.

Life cycle assessment (LCA) methodology will be used to identify opportunities for environmental aspects improvement at different points of the microalgae-based biofuel chain production. The LCA is based on ISO 14040 (ISO 2006b) and ISO 14044 (ISO 2006a) standards, that allow to analyse different phases of the productive process of goods and services, seeking to identify possible environmental and social damages, as well as, the environmental friendliest routes and technological processes. According to Sander and Murthy (2010) the LCA tools have a wide applicability and can be used for product development, eco-labelling, regulation of environmental policy and definition of priority scenarios.

Values on energy consumption, nutrients, water and materials will be used to create an inventory of inputs and outputs of raw materials and energy used in the biodiesel production process. These data, as well as previous data from the laboratory or industry, will be used as the foundation to produce process flowsheets that will then enable a more realistic LCA to be performed, using the SimaPro® Software 7.3.3 to evaluate the environmental impacts of biofuels production, using both upstream and downstream data.

The propose of this work it is to perform a quantitative sustainability analysis of the process using LCA as a tool to propose improvements, mitigations and possible influences of different technology routes for microalgae biomass cultivation, as well as downstream processing, to contribute for environmental and economic feasibility of this process, considering the political and economic reality of these two regions (Europa and Latin America).

The dataset of upstream process have been inventorying into LCA software and they were obtained from prototype plants localized at Chile and Brazil. According to the aims of this project, the authors are contacting industries of algae fields to establish a collaborative work, in order to obtain process data to analyse the environmental impacts of downstream route of biodiesel production.

This study intends to act as a benchmark for future upstream and downstream process development, as well as support the public policy decision-making, through the identification of critical factors to promote the development of sustainable pilot and large-scale algae-based biorefinary plants in Latin America, based on the European expertise.

References

Bradley, Tom, Daniel Maga, and Sara Antón. 2015. “Unified Approach to Life Cycle Assessment between Three Unique Algae Biofuel Facilities.” *Applied Energy* 154 (January): 1052–61.

Campbell, Peter K, Tom Beer, and David Batten. 2011. “Life Cycle Assessment of Biodiesel Production from Microalgae in Ponds.” *Bioresource Technology* 102 (1): 50–56.

Collet, Pierre, Laurent Lardon, Arnaud Hélias, Stéphanie Bricout, Isabelle Lombaert-Valot, Béatrice Perrier, Olivier Lépine, Jean-Philippe Steyer, and Olivier Bernard. 2014. “Biodiesel from Microalgae – Life Cycle Assessment and Recommendations for Potential Improvements.” *Renewable Energy* 71 (November): 525–33.

Demirbas, Ayhan. 2011. “Biodiesel from Oilgae, Biofixation of Carbon Dioxide by Microalgae: A Solution to Pollution Problems.” *Applied Energy* 88 (10): 3541–47.

ISO. 2006a. “Environmental Management: Life Cycle Assessment: Requirements and Guidelines.” *Technical Committee ISO/TC 207, Environmental Management. Subcommittee SC 5, Life Cycle Assessment, ISO 14040:2006*, 20.

ISO. 2006b. “Life Cycle Assessment - Principles and Framework.” *Technical Committee ISO/TC 207, ISO 14040:2006, Environmental Management.* https://www.iso.org/standard/37456.html.

Mata, Teresa M., António A. Martins, and Nidia. S. Caetano. 2010. “Microalgae for Biodiesel Production and Other Applications: A Review.” *Renewable and Sustainable Energy Reviews* 14 (1): 217–32.

Sander, Kyle, and Ganti S. Murthy. 2010. “Life Cycle Analysis of Algae Biodiesel.” *The International Journal of Life Cycle Assessment* 15 (7): 704–14.

Crambe abyssinica cultivation in Portugal: Field Study

E. Costa[1*], C. Alvim-Ferraz[2], M.F. Almeida[1], J.M. Dias[1]
[1]Lepabe, Metallurgic and Materials Engineering Dpt., Faculty of Engineering University of Porto, Porto, Portugal;
[2]Lepabe, Chemical Engineering Dpt., Faculty of Engineering University of Porto, Porto, Portugal;
[*]emanueltpmc@fe.up.pt

Keywords: *Crambe abyssinica*, non-food crops, cultivation, biofuel.

In the present study, the species *Crambe abyssinica* (seeds of FMS Brilhante variety) was cultivated in Northern Portugal to assess the adaptability to the Portuguese edaphoclimatic conditions and crop yield. The culture was made in the spring with a sowing density of 100 plants/m^2 and lasted 95 days. The sowing with a density of 100 plants/m^2, the harvest and the weeds control were performed by hand. Organic manure and irrigation were used and the climatic conditions were monitored. The seeds yield was 742 kg/ha, showing potential for cultivation but lower when compared to the yield reported in some studies in Brazil. This crop can be a real alternative for biodiesel production, considering that it easily completes the life cycle in the Portuguese conditions, although it is necessary to perform more studies in order to make possible the improvement of the yield.

Introduction

The production of biofuels from vegetable oils (renewable energy sources) started to have high impact by the end of 20th in replacing fossil fuels. Biodiesel can be obtained from several food plants species, like soybean, rapeseed or sunflower. Given that these species are also used for human consumption, creating competition between the energy market and the food market, non-edible vegetable oils, such as from *Crambe abyssinica*, emerge as important sources for the sustainable production of that biofuel. This species is from the Mediterranean region but it is capable to adapt to colder and drier weathers and it can be harvested in 90-120 days, which makes possible sowing twice a year or more. The seeds are typically very small (0.8 – 2.6 mm) and the weight is approximately 6 to 10 g/1000 seeds (Falasca et al. 2012). Non edible content oil from the seeds can vary between 36 and 43 wt.% (Falasca et al. 2010).

Materials and Methods

The seeds used in this study belong to the FMS Brilhante variety and were donated by Fundação MS, Brazil. Prior sowing, the germination rate was determined during 25 days, in a room with controlled temperature at 22 – 24 °C, without light. The amount of seeds used were as need to ensure the crop density established. The culture was at the Northern Portugal (40°59'07.2"N; 8°32'43.6"W). Since it is a Winter-Spring crop, well adapted to warm weather and very sensible to frost, it was chosen to sow only at the end of April (2016), when precipitation decreased, which directly influences the compaction of the soil and the number of germinated seeds. The seeds were sowed in low deep (approximately 3 cm). The area of cultivation was 50 m^2 and the density of sowing was 100 plants/m^2, with 0.35 m between rows. Sowing was performed by hand. Pivot irrigation with frequency of 3 times/week, using 120 – 150 L of water during the period of germination (16 days) and 80 L in the following period (70 days), avoided the subsurface irrigation of the crop. Before sowing soil was characterized and the results showed adequate conditions concerning the most important macro and micronutrients (phosphorus >200 mg/kg). For this reason, only a small amount of organic fertilizer was applied (Fertigranu, from animal manure, 1000 kg/ha), in agreement with the supplier recommendations.

Results and discussion

The germination rate of the seeds was 84% which indicated feasibility for sowing. During the development of the crop, weeds were removed to decrease the competition for nutrients and light. The climatic conditions verified were: 250 mm of cumulative precipitation; mean temperature of 18.5 °C and 70% of mean relative humidity. During crop growth, some extreme events of precipitation occurred (20 mm/day). Cumulative precipitation was 991.3 mm in 2016 and May was the month with the highest deviations of the year (around +70 mm) in relation to what occurred in the 1971-2000 period. Around 16 days were required for germination and 52 days for flowering (Figure 1). After 95 days, the crop had brown colour, indicating the end of the life cycle. The harvest was made by hand collection of the biomass from the roots.

Figure 1. Life cycle of *Crambe*, namely flowering (A and B) and end of the life cycle the harvest (C).

A seed yield of 742 kg/ha was obtained despite climatic unfavourable conditions along the period. Studies developed in Brazil report yields between 989 kg/ha and 1347 kg/ha and consider that *Crambe* production has economic viability for yields higher than 800 kg/ha (Carlos Pitol 2011). With normal climatic conditions yields higher than 800 kg/ha seems to be expectable in the Northern region of Portugal.

Conclusion

Crambe abyssinica seems to have potential to be cultivated in Portugal. Despite seeds yield of 742 kg/ha was lower than that reported in Brazil, higher yields are expected under typical climatic conditions without the atypical intensive precipitation periods registered during this study. The life cycle close to 90 days confirms the possibility to sow twice a year in Portugal.

References

Carlos Pitol, Renato Roscoe, Elton José Erbes, Thiago da Silva Romeiro, Jaimir Freitas dos Santos. 2011. Cultura do Crambe: Resultados e Experimentação. Maracaju, Brasil: Fundação MS.

Falasca, S. L., N. Flores, M. C. Lamas, S. M. Carballo, and A. Anschau. 2010. "Crambe abyssinica: An almost unknown crop with a promissory future to produce biodiesel in Argentina." *International Journal of Hydrogen Energy* no. 35 (11):5808-5812. doi: http://dx.doi.org/10.1016/j.ijhydene.2010.02.095.

Falasca, Silvia L., Ana C. Ulberich, and Eliana Ulberich. 2012. "Developing an agro-climatic zoning model to determine potential production areas for castor bean (Ricinus communis L.)." *Industrial Crops and Products* no. 40:185-191. doi: http://dx.doi.org/10.1016/j.indcrop.2012.02.044.

Sustainability Assessment of Agricultural Production Units (UPA) of Southern Bahia-Brazil: a study with organic cocoa farmers associated to Cabruca Cooperative

F. Regivaldo[1*] and A. Jaênes[1]
[1]Dpt. de Ciências Exatas e Tecnológicas, Universidade Estadual de Santa Cruz, Ilhéus, Bahia, Brasil;
*regivaldo.santos.silva@gmail.com

Keywords: Sustainability Assessment, Sustainability Indicators, Agroforestry Systems, Organic Cocoa.

Introduction

We have sought ways of more sustainable consumption and production, and agroforestry systems (SAF) are a good alternative to conventional agriculture. These systems in the south of Bahia are boosted by the establishment of the cocoa crisis, and are vulnerable in agronomic, economic and socio-environmental terms. Local producers have seen in organic agriculture an economically viable and beneficially environmental production. However, not all SAF, although agro-ecological, is obligatorily a sustainable agro-ecosystem. The use of environmental indicators constitutes an important strategy for the analysis of the sustainability of agricultural production units (UPAs). Thus, we sought to evaluate the environmental, economic and social sustainability of SAF composed of UPA organic cocoa from the south of Bahia associated with the CABRUCA cooperative.

Methodology

CABRUCA cooperative has 29 associates with operations in the municipalities of Barro Preto, Buerarema, Ilhéus, Itacaré, Pau-Brasil, Una and Uruçuca. The indicators' data was obtained through the application of a semi-structured questionnaire to the cacao growers, who volunteered to participate in the research. Sustainability was evaluated with SAF's indicators, typical of the southern Bahia region, developed by Passos (Passos, 2008), resulting in 13 descriptors, composed of 37 original indicators, synthesized in 15 aggregate indicators. The later are distributed in five criteria (productivity, stability, equity, resilience and autonomy) and in three dimensions (environmental, economic and social). Sustainability indicators and indices are calculated using the harmonic mean, plus a constant of 4 for each original indicator. This procedure does not change the comparability or the graphical reproduction of the original indicators, it only transfers the classification level of the values evenly above. Consequently, the variation of the original indicators from 0 to 1 will change from 4 to 5. After adding the constant, the aggregate indicators of the five criteria of each dimension will be calculated with the harmonic average of each UPA. We obtained 15 aggregate indicators for each UPA, ranging from 4, weak sustainability, to 5, strong sustainability. The original indicators with unit of measure or that exceed the interval of [0,1] are transformed to this scale before adding the constant 4 and computing the aggregate indicator, using the formula from (Sepúlveda, Chavarría And Rojas 2005). With the harmonic average, Index of Sustainability of each Dimension (ISD) and of each

Criteria (ISC), for each UPA, respectively, are computed and plotted in radar-type graphs for comparative analysis between the levels of sustainability of each UPA, representing each typical SAF studied.

Results and discussions

Regarding the Sustainability Indices of each Dimension (ISDs), shown in Table 1, it can be verified that only SAF 1 presents indices of the economic and social dimension tending to situations of weak sustainability, even if the social dimension is still close to 4,5.

Table 1. Sustainability Indices of each Dimension (ISD) of the SAF studied, Bahia, Brazil, 2016

SAF	Environmental	Economic	Social
1	4,54	4,41	4,49
2	4,64	4,50	4,57
3	4,69	4,55	4,58

After calculating the above indexes, the Sustainability Index (IS) are measured using the criteria or dimensions. The results are set forth in Table 2.

Table 2. Sustainability Index (IS) of the SAF studied, Bahia, Brazil, 2016

SAF	IS
1	4,48
2	4,57
3	4,61

SAF 3 is the strongest and SAF 1 is weakest, in terms of sustainability. The indices of the three SAFs show little discrepancy between them. It is verified that the highest value index is the one that presents the best balance between its various indicators and indexes. Looking at the results achieved by the three systems for each index of the IS, one can say that the types of permanent crops adopted in the SAF do not constitute the decisive reason for the level of sustainability achieved by each one of them, although all are crops with enormous financial potential capable of diminishing the financial instability of producers.

Conclusions

Based on the concept of sustainability of agroecosystems and the aspects that lead to the sustainability of these in the region, it is concluded that SAFs constitute an alternative system capable of reducing environmental, economic and social vulnerabilities and develop the long-term maintenance and reproduction of UPA and producers and families of the southern region of Bahia.

References

PASSOS, H. D. B. Indicadores de sustentabilidade: uma discussão teórico-metodológica aplicada a sistemas agroflorestais no Sul da Bahia. 2008.

SEPÚLVEDA, Sergio; CHAVARRÍA, Hugo; ROJAS, Patricia. Metodología para estimar el nível de desarrollo sostenible en territorios rurales: el Biograma. San José, Costa Rica: Instituto Americano de Cooperação para a Agricultura – IICA/Dirección de Desarrollo Rural Sostenible, 2005.

Author index

ISBN: 978-972-752-218-7

Follow us:

www.fe.up.pt/dce17

dce@fe.up.pt